Experimental and Theoretical Study of Carbon Dioxide Corrosion Inhibition Persistency

A dissertation presented to

the faculty of

the Russ College of Engineering and Technology of Ohio University

In partial fulfillment

of the requirements for the degree

Doctor of Philosophy

Kasra Shayar Bahadori

August 2025

This dissertation titled

Experimental and Theoretical Study of Carbon Dioxide Corrosion Inhibition Persistency

by

KASRA SHAYAR BAHADORI

has been approved for

the Department of Chemical and Biomolecular Engineering

and the Russ College of Engineering and Technology by

Marc Singer

Professor of Department of Chemical and Biomolecular Engineering

Patrick Fox

Dean, Russ College of Engineering and Technology

Abstract

SHAYAR BAHADORI, KASRA, Ph.D., August 2025, Chemical and Biomolecular Engineering

Experimental and Theoretical Study of Carbon Dioxide Corrosion Inhibition Persistency

Director of Dissertation: Marc Singer

Metallic corrosion remains a persistent challenge in oil and gas pipelines. Chemical inhibitors represent a widely employed mitigation strategy, typically administered through continuous treatment or batch application. In continuous treatment, inhibitors are continuously injected into the pipeline to form a protective layer on the pipe wall. In batch treatment, the inhibitor is directly applied to the pipe wall during shutdown or slowdown operations. A common issue in both treatments is the loss of inhibition after inhibitor application ceases, known as inhibitor persistency. Understanding persistency is crucial for operators to schedule production interruptions and implement additional inhibitor treatments to prevent significant pipeline corrosion. While numerous studies have investigated inhibitor persistency, limitations exist in comparing these methodologies to real-world field conditions. In addition, there is a notable lack of comprehensive parametric studies and modeling efforts.

The primary objective of this study was to investigate inhibitor persistency behavior and identify influencing parameters in both continuous and batch treatments. To achieve this, the research was divided into two sections: continuous treatment and batch inhibition. A novel methodology was developed for each section to more accurately reflect real-world field conditions. Parametric studies were conducted to pinpoint key

influencing parameters within each treatment. The final stage of the research focused on descriptive and mechanistic modeling and on analyzing inhibitor persistency behavior in the respective treatment contexts.

For the continuous treatment persistency study, a new dilution methodology was employed to completely remove all inhibitor residuals, mimicking field conditions where inhibitor injection is interrupted. Parametric studies were conducted to investigate the effects of temperature, longer pre-corrosion, and contact time. The Langmuir isotherm model was utilized to model inhibitor desorption behavior during the persistency phase.

For the batch treatment persistency study, a novel methodology was developed to address the limitations of previous studies and more accurately simulate real-world field conditions. Key features of this methodology included the ability to apply inhibitors in a deoxygenated environment and the continuous replenishment of brine to replicate field conditions. Parametric studies were conducted using commercial and model compound inhibitors to elucidate the factors influencing batch inhibitor persistency. A comprehensive protocol for evaluating inhibitor persistency in batch treatment was established, along with insights into potential modeling applications, providing a valuable framework for future research relating to batch inhibition persistency.

Dedication

To my mother, Azita Hosseinpour, for her endless support and sacrifices, even as my Ph.D. kept us apart for years.

To my wife, Bita Kamizi, for her unwavering love and for always standing by my side.

To my sister, Ayie Bahadori, who is always in my heart.

Acknowledgments

I would like to begin by expressing my heartfelt gratitude to my academic advisor and life mentor, Prof. Marc Singer. His support extended far beyond academics. He guided me not only throughout my Ph.D. journey but also through personal challenges. His mentorship was a guiding light during difficult times and continuously inspired me to stay motivated.

I offer special thanks to Dr. Bruce Brown, who was always present and never let me face a problem alone. His unwavering support and willingness to help with practically everything meant a great deal to me. I am also deeply grateful to Dr. Young for his valuable guidance in academic writing and for synthesizing inhibitors for my research.

I would like to thank Prof. Srdjan Nesic for his continuous support and kindness. His deep knowledge and teaching opened my eyes to new perspectives, especially during the courses I had the privilege to take with him.

Special thanks go to Alexis Barxias, Cody Shafer, Rebecca Matthews, and all the other members of the ICMT family for their camaraderie and support throughout this journey.

I am sincerely thankful to my doctoral committee members, Dr. Lauren E.H. McMills and Dr. Rebecca Barlag, for their time, insights, and encouragement.

Finally, I want to extend my appreciation to all my friends, colleagues, professors, and classmates at Ohio University. Thank you for making my Ph.D. experience both meaningful and memorable.

Table of Contents

Page

List of Tables

Page

List of Figures

Page

Chapter 1: Introduction

When a metal is subjected to an aqueous or otherwise aggressive environment, it may experience electrochemical degradation; a phenomenon referred to as metallic corrosion. In atmospheric corrosion, the metal typically undergoes conversion to its oxide form, in various other environments different products may develop [1]. Given the widespread use of metals globally, corrosion has substantial impacts, particularly concerning safety and economic costs. Numerous incidents have been attributed to metal corrosion. One of the most severe occurred in 1992 in Guadalajara, Mexico, where consecutive gas explosions adjacent to a sewer system destroyed 8 kilometers of roadway. This disaster was precipitated by the corrosion of pipelines near water and sewer lines; their leakage caused nearby gas pipelines to corrode and ultimately fail, leading to a catastrophic explosion. This tragedy resulted in 252 fatalities, 1,500 injuries, and 15,000 individuals being rendered homeless [2]. In another tragic incident on April 28, 1988, a flight attendant lost their life and numerous passengers sustained injuries when the airplane fuselage collapsed due to metal fatigue exacerbated by corrosion [1].

Studying and understanding the mechanisms of metallic corrosion can prevent such catastrophic incidents and save lives. While this proposed research focuses on corrosion in the oil and gas industry, its general findings on corrosion and mitigation strategies can be applied, to some degree, to other areas, including the protection of metallic structures such as bridges and buildings.

Metallic corrosion is particularly significant in the oil and gas industry. CO_2 plays a crucial role in the corrosion of pipelines within this sector and more broadly in the

energy industry. Natural gas containing CO_2 is transported from reservoirs to various production and processing units through low-alloy steel pipelines [3]. Internal corrosion of a pipeline steel can occur when an aqueous phase is present together with gaseous CO_2 dissolving and hydrating therein to form the corrosive weak acid H_2CO_3 (carbonic acid) [4].

Various methods exist to mitigate pipeline corrosion in the oil and gas industry, with the use of corrosion inhibitors being particularly common given their economy. These chemical compounds are introduced into pipelines through different techniques, where they act to alter active surface areas and mitigate corrosion [5].

There are different methods for applying corrosion inhibitors (CIs) in upstream oil and gas pipelines, with two being dominant. The first, and most convenient, method is called continuous treatment; CI is continuously injected, at a relatively low dosage, into the pipeline flow in the aqueous phase using a pump. The purpose of this method is to maintain CI concentration at a relatively constant value along the pipeline to achieve the required protection. However, there are particular environments and conditions where continuous treatment is ineffective for protecting the entire internal pipeline surface area (in case of multiphase flow and consequent gas-liquid stratification in horizontal pipelines, for example, where there is no straightforward methods to transport the CI injected at the bottom of the pipe to the top). In these cases, another method termed batch treatment is used to directly apply the CI to the entire internal tubular surface. In the most common variant of this method, especially applicable to pipelines, a very high concentrated slug of the inhibitor is placed between two moving “pigs” (cylindrical

devices inserted inside the pipe that can be used for cleaning and inspection without completely interrupting production), the inhibitor forming a protective film on the pipeline as the pigs move. When pigs cannot be used easily, as is the case for downhole tubulars of producing wells, the inhibitor slug is injected at the wellhead and is pumped to the bottom, typically through the annulus between the production tubing and the casing. The inhibitor then flows back up through the tubing, together with the produced fluids and a protective film is meant to be formed as the inhibitor covers the wall [6-9]. However, each treatment method presents distinct operational and corrosion control challenges. In continuous treatment, issues such as injection pump failure or insufficient inhibitor supply can arise. Under these circumstances, corrosion protection can revert to unsafe levels as inhibitor can desorb relatively quickly. The corrosion inhibitor (CI) persistency represents the period during which the inhibitor remains effective after CI injection has ceased. Understanding the CI persistency in continuous treatment is crucial for identifying safe operational windows, thereby preventing serious and costly damage to the pipeline. Conversely, in batch treatment, the inhibitor is initially applied directly to the pipeline, after which normal operations resume. Over time, depending on various factors, the inhibitor gradually desorbs from the metal surface, leading to a loss of protection. This inhibition duration also represents the CI persistency in batch treatment, which is even more critical compared to continuous treatment as it is an essential aspect of the corrosion control process. Therefore, CI persistency is a paramount parameter in corrosion mitigation using chemical inhibitors. Accurately predicting CI persistency behavior in both treatment methods is crucial for effective corrosion management in the

oil and gas industry [7-9]. Hence, the objective of the research described in this dissertation is to enhance understanding of the parameters influencing inhibitor persistency. This goal is accomplished by considering several key steps. Firstly, an experimental methodology is developed to accurately simulate inhibitor treatments under controlled conditions. Secondly, a systematic study is conducted to investigate the effects of various controlling parameters on the persistency of model compounds. Finally, a mechanistic model is constructed to predict the persistency of CO_2 corrosion inhibitors. By integrating these approaches, the research aims to provide comprehensive insights into the factors that govern inhibitor persistency, considering both continuous and batch treatments, thereby advancing the efficacy of corrosion mitigation strategies in the oil and gas industry.

Chapter 2: Literature Review

This chapter presents the fundamentals of CO_2 corrosion of mild steel as well as of corrosion inhibition mechanisms.

2.1 Mild Steel Corrosion in Acidic Environments

There are two primary concurrent reactions that contribute to the corrosion of mild steel: the cathodic and anodic reactions. In typical acidic aqueous environments encountered in oil and gas production, the predominant cathodic reaction is the reduction of hydrogen ions [10]:

$$2H^+(aq) + 2e^- \rightarrow H_2(g) \qquad (1)$$

The dominant anodic reaction results in iron oxidatively dissolving into solution:

$$Fe(s) \rightarrow Fe^{2+}(aq) + 2e^- \qquad (2)$$

2.2 Corrosion in CO_2 Environments and Associated Reactions

When gaseous CO_2 dissolves in the aqueous phase, it creates an acidic environment that can induce severe corrosion of mild steel. This acidic environment is a primary source of corrosion in oil and gas pipelines [11]. Over the past 30 years, CO_2 corrosion in aqueous systems has been the subject of extensive research. Mechanistically, dissolved CO_2 hydrates to form H_2CO_3 (carbonic acid), which can increase the reduction current associated with the corrosion of mild steel [12-16]. More details on this are provided in Appendix A: Electrochemical and Transport Processes in CO_2 Environments [17].

2.3 Corrosion Inhibition

Various methods are employed to mitigate corrosion in the oil and gas industry. These include material selection, the application of protective coatings, cathodic protection, the use of nonmetallic materials, environmental control, and chemical inhibition. Given their economy, effectiveness, and relative ease of application, the use of corrosion inhibitors is very common in the industry [18-20]. This section focuses on discussing the application and effectiveness of corrosion inhibitors as a means of preventing corrosion in oil and gas pipelines.

The selection of appropriate inhibitors is a critical aspect of corrosion protection strategies [5]. Corrosion inhibitors are chemical compounds employed to mitigate the corrosion rate in production tubulars and pipelines, typically at concentrations of less than 100 parts per million (ppm) [21, 22]. Generally, inhibitors operate by either reducing the corrosivity of the environment or by adsorbing onto the metal surface, thereby forming a protective film that shields the metal from corrosive agents. Consequently, inhibitors are often categorized into two main groups based on their mechanism of action: environment modifiers and adsorption inhibitors [23]. Environment modifiers function by altering the chemical properties of the corrosive environment, thereby decreasing its ability to cause damage. Therefore, these types of inhibitors need to be injected at higher concentrations compared to adsorption inhibitors. In contrast, adsorption inhibitors work by attaching to the metal surface, thereby creating a physical barrier that prevents corrosive substances from reaching the metal and/or by decreasing the reactivity of the metal itself. The careful selection and application of these inhibitors are essential to

ensuring the longevity and integrity of pipelines and production systems in the oil and gas industry. In addition to this classification, inhibitors are also categorized into organic and inorganic inhibitors based on their compositional characteristics. Inorganic inhibitors are mostly chromium, molybdenum, zinc, phosphate, sulfite and hydrazine compounds, many of which are toxic and not environmentally friendly [18, 24, 25]. On the other hand, organic molecules have been commonly used as corrosion inhibitors in the oil and gas industry over the past decades. In general, organic inhibitor molecules have two main parts: a polar or charged functional group that has hydrophilic characteristics (the head group); and an alkyl tail which has hydrophobic characteristics (the tail) [24]; such molecules are termed amphiphilic. A wide range of organic compounds can function as organic inhibitors, including acetylenic alcohols, aromatic aldehydes, amines, amides, imidazolines, pyrimidines, thiols, and phosphate esters [25]. Among these, imidazoline-type compounds and quaternary ammonium salts are particularly prevalent in inhibitor formulations [26]. Commercial inhibitor formulations comprise a blend of several types of corrosion inhibitors along with additional additives such as dispersants and film enhancers to optimize performance [26]. Inhibitors operate by targeting specific aspects of the corrosion process. They can mitigate corrosion by slowing the rate of the cathodic reaction (cathodic inhibitors), the anodic reaction (anodic inhibitors), or both reactions simultaneously; inhibitors that impact both are referred to as mixed inhibitors [26]. The use of mixed inhibitors is advantageous because they provide a more comprehensive defense against corrosion by addressing both key components of the electrochemical corrosion process [27, 28]. However, discrepancies exist in the open literature regarding

the definition of anodic and cathodic inhibitors. Some researchers argue that an inhibitor is classified as either anodic or cathodic based on the shift in corrosion potential it induces through anodic or cathodic polarization. Others, however, contend that this classification should be based on the ability of inhibitor molecules to participate in specific reactions that block either anodic or cathodic sites. However, actual proof of an inhibitor's ability to target specific active sites or reaction remains elusive.

In practice, the effectiveness of these inhibitors is influenced by their chemical structure and the specific environment conditions in which they are used. Consequently, the development and selection of suitable inhibitors require a thorough understanding of their interactions with both the metal surface and the corrosive medium. This complexity underscores the necessity for continued research and innovation in the field of corrosion inhibition, particularly in industries such as oil and gas where the integrity of infrastructure is paramount [23].

Over the past few decades, numerous studies have documented the extensive use of organic inhibitors containing heteroatoms such as nitrogen (N) in their molecular structures for combating sweet corrosion [18, 26]. The head groups of these inhibitors predominantly include derivatives of amines, imidazolines, and quaternary ammonium species. Due to their cationic nature and film-forming capabilities, protonated imidazoline (imidazolinium) and quaternary ammonium derivatives are regarded as some of the most effective inhibitors available [18]. The efficacy of these inhibitors lies in their ability to form an adsorbed film on the metal surface. This film has been described by acting as a barrier, "blocking" corrosive species from reaching the metal and thereby

reducing the rate of corrosion [18]. However, the ability of such films to limit mass transfer is dubious as they are often very thin (several molecular lengths thick) and it is more likely that the adsorption of CI molecules affects the kinetics of electrochemical reactions. Figure 1 depicts an example of a quaternary ammonium type inhibitor that exhibits the characteristics described above.

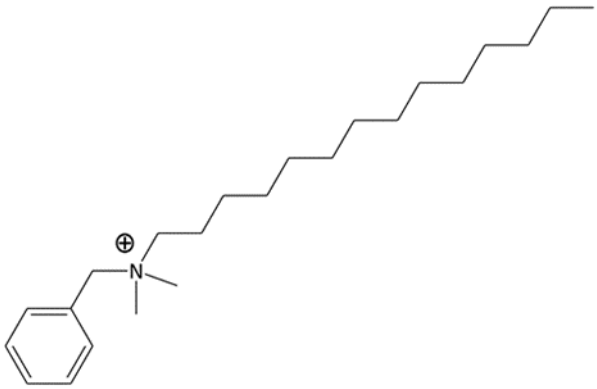

Figure 1. Example structure of a quaternary ammonium inhibitor with a tetradecyl tail and a benzyldimethylammonium head (identified as BDA-C14 at ICMT).

2.3.1 Inhibitor Adsorption Mechanism

Most organic inhibitors mitigate corrosion through three primary mechanisms: physical adsorption, chemisorption, and layer formation. When inhibitor molecules adsorb onto the surface, a process known as physisorption can occur due to electrostatic interactions between the charged inhibitor molecules and the metal surface. These interactions include van der Waals forces, dipole-dipole interactions, and London dispersion forces. This process is relatively fast and creates weak bonds that are easily disrupted (Figure 2) [29-31].

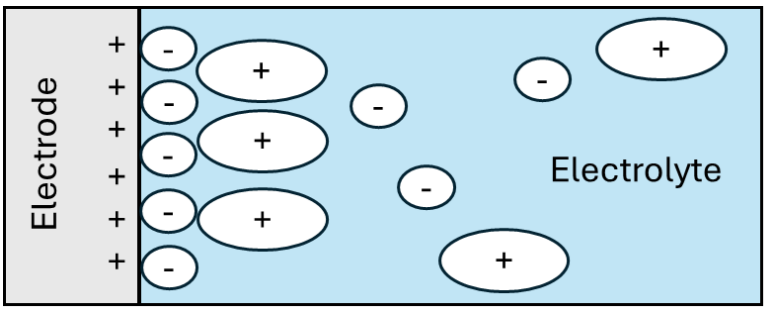

Figure 2. Adsorption of negatively charged inhibitor on a positively charged metal surface.

Conversely, chemisorption has been postulated to involve interaction between lone pair or π-electrons of the inhibitor head group and orbitals at the metal surface, leading to the formation of strong, stable donor-acceptor bonds. This process is slower but results in a much more durable protective layer that is significantly harder to break [32, 33]. Furthermore, adsorbed inhibitors can interact with the corrosion products of the metal or reactive components in the medium, resulting in formation of various complex compounds or precipitated layers on the metal surface [28, 34, 35]. This layer formation enhances corrosion mitigation by providing an additional barrier against corrosive agents. The effectiveness of these mechanisms is influenced by the chemical structure of the inhibitors, the nature of the metal surface, and the environmental conditions [36]. However, there is no strong evidence in the current literature confirming the chemisorption of corrosion inhibitors. It is generally assumed that adsorption is classified as chemisorption if the standard free energy of adsorption exceeds 40 kJ/mol. However, Kokalj *et al*. [32] highlighted several weaknesses in this criterion for distinguishing between physisorption and chemisorption. First, there are uncertainties in measuring the

Gibbs free energy of corrosion inhibitor adsorption. Additionally, entropy contributions can lower the Gibbs free energy, even in cases of chemisorption. Lastly, chemisorption is a slow and irreversible process that often conflicts with the fast adsorption kinetics and the low persistency of common inhibitors.

2.3.2 Inhibition Efficiency

The efficiency of an inhibitor can be evaluated using the equation below [23, 29]:

$$\varepsilon = \frac{CR_{uninhibited} - CR_{inhibited}}{CR_{uninhibited}} \quad (3)$$

where ε is the corrosion inhibition efficiency, $CR_{uninhibited}$ is the steady state corrosion rate (mm/year) without inhibitor and $CR_{inhibited}$ is the steady-state corrosion rate (mm/year) in the presence of inhibitor.

2.3.3 Adsorption Isotherm Models

In the realm of corrosion inhibition, the exploration of correlations between inhibition effectiveness and adsorption behaviors is fundamental and often facilitated through the utilization of isotherm models [23, 37]. In the extensive body of literature dedicated to this subject, numerous isotherm models have been proposed and investigated [37]. Predominantly, the Langmuir, Frumkin, Bockris-Swinkels, and Virial Parson isotherms emerge as the most frequently employed models for elucidating the interaction mechanisms between inhibitor molecules and the metal surface [23, 38]. Among these models, the Langmuir isotherm stands out as the most prevalent and straightforward, finding widespread application across various studies in the field. In general, inhibitor adsorption has been considered as an exchange between adsorbate molecules and solvent molecules on the surface [39, 40]:

$$I_{aq} + x(H_2O)_{sur} \rightarrow I_{sur} + x(H_2O)_{aq} \quad (4)$$

where I corresponds to inhibitor adsorbate molecules and (aq) and (sur) represent the molecules in the bulk and at the surface, respectively. The parameter x accounts for the displacement of water molecules and represents the ratio of desorbed solvent molecules to adsorbed inhibitor molecules at the surface. Isotherm models are generally expressed as:

$$f(\theta, x)\exp(-\alpha\theta) = Kc \quad (5)$$

where K is the equilibrium constant and α is a parameter that accounts for molecular interaction between molecules in the adsorbed layer. Thus, this expression consists of two factors that consider species substitutability ($f(\theta, x)$) and molecular interactions between adsorbed molecules ($\exp(-\alpha\theta)$). The Langmuir isotherm model is the result of considering x as 1 and α as zero. The Langmuir isotherm model operates on the assumption that adsorption occurs through the formation of a monolayer on the surface, with negligible intermolecular interaction between the adsorbate molecules. Mathematically, the Langmuir isotherm model, commonly employed to describe the adsorption phenomenon of a substance onto a surface, is expressed by the following equation [41, 43]:

$$\frac{d\theta}{dt} = k_A C_{inh}(1-\theta) - k_D\theta \quad (6)$$

which relates surface coverage factor to adsorption ($k_A\, in\, \mathrm{M^{-1}.s^{-1}}$) and desorption ($k_D\ in\ \mathrm{s^{-1}}$) constants and inhibitor concentration (mol/L).

The equilibrium surface coverage and the concentration of inhibitor are related by the equation below [37, 41, 43]:

$$C_{inh} = \frac{1}{K_{AD}}\left(\frac{\theta_{eq}}{1-\theta_{eq}}\right) \quad (7)$$

where C is the inhibitor concentration (mol/L) and K_{AD} is the equilibrium constant (L/mol) for the adsorption-desorption process. This equation relates the surface coverage factor, the inhibitor concentration (which can be measured experimentally) and the adsorption-desorption equilibrium constant.

2.3.4 Corrosion Inhibition Models

Various studies in the open literature have attempted to model the mechanisms and kinetics of corrosion inhibitors. The most significant studies are highlighted here.

2.3.4.1 Corrosion Inhibition Model Based on Surface Coverage. The model known as the "geometrical blocking effect" uses the idea that inhibitor molecules decrease the corrosion rate by adsorbing on the surface and blocking the actively corroding areas [29, 43-45]. This model also assumes that the areas covered by inhibitor molecules are uncorroded while the areas without inhibitor coverage are corroded at the bare steel rate [43, 46]. Thus, using this assumption, the surface coverage by the inhibitor can be equated to the inhibitor efficiency:

$$\theta = \varepsilon = \frac{CR_{uninhibited} - CR_{inhibited}}{CR_{uninhibited}} \quad (8)$$

where θ is defined as the surface coverage factor.

However, this approach has some limitations since full inhibitor coverage (θ =100%) never practically translates to an efficiency of 100% [43]. Consequently, the parameter θ is ill-defined since it does not represent the actual coverage of the surface by the inhibitor molecules. However, this definition is mentioned here as it is a very commonly used parameter in corrosion mitigation studies, although it can be misleading.

Hackerman *et al*. defined the surface saturation concentration (SSC) of an inhibitor as the concentration that yields the highest corrosion inhibition efficiency. This concentration corresponds to the maximum surface coverage, assuming monolayer adsorption by the inhibitor. Beyond this saturated concentration, further increases in inhibitor concentration do not affect the surface coverage factor or the inhibitor's efficiency [47]. This definition addresses limitations in previous assumptions regarding the surface coverage factor and inhibitor efficiency by not assuming zero corrosion at full inhibitor coverage. Additionally, it provides a definition of the time dependence of coverage as follows [47]:

$$\theta(t) = \frac{(i_{corr})_{\theta=0} - (i_{corr})_{\theta=t}}{(i_{corr})_{\theta=0} - (i_{corr})_{\theta=1}} \quad (9)$$

In the equation above, the corrosion rate is represented as current density i_{corr} (A/m^2). $(i_{corr})_{\theta=0}$ is the corrosion rate without inhibitor, $(i_{corr})_{\theta(t)}$ is the corrosion rate at time (t) and considering the applied CI concentration, and $(i_{corr})_{\theta=1}$ is the steady-state corrosion rate at surface saturation concentration (full coverage).

2.3.4.2 Mechanistic Model Based on Activation Energy. Dominguez, *et al.*, developed a mechanistic model for quaternary ammonium type inhibitors, such as of the type shown in Figure 1 above, based on changes in activation energy (ΔG) in the electrochemical processes occurring during CO_2 corrosion, using this parameter as a key indicator of inhibitor efficiency [43]. The fundamental assumption of this approach is that the presence of corrosion inhibitor molecules influences the chemical component of the activation energy while leaving the electrochemical component unchanged, evidenced by the fact that the Tafel slope and limiting current are not influenced by the presence of the

inhibitor. The activation energy, both in the presence and absence of the inhibitor, was determined using an Arrhenius plot at the potential of zero charge (PZC). Dominguez postulated that the total activation energy of the corrosion process in a system without an inhibitor ($\theta = 0$) gradually increases as the inhibitor is introduced, reaching a maximum value (ΔG_{MAX}) at surface saturation ($\theta = 1$), as illustrated in Figure 3.

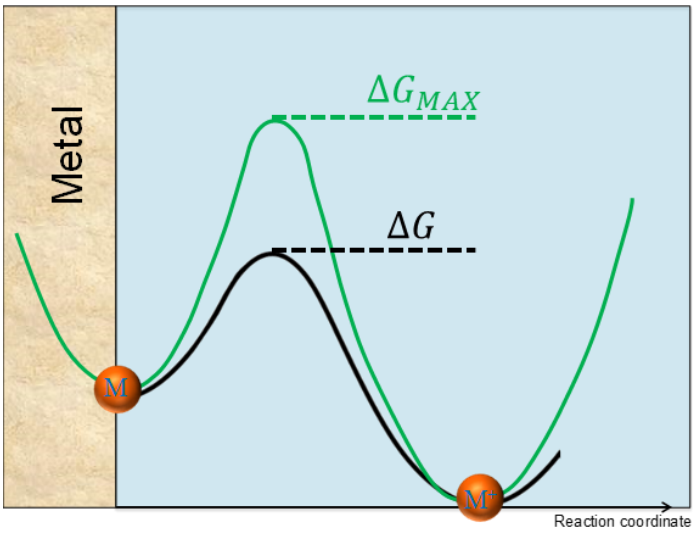

Figure 3. Activation energy change in presence of the inhibitor (reprinted with permission from [43]).

Based on this model, total activation energy in the presence of the inhibitor at any coverage can be calculated using the equation below:

$$(\Delta G)_{inh} = (\Delta G)_{\theta=0}(1-\theta) - (\Delta G)_{\theta=1}\theta \quad (10)$$

where $(\Delta G)_{inh}$ is the activation energy in the presence of the inhibitor, $(\Delta G)_{\theta=0}$ is activation energy with no inhibitor, and $(\Delta G)_{\theta=1}$ is the activation energy at surface saturation concentration. Dominguez *et al*. modeled the polarization curves for anodic and cathodic reactions in the presence of an inhibitor under the assumption that the

inhibitor influences only the charge transfer process of corrosion, without affecting diffusion or chemical reaction processes. The author also successfully showed that adsorption/desorption constants of the inhibitor could be calculated using the Langmuir isotherm model. By integrating equation (6) and considering $\theta = 0$ at initial time ($t = 0$), the surface coverage (θ) function with respect to time can be obtained:

$$\theta(t) = \left(\frac{K_{AD}C_{inh}}{1+K_{AD}C_{inh}}\right)\left(1 - e^{-(k_A C_{inh}+K_D)t}\right) \quad (11)$$

where t is time, k_A and k_D are adsorption and desorption constants, respectively, C_{inh} is initial concentration of the inhibitor and K_{AD} is the ratio of adsorption and desorption constants. By using non-linear regression analysis, Dominguez was able to determine the adsorption/desorption constants [43].

2.3.4.3 Improved Inhibition Model Based on Activation Energy. Although the inhibition model developed by Dominguez *et al*. provided a more comprehensive mechanistic understanding of inhibition behavior in CO_2 corrosion compared to the earlier inhibition models, it still has certain limitations. The model relies on calculating activation energy in the presence and absence of an inhibitor at the potential of zero charge (PZC). However, determining the PZC and activation energy using an Arrhenius plot is a complex and labor-intensive process, making the model difficult to apply and, in some cases, inapplicable to inhibitor molecules other than quaternary ammonium compounds. Additionally, the model assumes that both anodic and cathodic reactions exhibit the same change in activation energy upon inhibitor addition, which does not hold true for all inhibitors. To address these limitations, Ren *et al*. [48] introduced an updated version of the fundamental mechanism proposed by Dominguez *et al*. Instead of directly calculating

the activation energy, Ren *et al*. employed derived equations fitted to experimental data, determining the change in activation energy using analysis of potentiodynamic polarization. This approach allowed for the modeling of polarization curves for both uninhibited and inhibited conditions by separately incorporating the activation energy changes into the current density equations for anodic and cathodic reactions. By doing so, the model resolved some of the limitations of the Dominguez *et al*. approach, offering a more straightforward method for calculating activation energy changes and extending its applicability to a broader range of inhibitors. Furthermore, by incorporating the Langmuir isotherm model and the inhibitor kinetic constant, the approach enabled the calculation of transient-phase surface coverage changes and model polarization behavior under non-steady-state conditions. However, this model also has its own limitations, as it is only validated in CO_2 corrosion in the absence of corrosion products, and the transient-phase calculations remain valid only when the inhibitor follows Langmuir adsorption behavior.

2.4 Inhibition Treatment

In the downhole and upstream sectors of the oil and gas industry, two primary methods are employed for mitigating internal pipeline corrosion using inhibitors: continuous treatment and batch treatment. The choice between these treatment methods is typically determined by factors such as the accessibility of the pipeline and the associated costs [5, 7-9, 21, 29].

2.4.1 Continuous Treatment

In the upstream oil and gas industry, the predominant method for corrosion inhibition involves the continuous injection of a carefully formulated chemical package

to maintain a consistent concentration of inhibitor within the fluid flowing through the pipeline [7-9]. This approach is preferred over batch treatment because it eliminates the need for production interruptions or slowdowns while enabling more precise control of inhibitor concentration [21, 49]. The continuous injection method involves the constant supply of the inhibitor into the pipeline via an injection port. This system typically includes a pump and a filter to remove any solid particles that could obstruct the injection port, as well as a capillary tube for precise delivery [21]. The design of the injection system is tailored to the specific application, whether for transport pipelines or downhole tubulars, ensuring optimal performance under various operational conditions [21, 50]. Water-soluble inhibitors, such as imidazolinium and quaternary ammonium compounds, are commonly used in continuous treatment due to their effectiveness and compatibility with this delivery method. These types of inhibitors, discussed in section 2.3, are particularly suited for maintaining the integrity of pipelines by forming protective films that prevent corrosive agents from attacking the metal surfaces [18]. The advantages of continuous treatment extend beyond the uninterrupted operation of production processes. This method provides enhanced control over the inhibitor dosage, leading to more effective and reliable corrosion protection. The continuous supply of inhibitors ensures that the protective film remains intact even under fluctuating operational conditions, thereby reducing the risk of corrosion-related failures and extending the lifespan of critical infrastructure. However, this method presents several challenges and limitations. The continuous injection of corrosion inhibitors (CIs) necessitates a system comprising an injection pump, an inhibitor storage tank, and tubing, all of which require a substantial

volume of inhibitor. This not only increases operational costs but also renders the approach impractical in harsh operating environments. Furthermore, the selection of an appropriate inhibitor for specific conditions requires laboratory experimentation, which is inherently limited in its ability to fully replicate real-world conditions. Additionally, any system failure can rapidly restore the environment to highly corrosive conditions, necessitating continuous monitoring to ensure the effectiveness of the inhibition treatment [51, 52].

2.4.2 Batch Treatment

There are some cases where continuous treatment is impractical or not adapted to address specific corrosion threats. For example, most continuous inhibitors are water-soluble and do not evaporate. Consequently, they remain confined to the bulk water phase and are unable to provide effective protection against corrosion under dewing conditions (*i.e.*, with respect to top-of-the-line corrosion (TLC) mitigation). In complex flow regimes, such as downhole tubulars, the partitioning of inhibitors between the oil and water phases can limit their contact with the steel surface, reducing corrosion protection. This occurs because inhibitors that preferentially dissolve in the oil phase become unavailable in the aqueous phase, where corrosion primarily takes place. As a result, the inhibitor concentration in the bulk water decreases, leading to a reduction in continuous inhibition efficiency [53, 54]. In these cases, batch treatment can be viewed as a useful alternative [5, 7-9, 55, 56]. The inhibitors that are used in batch treatment are mostly oil-soluble type inhibitors while water-soluble organic inhibitors are mostly used in continuous treatment [5]. Long-tail primary amines, imidazolines, fatty acids and

phosphate esters are examples of oil-soluble inhibitors that are used in batch treatment [18].

In cases of downhole tubulars, a highly concentrated inhibitor slug is often injected from the wellhead during periodic shutdowns. The inhibitor slug slowly flows along the tubing or the casing, forming a film on the metal surface. Also, the inhibitors used in this method are selected for their superior film forming abilities [57, 58]. After the inhibitor film formation step, production is restarted, and operators count on the high persistency of the inhibitor to provide protection against corrosion. This procedure is repeated at defined time intervals when it is assessed that the CI persistency is about to be lost.

For transport pipelines, batch treatment of the inhibitor is usually done between two cylindrical tools, also called pigs. This treatment necessitates either a temporary interruption or a significant reduction in production rates. The highly concentrated inhibitor solution is loaded between the two pigs at the pig launcher (a device at the inlet and outlet of the pipeline that enables insertion or retrieval of the pigs). Using back pressure, the pigs/inhibitor slug system flows along the pipeline, applying an inhibitor film on the pipe wall (Figure 4). In some cases, the inhibitor is sprayed at the top of the line by a specially designed front pig (Figure 5) [21]. The term pig is a broad name that is used to describe a wide range of tools, with various degrees of complexity, from a simple cleaning scrapper to highly instrumented “intelligent" pigs used for inspection [21]. Its name originates from the early design of scraper pigs, which initially involved pushing a large rubber ball through a pipeline. The friction between the ball and the pipe surface

produced a screeching noise, resembling the squeals of a pig, hence the name. In all batch treatments, whether downhole or upstream, periodic application is essential because the inhibitor film gradually deteriorates over time. This degradation occurs due to factors such as dissolution, mechanical shear from fluid flow, and desorption from the metal surface, ultimately reducing the effectiveness of corrosion protection [21].

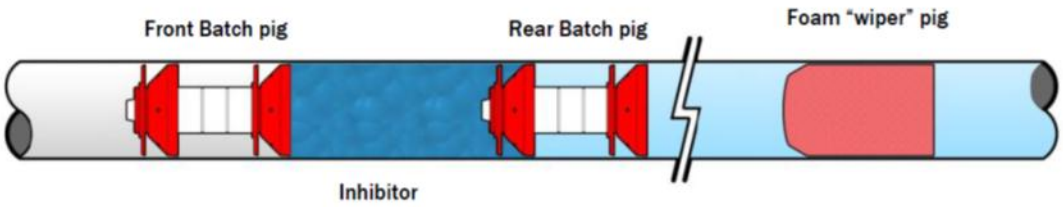

Figure 4. Batch inhibition application in pipeline with the CI slug place between two moving pigs (reprinted with permission from [59]).

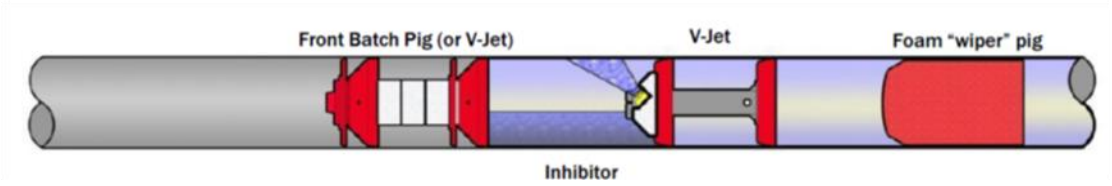

Figure 5. Batch inhibition application in pipeline using spraying pig (reprinted with permission from [59]).

2.5 Inhibitor Film Persistency

The inhibitor forms a protective film when it is applied on the pipe walls. The film protective characteristics are governed by its effect on the kinetics of electrochemical reactions, in some cases its thickness, and the adsorption/desorption dynamic equilibria involved, which depends on several parameters such as the inhibitor concentration in the bulk fluid, the inhibitor structure, and temperature. Many scenarios

can lead to the sudden or gradual removal of the film. This film can be removed by fluid flow (mechanical shear), especially in highly turbulent situations that can damage the adsorbed film. If the bulk fluid is suddenly replenished by an uninhibited solution (*i.e.*, if the inhibitor injection stops), the film will gradually desorb, eventually exposing the surface to the corrosive environment. The time it takes for the film to effectively desorb (*i.e.*, for the corrosion protection to be lost) is defined as the persistency of the inhibitor. Inhibitor persistency is a critical factor for both continuous and batch treatment methods. While continuous treatment offers the advantage of continuous application, interruptions in inhibitor injection can lead to a rapid loss of inhibition effectiveness and persistency. Batch treatment, on the other hand, requires periodic reapplication by design, while the inhibitor persistency is much higher than for continuous CIs due to the inherent decline in inhibitor potency over time. In both cases, the persistency of the inhibitor is a critical characteristic that needs to be known and understood for determining the time window of safe operation and defining the frequency of the batch treatment. So, obtaining a better understanding of the parameters affecting an inhibitor molecule persistency is very important to optimize the design of future inhibitor packages for superior corrosion mitigation [7-9, 60].

2.5.1 Literature Review on CI Persistency in Continuous Treatment

One of the most notable studies on inhibitor persistency was conducted by Dougherty, *et al*., published in 2002 [61]. The experimental system and procedure employed in this investigation utilized a flow-through system designed to simulate continuous inhibitor treatment as well as sudden treatment interruption. To validate the

results from the experimental flow-through test, a field test was also conducted. Dougherty, *et al*., demonstrated that oil-soluble inhibitors exhibit superior film persistency compared to water-soluble types. Additionally, they found that increasing the initial inhibitor concentration positively impacted film persistency without significantly affecting inhibitor efficiency. The flow-through tests were carried out using a standard rotating cylinder electrode (RCE) system with three electrodes. The main steps of their procedure included:

1- Pre-corroding the sample in a corrosive brine without an inhibitor for 1.5 hours.

2- Adding the inhibitor in ppm concentrations to the main solution using a solvent.

3- Flushing the inhibited solution by continuously adding an uninhibited solution 1.5 hours after the inhibitor addition.

This dilution method gradually decreased the concentration of the inhibitor in the solution until it was undetectable, simulating an interruption in inhibitor injection (*i.e.*, continuous treatment) after a specific contact time with the metal surface. The results of the flow-through test (Figure 6) showed that immediately after the inhibitor was added, the corrosion rate decreased, indicating rapid adsorption of the inhibitor. The corrosion rate continued to decrease until reaching a steady-state value, reflecting equilibrium in the adsorption/desorption process. Although the inhibitor concentration dropped to the lowest detectable level after 11 hours, desorption did not occur until after 18 hours, highlighting its persistency. Once the inhibitor lost its persistency, the corrosion rate

sharply increased to the blank corrosion rate, confirming the complete desorption of inhibitor molecules from the metal surface. While the experimental design and procedural execution in this study aimed to replicate field conditions for continuous corrosion inhibitor (CI) treatment, a critical methodological limitation still existed. Specifically, the authors failed to validate the calculated CI concentration through direct measurement. This omission raises concerns regarding the potential for residual inhibitor adsorption onto system surfaces, which could have significantly altered the bulk CI concentration and, consequently, influenced the observed inhibitor desorption rate. Therefore, the presented data does not provide conclusive evidence for CI persistency.

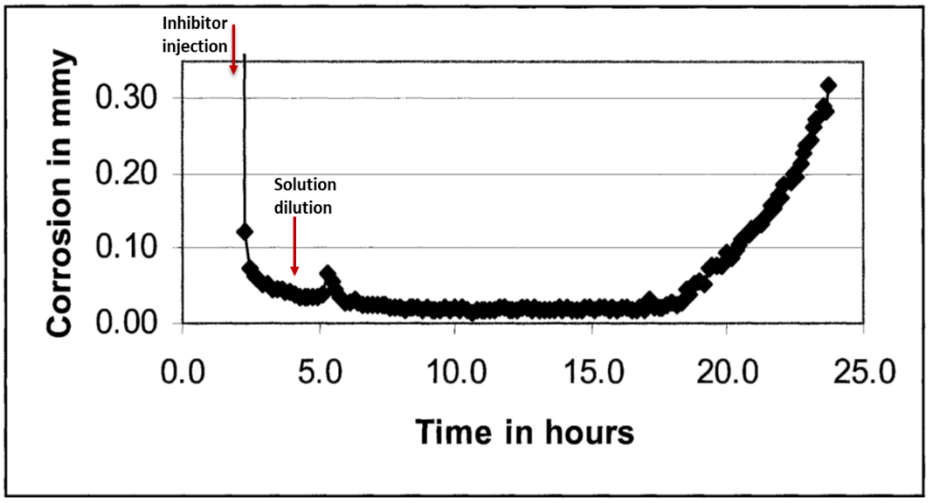

Figure 6. CI persistency test: Corrosion rate (mm/year) vs. time plot corresponding to an "interruption in continuous treatment" (reprinted with permission from [61]).

Ramachandran, *et al.,* employed a distinct approach to investigate inhibitor film persistency by utilizing the Langmuir isotherm model to calculate the adsorption and desorption kinetics of the inhibitor on the metal surface [62]. The authors conducted their

study using a kettle test, analogous to the rotating cylinder electrode (RCE) system, to examine the film persistency of a water-soluble inhibitor in continuous treatment. The experimental procedure involved similar steps to those in previous studies, including pre-corrosion, inhibition, and dilution phases. Figure 7 shows an example of their results for persistency experiments in continuous treatment. The adsorption and desorption kinetics for each experimental condition were determined by applying equations derived from the Langmuir isotherm model and fitting them to the empirical data. This analysis was established on the assumption of immediate desorption upon the exchange of inhibited brine with uninhibited brine, thereby neglecting any potential persistency. The study concluded that while continuous inhibition did not demonstrate measurable persistency, the desorption kinetics, in conjunction with the Langmuir isotherm model, could be utilized to estimate the time required for the corrosion rate to return to uninhibited levels. Although the Langmuir isotherm model was proposed as a suitable technique for analyzing continuous corrosion inhibitor (CI) adsorption and desorption behavior, several methodological limitations were identified. Specifically, the kinetic calculations were performed using data from a single CI concentration, precluding the determination of maximum surface coverage. Consequently, the reliability of fitting a solitary data set to the Langmuir isotherm model for comprehensive adsorption and desorption analysis is questionable. Furthermore, the solution exchange procedure, a factor known to significantly influence desorption behavior, was not adequately documented.

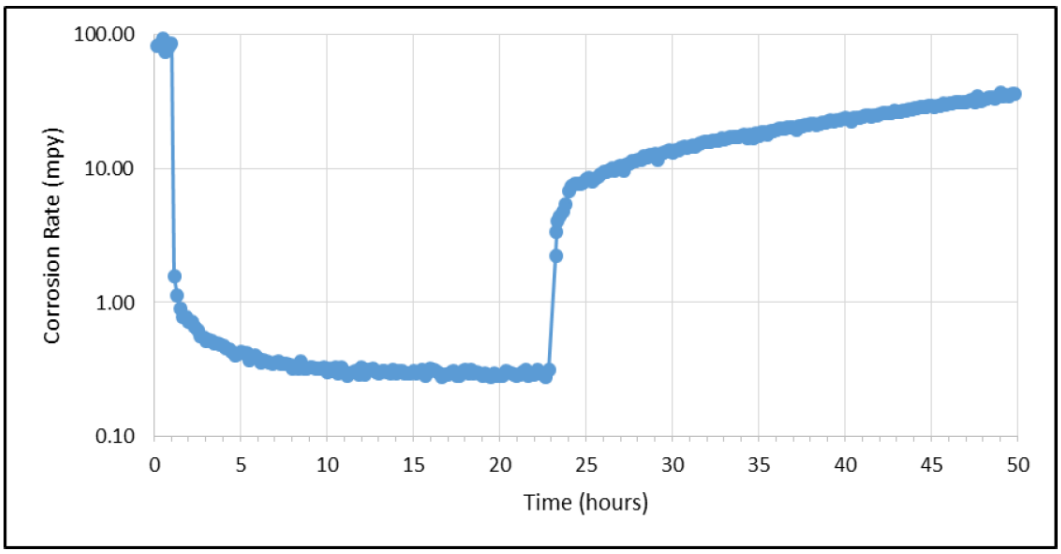

Figure 7. Corrosion rate versus time for persistency experiment (2 hours pre-corrosion, solution exchange after 22 hours) (reprinted with permission from [62]).

In another study again done by Ramachandran, *et al*. [63], inhibitor persistency behavior in continuous treatment was investigated using two different commercial inhibitors. The experimental methodology largely mirrored that of their previous study, with a notable modification in the desorption protocol. Specifically, following inhibitor exposure, the working electrode was transferred to an uninhibited brine solution within a separate container. Corrosion rate analyses, depicted in Figure 8, revealed that both inhibitors exhibited desorption kinetics below 80°C. However, at 80°C, a distinct phenomenon was observed. After a 24-hour inhibition period, followed by transfer to the uninhibited brine, the corrosion rate initially displayed a marginal elevation. Subsequently, the rate gradually converged towards the pre-sample transfer, inhibited value. The authors attributed this observed behavior to the precipitation of iron carbonate and the formation of complexes between the inhibitor molecules and the precipitated species, resulting in the establishment of a persistent protective film. However, the initial

increase in corrosion rate remains unexplained. Furthermore, this methodology, which involves transferring the electrode to the uninhibited environment, may alter the inhibitor film on the surface, potentially affecting the electrochemical behavior. Additionally, there is no control over the inhibitor concentration in the second container, introducing variability that could impact the reliability of the results.

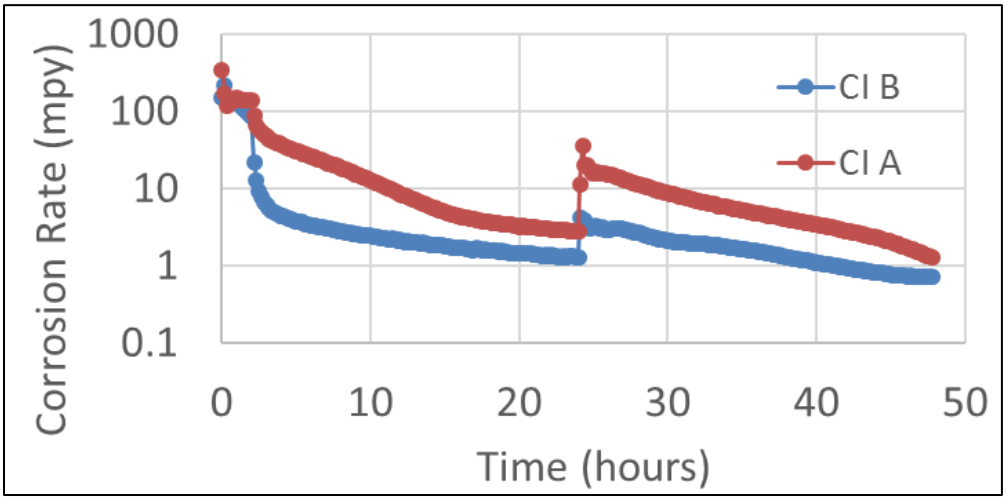

Figure 8. Corrosion rate versus time for persistency experiment (2 hours pre-corrosion, solution exchange after 24 hours) (reprinted with permission from [63]).

As shown above, some efforts, albeit limited, have been published in the literature to study inhibition behavior under continuous treatment conditions. However, the specific phenomenon of inhibitor persistency within such treatments remains comparatively under-investigated in the aforementioned works.

2.5.2 Literature Review on CI Persistency in Batch Treatment

One of the most challenging aspects of batch inhibition studies is developing laboratory methodologies that accurately simulate field applications. The literature

review shows that two primary methods have been employed to study inhibitor film formation. The first method involves immersing the specimen in a neat or diluted inhibitor solution for a defined period, representing the contact time. After this period, the specimen is allowed to drip dry before being transferred into an uninhibited brine, where electrochemical measurements are conducted. This step is often associated with some level of brine renewal [64-67]. This technique is referred to as the "*ex situ* dip and drip" method. The second method involves applying the inhibitor to the specimen within a deoxygenated glass cell, either by using the dip and drip method or a spray nozzle to achieve controlled coverage. Following this, uninhibited brine is introduced into the glass cell without transferring the specimen, with a limited brine renewal [68, 69]. This technique, known as the "*in situ* modified dip and drip" method, offers less control over uniform inhibitor film formation. In one approach, the inhibitor is sprayed onto the specimen, which can lead to incomplete coverage; in the other, the glass cell is completely filled with inhibitor solution, which can result in varying contact times across different areas of the specimen. These two different methodologies aim to replicate the conditions of field applications to better understand the inhibitor film formation and its effectiveness. Table 1 summarizes the differences between these two methodologies for batch inhibition studies:

Table 1. Differences between batch inhibition methodologies.

Parameter	***Ex situ* dip and drip**	***In situ* modified dip and drip**
Inhibitor application	Immerse specimen into a neat or diluted inhibitor in dedicated cell and then transfer to the uninhibited system	Apply inhibitor to the specimen in a deoxygenated environment
Dilution method	Exchange solution at fixed intervals (if any)	Exchange solution at fixed time intervals
Advantage	Easier to implement experimentally	Limits oxygen contamination
Disadvantage	Oxygen contamination No complete removal of inhibitor residual	No complete removal of inhibitor residual Less control on inhibitor film formation

Most published studies have utilized one of the aforementioned methods, with some variations, to investigate batch inhibition persistency. The most relevant studies on batch inhibition persistency are mentioned in this section.

Tan, *et al.*, used electrochemical impedance spectroscopy (EIS) to study formation and destruction of an imidazoline-type inhibitor film on mild steel [70]. The authors used an electrochemical cell containing a rotating sample (working electrode) and a counter and reference electrode using a 3 wt.% NaCl aqueous electrolyte containing 50 ppm inhibitor sparged with CO_2. Impedance measurements were done in solutions containing the full inhibitor dosage, diluted inhibitor, and no inhibitor by transferring the specimen similar to the dip and drip method. The authors concluded that the inhibitor formed a multi-layer structure, rather than just a monolayer on the surface, using Nyquist and Bode plots. The authors proposed a model wherein the initial adsorbed layer exhibits chemisorption characteristics, indicative of strong interactions between inhibitor

molecules and the metal substrate, while subsequent layers are associated with intermolecular interactions within the inhibitor film. Furthermore, the authors speculated that shear stress could induce film degradation by performing the same experiments but with RCE rotation. However, it is crucial to note that these interpretations are predicated upon the fitting of EIS data to an equivalent circuit model, where distinct resistive elements are used to represent inhibitor layers. Several methodological limitations warrant critical consideration. The transfer of the electrode to uninhibited brine introduces potential alterations to surface characteristics, risks oxygen contamination, and precludes precise control over inhibitor concentration due to dilution. These limitations collectively compromise the robustness and reliability of the study's conclusions.

Tan, *et al.*, also used electrochemical noise analysis (ENA) in two different studies to investigate the formation and removal of the corrosion inhibitor film on the metal surface [64, 65]. In one set of experiments, the steel specimen was first put into an electrolyte having 25 ppm of an imidazoline-type commercial inhibitor for several hours, it was then quickly transferred into the inhibitor-free brine. In another set of experiments, the steel specimen was first filmed in a more concentrated inhibitor solution, rinsed with the aqueous electrolyte, and then quickly transferred into inhibitor-free brine (this is known as the “dip-and-drip” method). In both experimental methodologies, Electrochemical Noise Analysis (ENA) was used to monitor film formation and removal from the metal surface, based on the assumption that the measured noise resistance correlates with linear polarization resistance (LPR). The authors hypothesized that ENA is preferable for continuous monitoring of inhibitor film behavior due to its rapid

response to system perturbations compared to Electrochemical Impedance Spectroscopy (EIS). However, this technique is complex and requires extensive data analysis, often involving significant uncertainties compared to the more straightforward LPR technique.

In general Tan, *et al.*, postulated that EIS and ENA can be used to monitor the inhibitor film persistency during formation and removal of the adsorbed film. They also suggested that these electrochemical techniques can address the nature of inhibitor adsorption and desorption. However, the studies conducted by Tan, *et al*., exhibit two primary methodological concerns. Firstly, the employed persistency testing protocol, involving the transfer of the electrode to an inhibitor-free solution, introduces a significant risk of oxygen contamination. This contamination can substantially alter surface characteristics and disrupt the adsorption process. Secondly, the conclusions drawn regarding inhibitor multilayer formation rely heavily on the fitting of experimental electrochemical impedance spectroscopy (EIS) data to an equivalent circuit. It is well-established that multiple equivalent circuits can often adequately fit the same EIS data, thereby rendering this approach insufficient to definitively substantiate the proposed multilayer formation mechanism. In addition, these two techniques involve extensive mathematical modeling and are highly complex.

Achour, *et al.*, [68], introduced an updated experimental system to study inhibitor film persistency in simulated batch treatment. The main goal in designing this system was to avoid exposing the working electrode to air which was the main problem in the standard dip-and-drip method (dipping the sample into the inhibited solution and then moving it to another solution without inhibitor). He successfully showed that this

methodology could simulate batch treatment and could be used to investigate the effect of different parameters on inhibitor persistency. The schematic of their experimental setup is shown in Figure 9. The system comprises two different RCE glass cells for testing the inhibitor film persistency simultaneously in different conditions. Two pumps can fill the cells with uninhibited brine and can also be used to flush the inhibited solution when needed. Several specimens can be mounted inside the cell for weight loss and LPR measurements. The inhibitor was applied by immersing the corrosion coupons in neat or diluted corrosion inhibitor placed in a test tube inside the cell. The inhibited solution was diluted with fresh uninhibited brine pumped through the cell every 24 hours. Figure 10 also shows the LPR results for this study. This shows the expected trend of the corrosion rate. After film was “stripped off” with uninhibited brine, corrosion rate remained stable for about 5 days and then started to increase to the blank value, indicating that the persistency of the tested inhibitor with this method was 5 days and corrosion rate results analysis can properly show the desorption of the inhibitor. This investigation advanced the methodology for assessing inhibitor persistency in batch treatments, notably mitigating oxygen contamination during inhibitor film formation. However, the dilution protocol, designed to eliminate residual inhibitor, was implemented at discrete 24-hour intervals, which may not have provided sufficient removal of all inhibitor residuals.

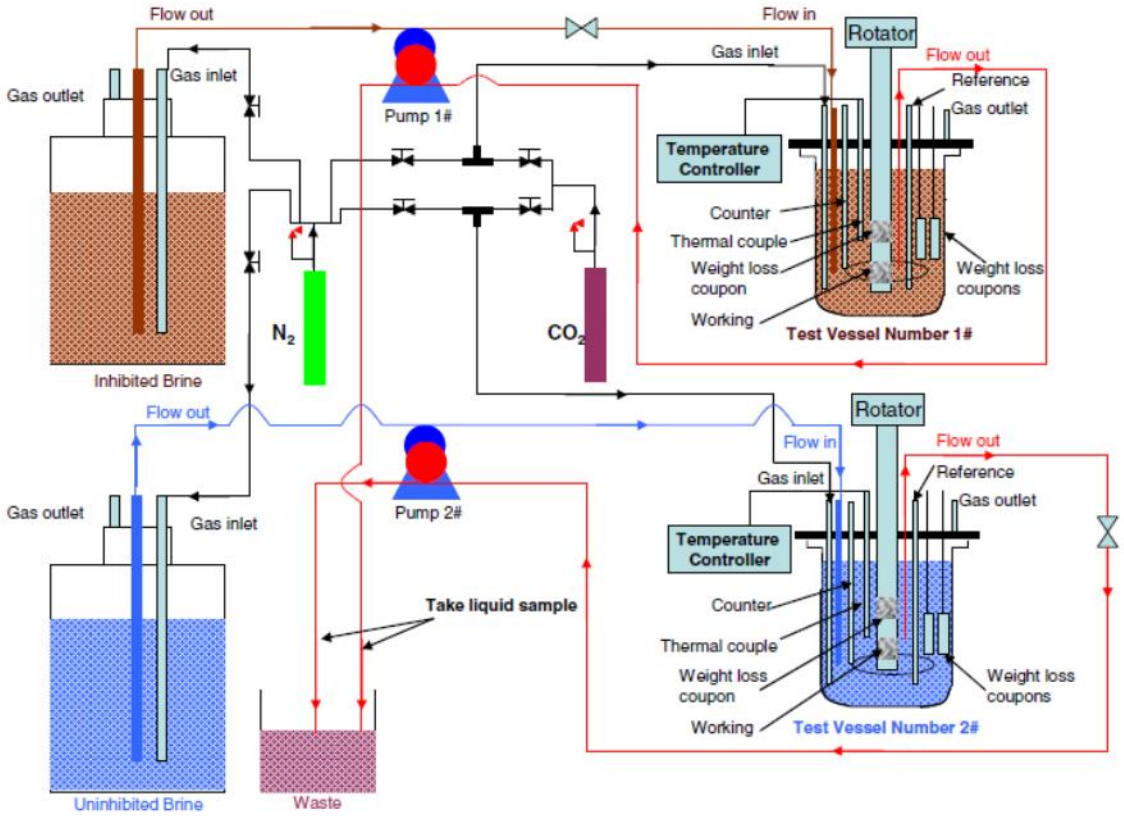

Figure 9. Schematic of batch corrosion inhibitor persistency test system (reprinted with permission from [68]).

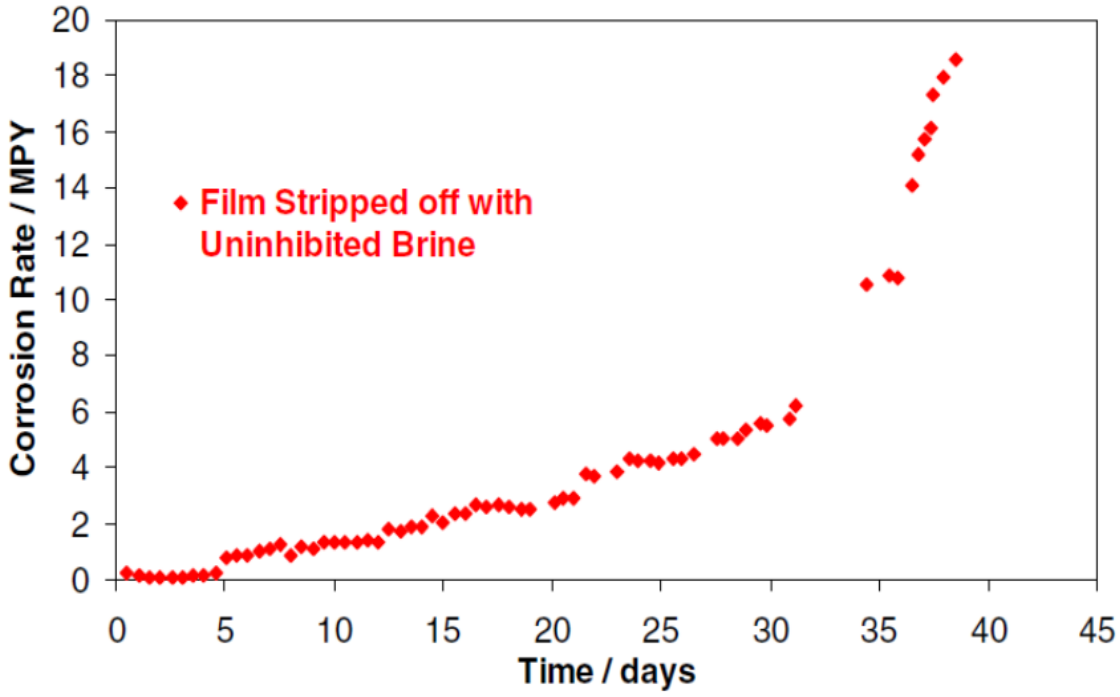

Figure 10. Inhibitor persistency: Corrosion rate vs. time for the RCE after introducing uninhibited brine. The Solution was replenished every 24 hours (reprinted with permission from [68]).

2.6 Parameters Affecting Persistency

Numerous studies have explored corrosion inhibitor (CI) persistency in both continuous and batch treatment methods. These investigations indicate that various parameters can influence CI persistency as well as the adsorption and desorption kinetics of inhibitor molecules. Some of these parameters apply to both batch and continuous treatments, while others are specific to a particular treatment method. This section discusses these parameters in detail.

Inhibitor type: Inhibitor molecules can generally be classified into two categories: water-soluble and oil-soluble inhibitors. Typically, water-soluble corrosion inhibitors (CIs) are employed in continuous treatment processes. These molecules are injected into

the aqueous phase, where they subsequently adsorb onto the metal surface to provide protection. Conversely, oil-soluble CIs are often utilized in batch inhibition methods. The oil-soluble nature of these inhibitors ensures that, once adsorbed onto the metal surface, they do not easily desorb into the aqueous phase. This characteristic enhances their persistency and prolongs their protectiveness. Organic corrosion inhibitor molecules are typically composed of a polar head group and a non-polar tail, conferring amphiphilic character. The head group of an inhibitor molecule imparts hydrophilic properties, facilitating its adsorption onto the metal surface. Conversely, the tail group confers hydrophobic characteristics, enhancing the molecule's ability to form a protective barrier against corrosive agents carried within the aqueous phase. The efficacy and type of the inhibitor are influenced by the nature of these groups as well as whether the inhibitor is a single molecule or a blend of different molecules, each with distinct properties. This combination of structural features determines the inhibitor's overall performance and suitability for specific applications [71-73]. Several studies exist in the literature on the type of the inhibitor typically selected in both treatments, although the formulation of commercial inhibitors is a trade secret. For example, de Marco, *et al*., demonstrated that the type of inhibitor head group is a key factor in determining adsorption behavior, which in turn leads to differences in persistency [66].

Contact time: The contact time is generally the duration of application of the neat inhibitor to the metal surface. The notion of contact time only makes sense for batch treatment where it is defined as the time duration that the inhibitor slug is in contact with the metal surface [74]. It is reported that in batch application, the contact time is in a

range of 10 to 15 seconds depending on the CI slug volume and the velocity [73-76]. In continuous treatment, the notion of contact time does not really apply since the inhibitor is applied continuously and is in contact with the steel surface, at the recommend dosage, for as long as the CI injection is maintained. Yet, as a limiting case, it can be defined as the time duration for which the CI concentration is maintained constant. This definition holds some meaning for the present experimental study, as explained in the relevant chapter in this dissertation.

Presence of hydrocarbon: One of the parameters that can affect inhibitor behavior and persistency is the presence of a hydrocarbon phase or the formation of an emulsion adjacent within an aqueous phase. Previous studies showed that both partitioning and oil wetting of the specimen can affect the corrosion rate and surface characteristics [77-81]. He, *et al*., investigated the effects of intermittent oil wetting and inhibitor emulsion using a model oil for tetradecyltetrahydropyrimidinium (THP-C14) [79]. Their study demonstrated that inhibitor molecules generally increase the hydrophobicity of the metal surface, leading to a greater affinity for hydrocarbon molecules to adsorb onto the surface. This adsorption facilitates interactions with the inhibitor layer, potentially enhancing corrosion inhibition by forming a protective barrier. Consequently, the presence of hydrocarbons can significantly influence the persistency and effectiveness of the inhibitor by altering its adsorption and interaction behaviors.

Pre-corrosion of the surface: Pre-corrosion of metal surfaces has been identified as a key factor influencing inhibitor performance. Various studies have demonstrated that corrosion products, such as Fe_3C, reduce inhibitor efficiency, particularly in CO_2

corrosion environments [82-88]. Fe_3C is part of the steel microstructure and is cathodic compared to the main ferrite phase. Corrosion of steel exposes the residual Fe_3C structure on the metal, which appears as a porous layer. The extent of this effect is influenced by the steel microstructure and the presence of carbides therein, albeit with conflicting findings reported in the literature. Ren, *et al*., investigated the impact of Fe_3C on two different steel microstructures under continuous inhibitor (CI) exposure, employing a methodology that allowed for better control over iron carbide formation with and without inhibitor at varying concentrations [48]. Their study revealed that the formation of Fe_3C on the metal surface increases the available cathodic area, thereby reducing CI efficiency and increasing the SSC. However, while higher inhibitor dosages could partially compensate for this negative effect, galvanic corrosion continued to undermine inhibitor performance. Although the authors hypothesized that corrosion product formation may act as an external diffusion barrier to hydrogen ions, the effect of these products on inhibitor adsorption and desorption kinetics was not examined. Therefore, pre-corrosion, which leads to the formation of corrosion products on the surface can significantly influence inhibitor adsorption kinetics and persistency.

Temperature: The effect of temperature on corrosion inhibitor adsorption/desorption and persistency behavior is a complex interplay, as demonstrated by several studies. Both Ding and Desimone found that while both adsorption and desorption rates increase with temperature; the effect on desorption is more pronounced, leading to a decrease in inhibitor persistency [89, 90]. Ameer and El-Nabey further support this observation, with Ameer noting a decrease in protection efficiency at higher

temperatures, and El-Nabey finding that a higher concentration of inhibitor was necessary to maintain high protection efficiency over a range of temperatures [91, 92]. These findings collectively underscore the importance of considering temperature in the design and application of corrosion inhibitors.

Flow velocity: Generally, the impact of high velocity in single-phase flow on inhibitor film layers can be assessed through the analysis of shear stress and mass transfer effects [93-96]. In turbulent flow, the mass transfer coefficient typically rises, which correlates with increased corrosion rates in uninhibited conditions [95]. Inhibitor film thickness typically falls within the nanometer range, which is considerably smaller than the boundary layer thickness, turbulent flow does not significantly affect the inhibitor film layer in single-phase flow [95, 97].

Chapter 3: Gaps and Motivation, Objectives, Methodologies, Hypothesis, and Dissertation Outline

3.1 Gaps and Motivation

Analysis of literature associated with corrosion inhibitor (CI) persistency in continuous and batch treatments reveals two significant research gaps: methodological and mechanistic.

Methodological limitations: Existing methodologies employed to evaluate CI persistency in both continuous and batch treatments exhibit limitations in replicating authentic field conditions. Specifically, the validity of the assessment of inhibitor effectiveness in the absence of bulk inhibitor, which defines persistency, is frequently compromised. Current experimental protocols, such as partial dilution and limited solution exchange, often fail to achieve complete inhibitor removal, leading to the presence of residual inhibitor that confounds persistency measurements. Furthermore, a lack of direct, real-time monitoring of CI concentration through systematic sampling precludes accurate control and quantification of the inhibitor environment. The practice of transferring electrodes to uninhibited brine, while intended to simulate field conditions, introduces artifacts, including potential oxygen contamination, thereby distorting the corrosion and inhibition mechanisms during the persistency phase.

Mechanistic deficiencies: a comprehensive mechanistic understanding of CI persistency remains absent from the current literature for both continuous and batch treatments, partly because the exact composition of inhibitor packages is a trade secret, and therefore unknown. Yet, some degree of commonality between the behaviors of all

CIs can be expected. While studies have investigated and modeled inhibitor adsorption/desorption kinetics in continuous treatment scenarios [43, 48, 62, 98], the specific parameters governing the prolonged retention of inhibitors on the surface, or the mechanisms delaying desorption, have not been elucidated. Similarly, the underlying mechanisms governing CI persistency in batch inhibition are unexplored. This represents a critical knowledge gap, as the identification of key parameters influencing persistency, coupled with the development of predictive models for batch treatment, is essential for optimizing corrosion inhibition strategies. Such mechanistic insights are currently lacking in the existing body of research.

Addressing the identified research gaps, the primary motivation of this study is threefold: first, to develop refined methodologies that more accurately simulate both continuous and batch inhibition treatments; second, to conduct comprehensive parametric studies to elucidate the factors influencing CI persistency; and third, to propose and validate mechanistic models describing CI persistency in both treatment modalities.

3.2 Objectives

The study described in this dissertation aims to enhance understanding of the mechanisms underlying inhibitor persistency by considering both continuous and batch inhibition treatment methods. The ultimate intent is to develop protocols for assessing inhibitor persistency in both treatment scenarios. To achieve this goal, several specific objectives are outlined at the outset of the study:

1. Develop an experimental system setup and methodology capable of more accurately assessing corrosion inhibitor persistency behavior under simulated field conditions, employing both continuous and batch treatment approaches.
2. Conduct parametric studies to identify the key controlling parameters influencing corrosion inhibitor behavior and to gain insights into the mechanisms underlying inhibitor persistency in both treatment methods.
3. Develop a mechanistic model describing corrosion inhibitor adsorption/desorption dynamics in continuous treatment, while exploring fundamental mechanisms underlying inhibitor persistency in batch treatment.

3.3 Hypotheses

To achieve the primary objectives of this research, the following hypotheses are tested:

- *In continuous treatment, the behavior of corrosion inhibitors (CIs) during the persistency phase is fundamentally governed by desorption kinetics. These kinetics, in turn, are affected by CI characteristics, temperature, and surface properties. Consequently, the prediction of CI desorption/persistency behavior necessitates a comprehensive investigation of the parameters influencing respective rate constants. It is hypothesized that lower temperatures and increased surface roughness, resulting from longer pre-corrosion time, retard the desorption of corrosion inhibitors (CIs), thereby enhancing their persistency.*

- *In contrast to continuous treatment, the persistency behavior of batch inhibition deviates from a strict adherence to adsorption/desorption mechanisms. In batch treatment, oil-soluble corrosion inhibitors (CIs) are applied, forming a substantially thicker film on the metal surface compared to continuous treatment. Consequently, the persistency is primarily governed by the dissolution rate of the film into the aqueous phase, followed by desorption kinetics. It is hypothesized that enhancing the oil-solubility of the inhibitor package will extend the persistency duration of the batch corrosion inhibitor (CI). Furthermore, supplementary parameters influencing the inhibitor dissolution rate, including viscosity and the presence of hydrocarbons, are anticipated to affect the observed persistency behavior.*

Two distinct methodologies and corresponding system setups are employed to evaluate the first hypothesis regarding CI inhibitor adsorption/desorption behavior under continuous treatment conditions. The Langmuir isotherm model is then utilized to analyze and interpret the experimental data. In addition, the influence of various parameters on the adsorption/desorption process is investigated.

For the second hypothesis focusing on batch inhibition persistency, the initial objective is to develop a methodology and system setup that closely mimicked real-world batch inhibition practices. A commercially available CI is subsequently used to verify this methodology. Building upon this foundation, the study explores the effects of different model compound CIs, presence of hydrocarbon, and solvent characteristics.

Ultimately, a mechanistic model for batch inhibition persistency behavior is proposed, incorporating both the dissolution rate and desorption kinetics.

3.4 Common Experimental Methodology

As one of the main objectives is the development of experimental methodologies to simulate continuous and batch treatment, it is essential to describe the main basic experimental procedures, measurement methods and analytical techniques that are used in this work. The experimental procedures specific to each inhibition treatment are described in full detail in each corresponding chapter.

All experiments were conducted under sweet corrosion conditions, simulating purely CO_2 corrosion in the absence of oxygen. Atmospheric pressure and a 1 wt.% NaCl solution prepared with deionized (DI) water were employed for each test environment. The main experimental configuration was in a 2-Liter glass cell with a three-electrode system setup (Figure 11). The glass cell contained the main working electrode, which was an RCE, a reference electrode (Ag/AgCl) and a counter electrode made of platinum coated titanium mesh. During each experiment, electrochemical measurements were performed at 20-minute intervals following this sequence:

1- Open Circuit Potential (OCP): Determination of the electrode potential after reaching steady state condition.
2- Electrochemical Impedance Spectroscopy (EIS): Quantification of the solution resistance.
3- Linear Polarization Resistance (LPR): Calculation of the corrosion rate.

The charge transfer resistance (R_{CT} in ohms/cm^2) was determined by subtracting the solution resistance (R_s in ohms/cm^2) from the polarization resistance (R_P in ohms/cm^2) measurement. Subsequently, the Stern-Geary equation was employed to calculate the corrosion current density (i_{corr} in A/cm^2) [99]:

$$i_{corr} = \frac{\beta_a \beta_c}{2.3 R_{CT}(\beta_a + \beta_c)} \tag{12}$$

where β_a and β_c are anodic and cathodic Tafel slope and were taken as 0.12 V/decade, as determined from baseline experiments. Since the presence of the corrosion inhibitor does not alter the fundamental corrosion mechanism, these values were assumed constant across all experiments. R_{CT} is charge transfer resistance (ohms/cm^2). Equation below (Faraday's law) was used to calculate corrosion rate (mm/year) from the corrosion current:

$$CR = \frac{i_{corr} M}{nF\rho} \tag{13}$$

where CR is corrosion rate (cm/s), M is atomic mass (g/mol), n is the number of electrons of the corrosion reaction, F is Faraday's constant (C/mol), and ρ is sample density (g/cm^3). *CR* was then converted to mm/year.

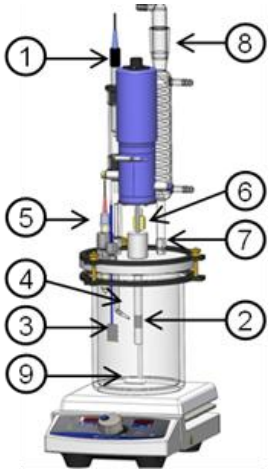

1. Reference Electrode (RE – Saturated Ag / AgCl)
2. Rotating Cylinder Electrode (WE)
3. Counter Electrode (CE)
4. Luggin Capillary
5. pH Meter
6. Thermocouple
7. Gas in
8. Gas out
9. Magnetic Stirrer

Figure 11. Glass-cell setup schematic.

3.4.1 Sample Preparation

A rotating cylinder electrode (RCE) fabricated from X65 carbon steel (C 0.035 wt.%, Cr 0.24 wt.%, Mn 1.42 wt.%, Mo 0.09 wt.% with the balance Fe) was employed for all experiments. Prior to each experiment, the sample underwent a meticulous surface preparation procedure. This involved sequential polishing with 180, 400, and 600 grit abrasive paper, followed by immersion in an ultrasonic bath for 3 minutes. Subsequently, the sample was rinsed with isopropanol and thoroughly dried using CO_2 gas.

3.4.2 Inhibitor Preparation

The quaternary ammonium and phosphate ester model compound inhibitors used in this study were synthesized by Dr. David Young for previous studies [43, 48]. In all experiments with model compound inhibitors, depending on the targeted CI concentration in the glass cell, a select mass of the solid inhibitor was put in a vial containing 3 mL of the appropriate solvent (isopropanol, methanol, etc.). The vial was then sparged with CO_2 for 10 minutes to eliminate any oxygen contamination. The

validity of this duration was previously verified experimentally by measuring oxygen concentration using an Orbisphere^{TM} oxygen meter. Following this, 2 mL of the prepared inhibitor solution was injected into the glass cell. This injection was done with a long needle that pierced a septum on the cell's lid, ensuring the inhibitor remained entirely within the bulk solution.

3.4.3 Inhibitor Concentration Measurements

Liquid samples are collected at each stage of the experiment to measure inhibitor concentration, ensuring the accuracy of the calculated values and verifying the initial concentration prior to dilution. This process is carried out using UV-visible (UV-vis) spectroscopy. In UV-vis spectroscopy, light within the ultraviolet or visible range is passed through a sample, and absorbance occurs to varying degrees, depending on the wavelength (λ). By measuring the absorbance of the samples at a wavelength corresponding to an absorbance peak and applying Beer's law, the concentration of the target species in the unknown samples can be directly determined if the molecule in question has appropriate spectrophotometric characteristics. Beer's law, as shown in equation (14), relates absorbance to concentration. A calibration curve must first be constructed using liquid samples with known inhibitor concentrations. Subsequently, the concentration of an unknown sample can be calculated by measuring its absorbance and applying Beer's law. However, it is important to note that UV-vis spectroscopy is only applicable to certain model compound inhibitors, specifically organic molecules that exhibit absorbance within the UV-Vis range. Consequently, this procedure was

successful in this study only when quaternary ammonium model compound inhibitors were used.

$$A = \epsilon l C \tag{14}$$

where A is the absorbance measured with UV-vis spectroscopy, ϵ is the absorption coefficient ($M^{-1}.cm^{-1}$), l is the path length of the cuvette (cm) and C is sample concentration (M). Figure 12 shows the calibration curve which was developed for the model inhibitor used in this study (BDA-C14) by measuring absorbance of the known samples for repeated times. Thus, BDA-C14 concentration was measured by determining the absorbance of the unknown sample and using the equation below:

$$CI\ concentration\ (ppm) = \frac{Absorbance}{0.0325} \tag{15}$$

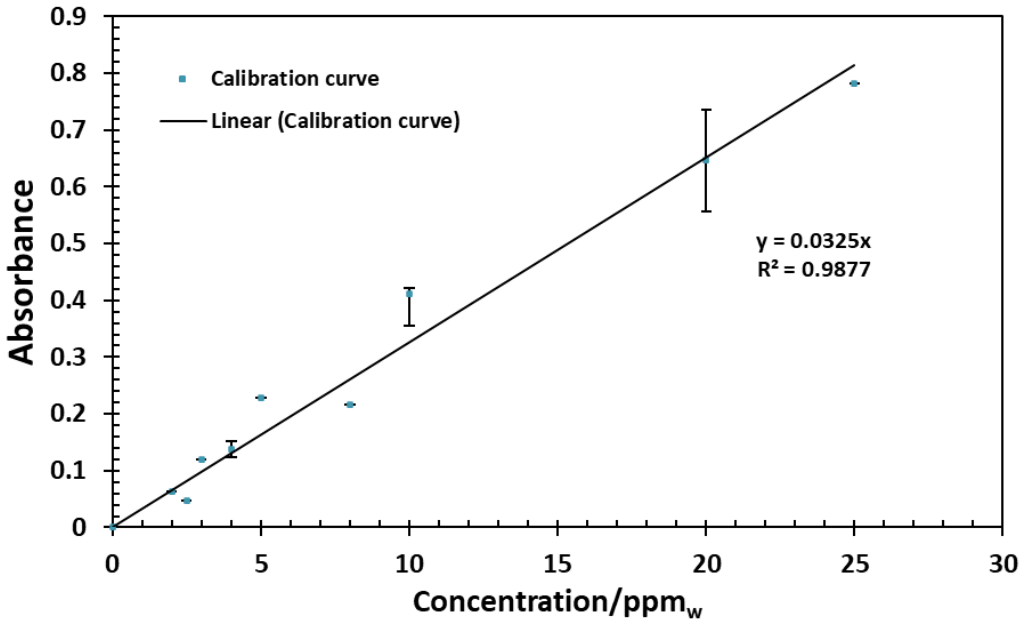

Figure 12. BDA-C14 UV-vis calibration curve.

3.5 Dissertation Outline

This study is primarily divided into two main sections: corrosion inhibitor (CI) persistency in continuous treatment and batch treatment. Each treatment method is further subdivided into two phases.

For continuous treatment, preliminary experiments were conducted using a system setup with a limited volume of uninhibited brine for dilution. Thus, the first phase of the continuous treatment involved replicating persistency experiments reported in the literature (using a stepwise dilution method) and identifying challenges specific to this study. After identifying these challenges, an improved system setup was implemented, incorporating a larger uninhibited brine container to enable continuous dilution of the solution.

For batch treatment, the first phase focused on evaluating CI persistency using a commercial batch inhibitor. To gain deeper insight into the underlying mechanisms of inhibitor persistency in batch treatment, the second phase involved studying CI persistency using various model compound inhibitors and solvents with a known inhibitor package.

Finally, conclusions regarding CI persistency in both continuous and batch treatments are presented, along with recommendations for future research directions.

Chapter 4: Study of Continuous Treatment Persistency Using Partial Dilution Methodology

4.1 Introduction

The initial phase of this dissertation research focused on assessing inhibitor persistency by examining the adsorption and desorption behavior of the inhibitor under simulated continuous injection conditions. This phase of the experimental work was conducted using a stepwise (*i.e.*, non-continuous) dilution method to simulate the interruption of corrosion inhibitor injection by using an experimental glass cell experimental configuration. This chapter discusses preliminary experiments aimed at replicating the general methodology found in the literature for evaluating CI persistency in continuous treatment, while also identifying the limitations and challenges associated with this approach to propose improvements. Benzyldimethyltetradecylammonium chloride (BDA-C14), a model compound inhibitor featuring a quaternary ammonium hydrophilic head group and a 14-carbon hydrophobic tail (Figure 1), was selected for testing; the product being synthesized and characterized in-house, exhibiting >99% purity [100]. The selection of this model inhibitor was driven by the widespread use of quaternary ammonium-based inhibitors in corrosion inhibition studies, as they are commonly found in commercial field formulations. Moreover, previous research has demonstrated the high efficacy of quaternary ammonium-type inhibitors for continuous injection in CO_2 environments, further supporting their relevance for this study. [43, 100, 101].

The following experimental sequence was implemented to investigate the adsorption and desorption behavior of the chosen inhibitor:

1. Baseline Corrosion Tests: Initial baseline corrosion rate measurements were established to provide a reference point for subsequent evaluations.
2. Inhibitor Adsorption Studies: The inhibitor adsorption behavior was then examined at various concentration levels to identify the surface saturation concentration.
3. Persistency Experiments: Following the adsorption studies, persistency experiments were conducted as the primary focus of this study. These involved a stepwise dilution of the inhibited solution to assess the inhibitor desorption characteristics and its impact on persistency.
4. Parametric Studies: To gain a more comprehensive understanding of inhibitor persistency, additional parametric studies were performed. These studies explored the influence of initial inhibitor concentration, pre-corrosion time, and temperature on persistency behavior.

4.2 Experimental Procedure and Test Matrix

The experimental procedure consisted of three distinct steps, aligned with previous studies on CI persistency in the current literature [61-63, 102]. These steps included pre-corrosion, an inhibition step (representing adsorption), and a subsequent dilution step (representing desorption), enabling a comprehensive evaluation of the inhibitor's adsorption and desorption behaviors under continuous treatment conditions. To conduct the experiments, a three-cell system configuration was employed (Figure 13),

comprising a main working glass cell, a reservoir for storing fresh uninhibited brine, and a collection cell for the effluent solution.

During the dilution stage, the inhibited solution was removed from the main working cell in a stepwise manner. This involved initially opening the outlet valve and draining 200 mL of the solution into the effluent container. Subsequently, the outlet valve was closed, and the inlet valve for the uninhibited brine cell was opened. Through this inlet, 200 mL of fresh uninhibited brine was introduced to replenish the working solution. This process of draining and replenishing was repeated until the uninhibited brine reservoir was depleted. The final inhibitor concentration could then be determined by considering the initial concentration and the total number of dilution cycles performed. Although this dilution method has limitations in completely removing all inhibitor residues, as mentioned previously, this system setup was employed to obtain preliminary results and investigate the persistency of the inhibitor when its concentration in the bulk phase significantly decreases.

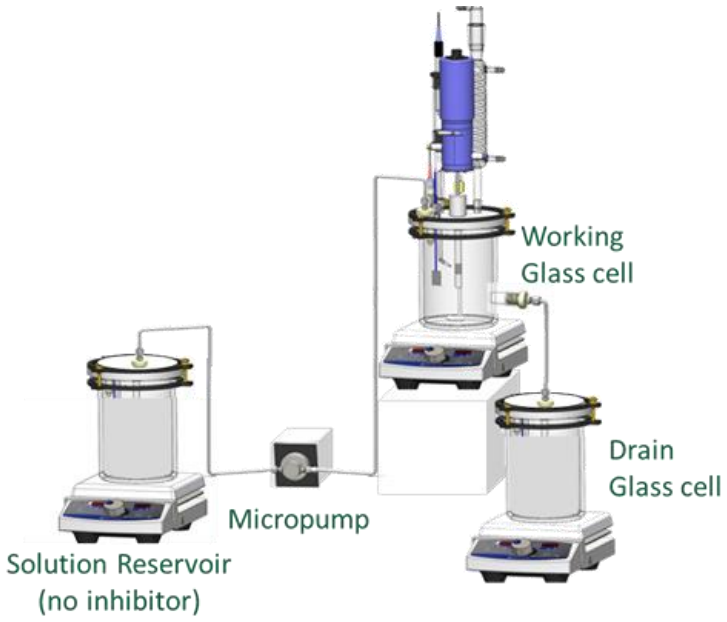

Figure 13. Schematic of the setup that was used for continuous treatment studies with partial dilution.

The variable parameters in this chapter include the initial concentration of the corrosion inhibitor, temperature, and pre-corrosion time. The rationale behind varying each of these parameters is discussed in detail in the following sections.

Table 2. Experimental matrix for continuous treatment experiments.

Parameter	**Conditions**
Working electrode	API 5L X65 (0.035 wt.%C)
Solution	1 wt.% NaCl
Sparge gas	CO_2
Total pressure	1 bar
Rotational speed	1000 RPM
Temperature	(30 °C, 40 °C) ± 1 °C
pH	4.0 ± 0.1
CI model compound	Quaternary ammonium type (BDA-C14)
CI concentration	50 ppm_w (SSC), 25 ppm_w, and 15 ppm_w
Measurement methods	OCP, LPR, EIS
Contact time (time before dilution)	When stable corrosion rate achieved (9 hours)
Initial inhibitor concentration	Variable
Presence of hydrocarbon	No – brine only
Pre-corrosion before CI injection	15 minutes, 2 hours

4.3 Results and Discussion

This section provides an outline of the experimental results. The persistency of BDA-C14 was tested at two different temperatures. First, BDA-C14 inhibition was examined at 30 °C to verify repeatability and inhibition efficiency. Then, CI persistency was investigated using stepwise dilution, where different CI concentrations and shorter

pre-corrosion times were tested to determine their effects on inhibitor desorption behavior. The research questions underlying each of these parametric studies are explained in their respective sections. Finally, BDA-C14 persistency was tested at 40°C to achieve a faster desorption rate and to compare BDA-C14 adsorption/desorption behavior at different temperatures. The Langmuir isotherm model was used to calculate adsorption and desorption kinetics at the tested temperatures, and initial modeling results are presented in this chapter.

4.3.1 Assessment of BDA-C14 Persistency at 30℃

As mentioned above, the first set of experiments with BDA-C14 were conducted at 30°C. Baseline inhibition and persistency tests were first performed. Subsequently, the effects of shorter pre-corrosion times were investigated. Finally, different initial CI concentrations were tested to examine their influence on desorption behavior.

4.3.1.1 Baseline Inhibition and Persistency of BDA-C14 at 30°C. The initial phase of investigating BDA-C14 persistency involved ensuring comparability and verification of the inhibition results with prior research conducted at ICMT on the same inhibitor. Therefore, temperature, pre-corrosion duration, and initial inhibitor concentration were chosen to be 30°C, 2 hours, and 50 ppm_w, respectively [100, 101, 103]. Previous studies by Moradighadi *et al.*, [100] indicated that under these conditions, the BDA-C14 surface saturation concentration lies between 25 and 50 ppm_w, while the critical micelle concentration (CMC, the highest concentration without micelle formation) is 53 ppm_w. Figure 14 presents the corrosion rate versus time data under the same experimental conditions as those in the work of Moradighadi, *et al*., to evaluate the

reproducibility of surface saturation concentration for BDA-C14. The results are consistent with the findings reported by Moradighadi, *et al*., indicating that the surface saturation concentration for BDA-C14 under these conditions ranges between 20 and 50 ppm_w.

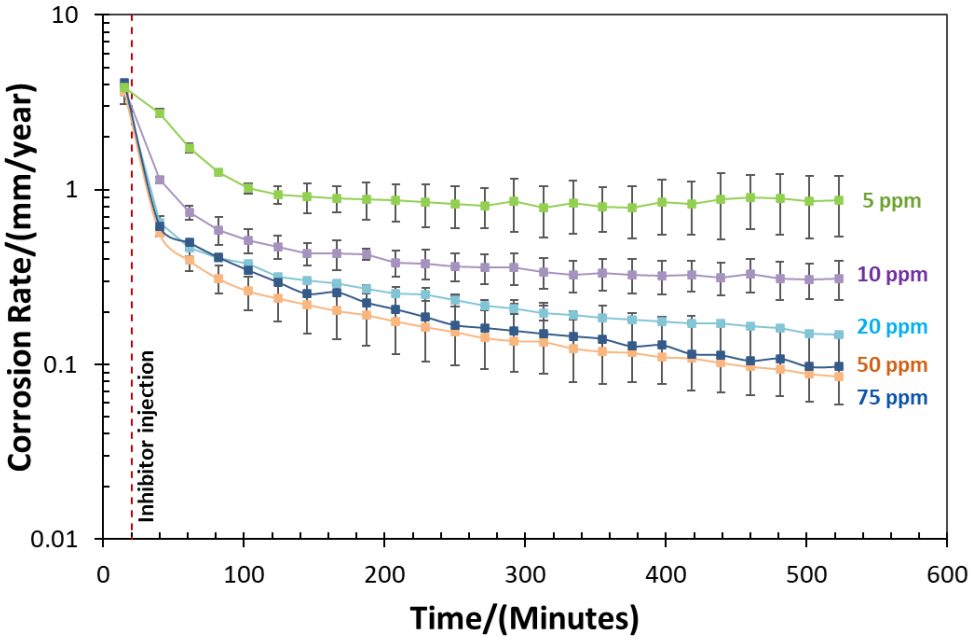

Figure 14. BDA-C14 inhibition at 30°C with different initial inhibitor concentrations (15 minutes pre-corrosion, 0.97 bar pCO_2, X65 RCE, 1000 rpm, BDA-C14 inhibitor).

Multiple pre-corrosion and inhibition experiments were conducted with a fixed 2-hour pre-corrosion period followed by inhibitor injection to track the corrosion rate and the time required for stabilization. The resulting corrosion rate versus time data for these repeated experiments with 50 ppm_w concentration are presented in Figure 15, demonstrating a trend similar to that reported by Moradighadi, *et al*. The observed consistency in the results for these initial steps (pre-corrosion and inhibition) serves as a

positive validation for each subsequent experiment. These findings allowed for the investigation to proceed further to the third stage: dilution experiments (persistency).

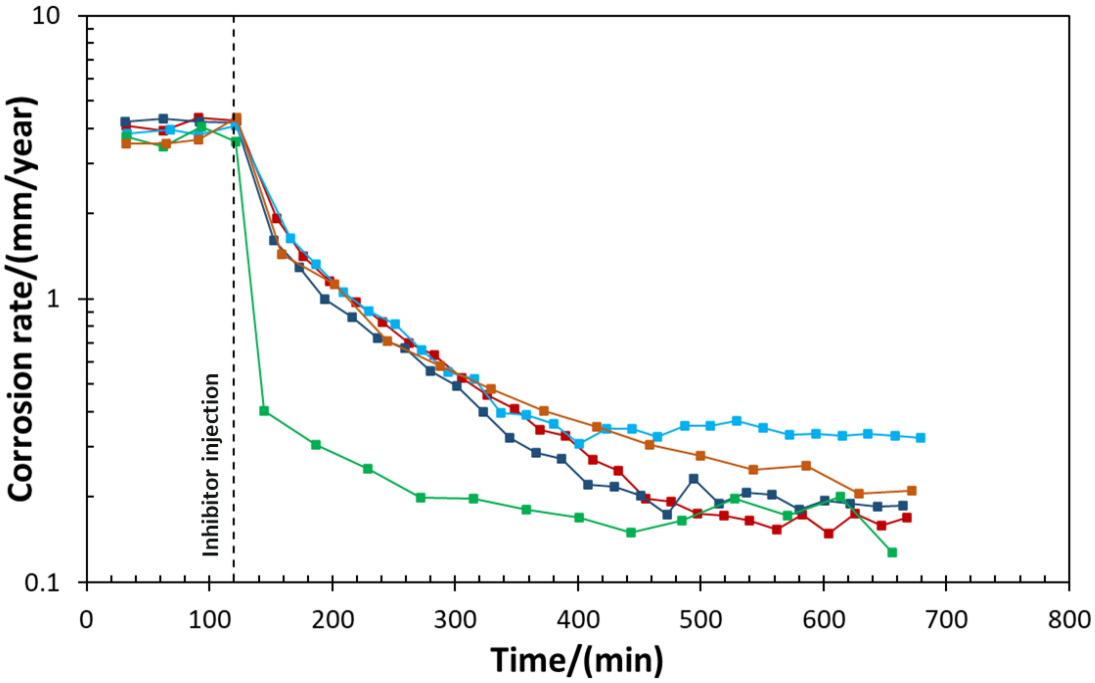

Figure 15. Inhibitor efficiency characterization - Corrosion rate *vs.* time for repeated baseline experiments (30°C, 0.97 bar pCO_2, X65 RCE, 1000 rpm, BDA-C14 inhibitor).

Two repeats of experiments were completed to evaluate the persistency of the quaternary ammonium type inhibitor BDA-C14 with 50 ppm_w concentration (which is the surface saturation concentration of BDA-C14 at 30°C). The common experimental conditions were: 1 wt.% NaCl solution, 1000 rpm, pH=4.00, and T=30°C. In the first repeat, 50 ppm_w of inhibitor was added after 2 hours of pre-corrosion. After 9 hours, the corrosion rate stabilized, and the solution was diluted to 10.5 ppm_w using the aforementioned stepwise dilution method. The experiment was run for another 12 hours.

However, there was no change in corrosion rate, which remained very low, so the solution was diluted again from 10.5 ppm_w to 2.2 ppm_w. The corrosion remained unchanged even after approximately 300 hours of exposure. In addition, different liquid samples were taken during every stage of the experiment to verify the inhibitor concentration in the solution using UV-vis spectroscopy. The high persistency level was somehow unexpected as the model inhibitor was never designed to be persistent and should have desorbed immediately after the dilution step. Nonetheless, different modifications, such as increasing the rotational speed and introducing hydrocarbons, were implemented to investigate the effect of these parameter on inhibitor desorption. A higher rotational speed was hypothesized to facilitate desorption by increasing shear stress forces. Additionally, the partitioning of CI molecules into the hydrocarbon phase was anticipated to accelerate the desorption rate. However, these efforts did not result in any significant changes in the corrosion rate. Figure 16 and Figure 17 show the results for this experiment with all the changes that were applied to help inhibitor desorption. To validate the results, the experiment was repeated and Figure 18 shows the comparison between these two repeats for 60 hours test duration.

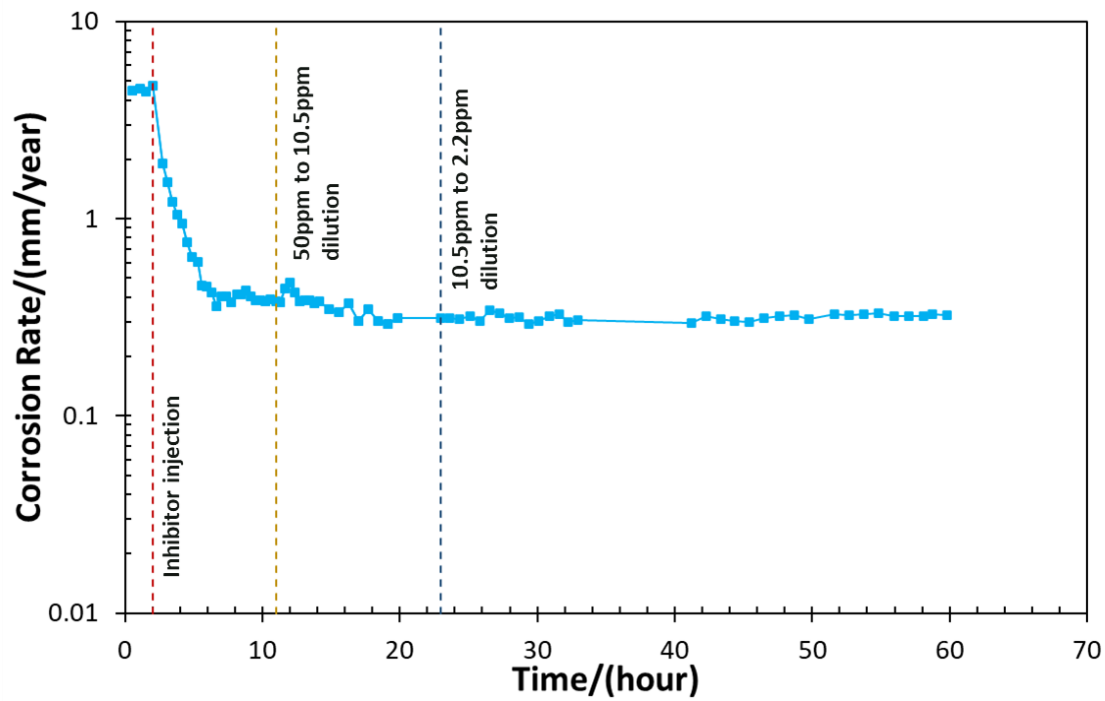

Figure 16. Inhibitor persistency evaluation - Corrosion rate *vs.* time, showing the three steps of the persistency experiment, first 60 hours (30°C, 0.97 bar pCO_2, X65 RCE, 1000 rpm, BDA-C14 inhibitor).

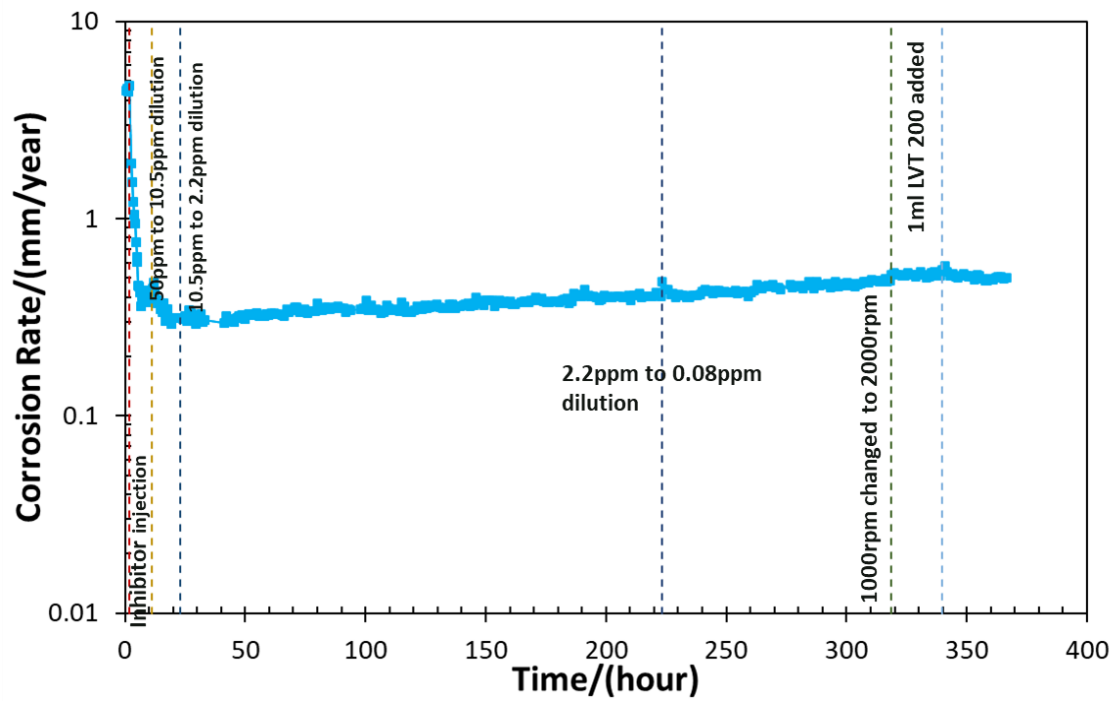

Figure 17. Effect of changing conditions (exposure time, increase in rotation speed, addition of LVT) on persistency - Corrosion rate *vs.* time, showing the three steps of the persistency experiment (30°C, 0.97 bar pCO_2, X65 RCE, 1000 rpm, BDA-C14 inhibitor).

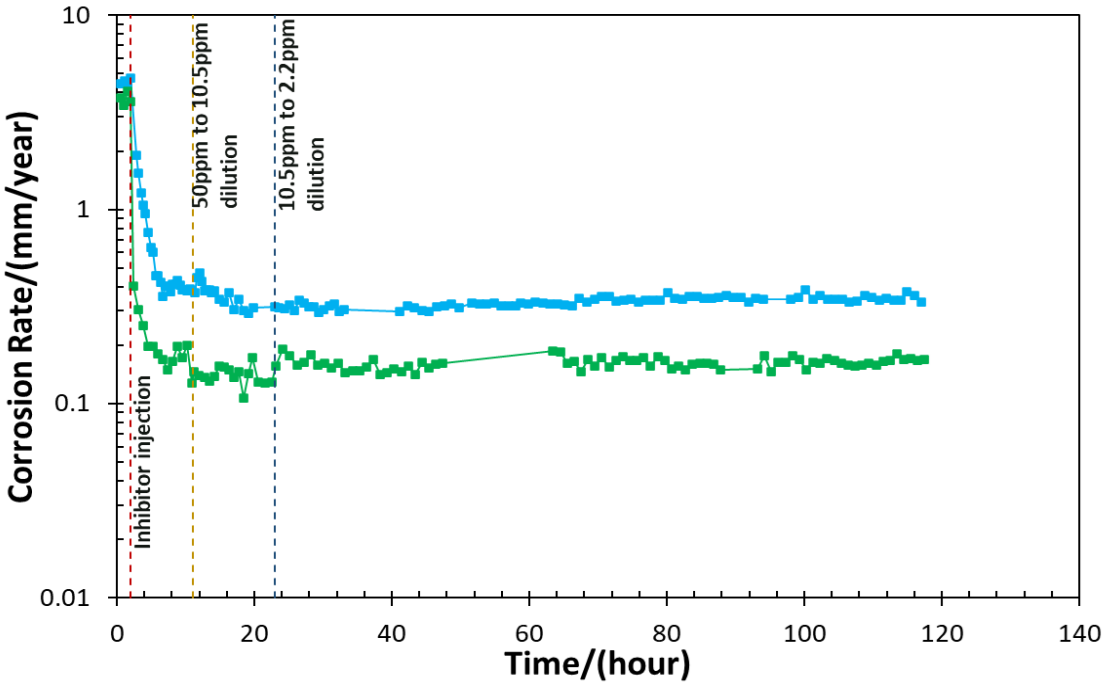

Figure 18. Repeatability of persistency results - Corrosion rate *vs.* time for persistency experiment with two stepwise dilutions (30°C, 0.97 bar pCO_2, X65 RCE, 1000 rpm, BDA-C14 inhibitor).

The results of this preliminary set of experiments were somewhat unexpected, as they indicated that BDA-C14 exhibited acceptable persistency under the test conditions and did not strictly adhere to adsorption/desorption isotherms, *i.e.*, desorption did not commence immediately upon dilution. It is important to note that the high persistency of BDA-C14 may have been influenced by the experimental procedure, particularly the incomplete removal of inhibitor molecules from the glass cell. Further experimentation was conducted to identify more severe conditions under which BDA-C14 loses or fails to exhibit persistency, as the primary objective of this study is to investigate the effects of controlling parameters on inhibitor persistency. Consequently, additional exploratory work was performed to determine conditions that promote desorption. Several

experiments were performed by modifying the pre-corrosion time and initial inhibitor concentration.

4.3.1.2 BDA-C14 Persistency Experiments With Shorter Pre-Corrosion at Surface Saturation Concentration. Additional experiments were conducted with a reduced pre-corrosion time of 15 minutes to investigate the impact of pre-corrosion duration on inhibitor persistency. The hypothesis was that a shorter pre-corrosion period would result in less surface roughness, and that inhibitor adsorption and desorption kinetics would be faster on a polished surface compared to a corroded surface, which contains more active sites requiring CI coverage. Figure 19 presents the results of two replicate experiments comparing 15-minute and 2-hour pre-corrosion times. In these new experiments, the specimen was corroded for 15 minutes before injection of 50 ppm_w BDA-C14 inhibitor. After 9 hours contact time (same contact time as for the 2 hours pre-corrosion experiment), CI dilution in the working glass cell solution was performed from 50 ppm_w to 6 ± 1 ppm_w.

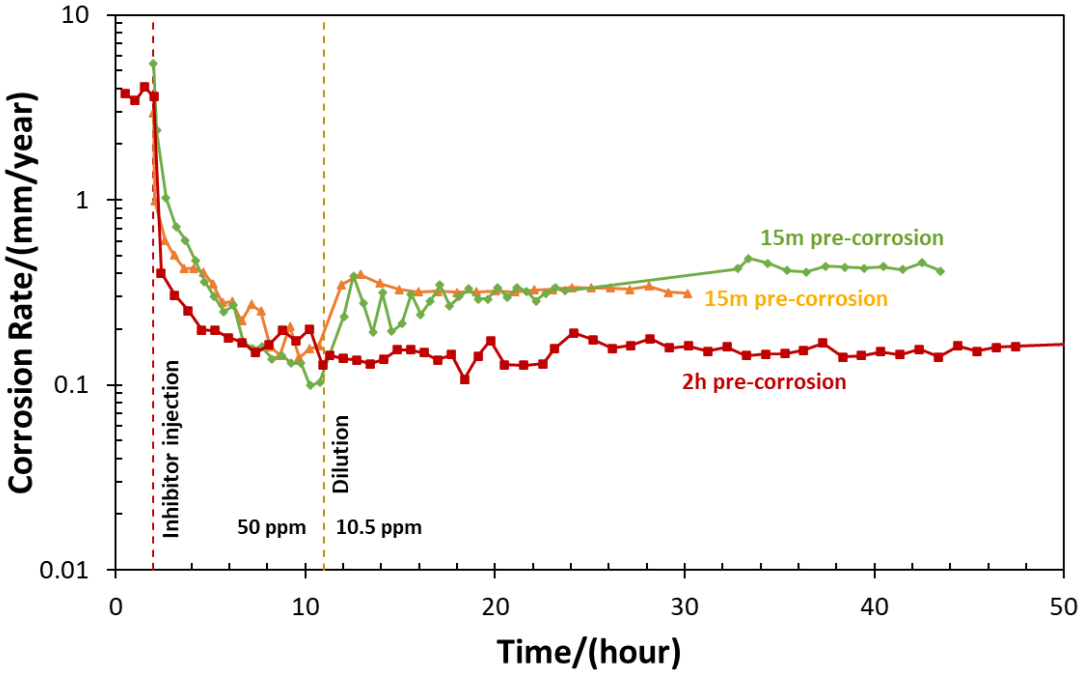

Figure 19. Corrosion rate *vs.* time for persistency experiment, comparison between experiments with 15 minutes pre-corrosion (orange and the green) and 2 hours pre corrosion (red). Results for 2 repeats with 15 minutes pre-corrosion were shifted in time axis to be more directly comparable with experiment with 2 hours pre-corrosion. (30°C, 0.97 bar pCO_2, X65 RCE, 1000 rpm, BDA-C14 inhibitor).

To facilitate comparison, the results of the 15-minute pre-corrosion experiments were shifted along the x-axis to align with those of the 2-hour pre-corrosion experiment within the same figure. In the 15-minute pre-corrosion experiments, 50 ppm_w BDA-C14 inhibitor was introduced after the pre-corrosion period. Subsequently, the solution was diluted using the established method following a 9-hour contact time. Each experiment was monitored until a new stable corrosion rate was achieved. A comparison of the 15-minute and 2-hour pre-corrosion experiments reveals no statistically significant difference in the uninhibited and inhibited corrosion rates before dilution. However, an increase of 0.2 mm/year in corrosion rates after dilution was observed in experiments

with a shorter pre-corrosion period. Although this finding is consistent with the hypothesis that adsorption and desorption kinetics are faster on an even surface, the increase in corrosion rate was not statistically significant.

Overall, the inhibitor persistency was retained for at least 40 hours. A decrease in pre-corrosion time slightly increased the stable corrosion rate after dilution. However, none of these results indicated a collapse in inhibitor persistency, as this model compound water-soluble inhibitor (BDA-C14) was expected to follow adsorption/desorption kinetics and was not expected to maintain strong inhibition after dilution.

At this point, two key questions arose to explain the unexpected inhibitor desorption behavior after dilution:

1. Could persistency be linked to initial corrosion inhibitor concentration?

2. Are corrosion inhibitor measurements after dilution accurate enough?

Additional experiments were performed with different corrosion inhibitor initial concentrations to answer these questions. The corrosivity of the diluted solution was also tested for validation of corrosion inhibitor content.

4.3.1.3 Impact of Initial CI Concentration on Inhibitor Persistency. In these experiments, various initial concentrations of the corrosion inhibitor were introduced into the solution after a 15-minute pre-corrosion period. The subsequent contact time was consistent with previous experiments. The solution was then diluted to a final concentration of 6 ± 1 ppm_w of BDA-C14 inhibitor. A freshly polished specimen was immersed in the solution post-dilution to assess the corrosivity of the diluted solution,

and to validate the concentration measurements. Figure 20 shows the results for these experiments which can be analyzed from two perspectives. One perspective is the impact of initial inhibitor concentration on persistency. Lower initial inhibitor concentrations of 25 and 15 ppm_w led to a higher stable inhibited corrosion rate of 0.3 mm/year compared to the higher concentration of 50 ppm_w, which resulted in a rate of 0.1 mm/year during the inhibition step. However, inhibitor persistency remained for at least 15 hours, indicating that the initial concentration had a minimal effect on persistency under the tested conditions. The corrosion rate after dilution to 6 ± 1 ppm_w for all three experiments with different initial CI concentrations was consistently between 0.2 and 0.4 mm/year. This indicates that inhibitor desorption behavior after dilution depends on the inhibitor concentration in the bulk solution rather than the initial CI concentration. Regarding the accuracy of inhibitor concentration measurements, the final inhibitor concentration after dilution was measured at 6 ± 1 ppm_w using UV-vis spectroscopy. A freshly polished X65 specimen immersed in the diluted solution exhibited corrosion rates similar to those observed in uninhibited solutions, confirming the low inhibitor concentration. However, a direct comparison with corrosion experiments using an initial injection of 6 ppm_w BDA-C14 had not been conducted. This behavior of the corrosion rate after dilution, when compared to that of a freshly polished sample in the same solution with the same CI concentration, indicates that inhibitor adsorption and desorption kinetics for the surface after dilution behave differently than on a freshly polished sample. Although this deviates from expectations, a possible explanation is that the inhibitor desorption behavior differs

after dilution due to variations in surface characteristics, which are not the same as those of a freshly polished surface.

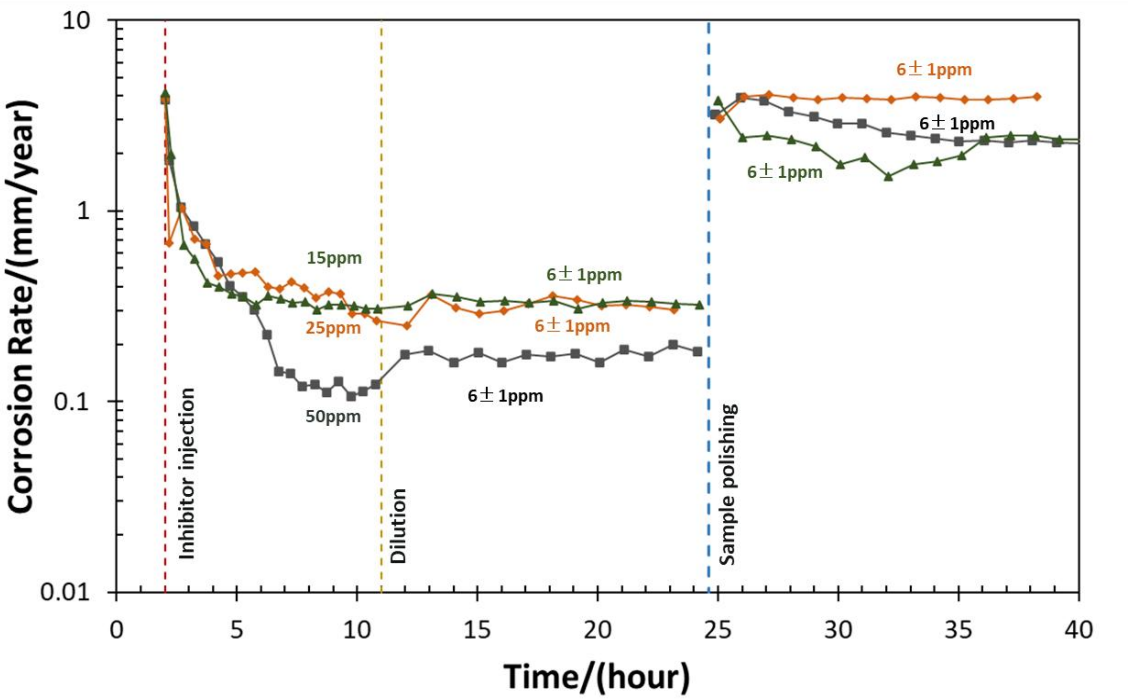

Figure 20. Corrosion rate versus time for 50, 25 and 15 ppm_w initial concentration. (30°C, 0.97 bar pCO_2, X65 RCE, 1000 rpm, BDA-C14 inhibitor).

4.3.2 Assessment of BDA-C14 Persistency at 40°C

Due to the high persistency of BDA-C14 at 30°C with partial dilution, more experiments were done at higher temperatures and 15 minutes pre-corrosion as higher desorption rates of the inhibitor were expected. The challenge was that while higher temperatures tend to promote desorption, they can also significantly diminish corrosion inhibition efficiency. Therefore, the first step was to verify whether the inhibitor provided acceptable inhibition at the tested temperature. Separate experiments were conducted at

60°C, 50°C, and 40°C, revealing that BDA-C14 exhibited no inhibition at 60°C and 50°C but remained effective at 40°C. Following this, inhibition experiments with varying initial concentrations were performed to determine the surface saturation concentration of BDA-C14 at 40°C. The results, presented in Figure 21, suggest that the surface saturation concentration for BDA-C14 at this temperature falls within the range of 25 to 50 ppm_w, as no further enhancement in inhibition was observed when the initial inhibitor concentration exceeded 50 ppm_w.

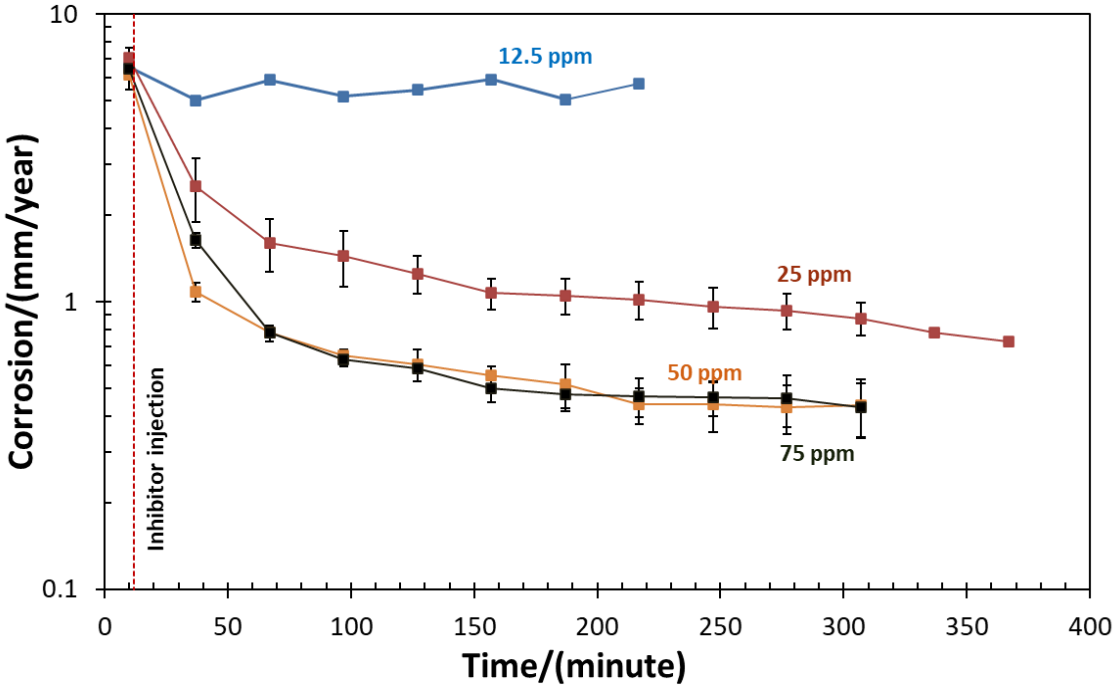

Figure 21. BDA-C14 inhibition at 40°C with different initial inhibitor concentrations (15 minutes pre-corrosion, 0.97 bar pCO_2, X65 RCE, 1000 rpm, BDA-C14 inhibitor).

Following the determination of the surface saturation concentration for BDA-C14 at 40°C, an investigation was conducted to assess inhibitor persistency at this

temperature. Dilution was done using the established stepwise dilution protocol previously utilized in experiments at 30°C while the corrosion rate was monitored over time. The results, depicted in Figure 22, reveal an initial increase in corrosion rate of approximately 0.5 mm/year immediately after the dilution. While a gradual and continued increase was observed thereafter, the data suggest that BDA-C14 retained a degree of inhibition efficiency and persistency. Notably, the corrosion rate increased by 0.5 mm/year at 40 °C, which exceeds the 0.2 mm/year increase observed at 30 °C right after the dilution. This observation is consistent with the expectation that desorption kinetics are accelerated at higher temperatures. The inhibition and persistency may be attributed to the presence of inhibitor residuals within the system, even after dilution, potentially influencing inhibitor desorption kinetics and the ultimate corrosion rate. Consequently, it is hypothesized that further experimentation is warranted to specifically elucidate the inhibitor desorption and persistency behavior under conditions where the bulk inhibitor concentration is effectively negligible.

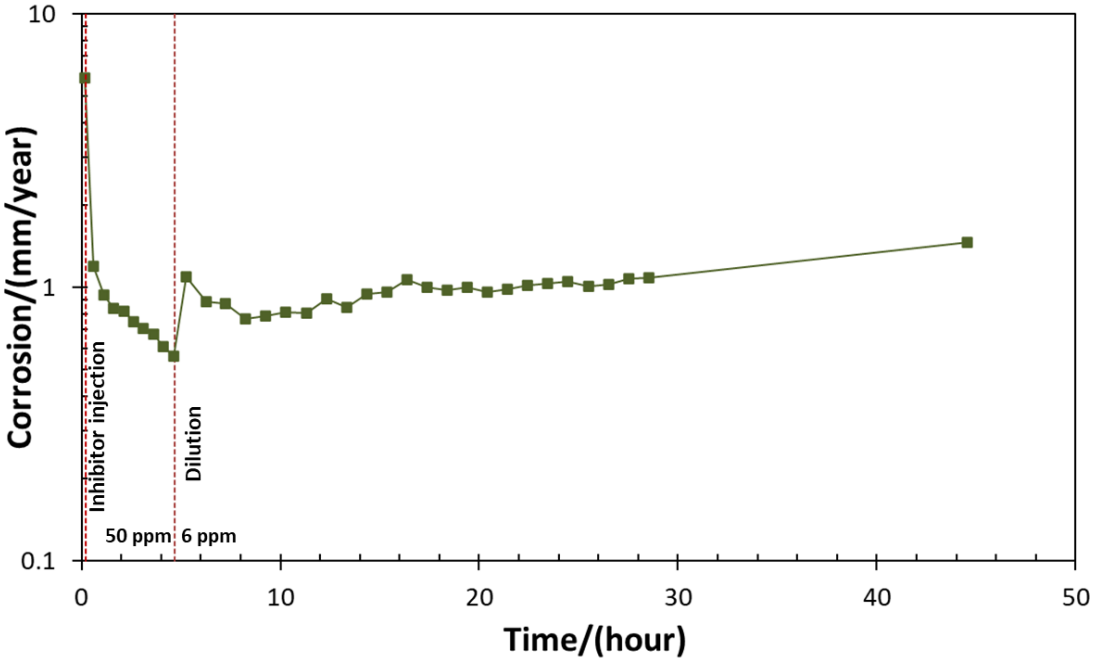

Figure 22. Corrosion rate versus time for the persistency experiment with only one dilution (40°C, 0.97 bar pCO_2, X65 RCE, 1000 rpm, BDA-C14 inhibitor).

Additional experiments were conducted at 40°C with an initial inhibitor concentration of 50 ppm_w to investigate the persistency behavior of BDA-C14 under further dilution steps, addressing the aforementioned hypothesis. Figure 23 presents the results of this persistency experiment with multiple dilutions for different experimental durations. In this experiment, the specimen was pre-corroded for 15 minutes before the introduction of 50 ppm_w BDA-C14. The corrosion rate stabilized after approximately 4.5 hours. Subsequently, the solution was partially diluted via the established stepwise dilution method. After flushing the inhibited solution with 5 L of uninhibited brine, the dilution was stopped, and the corrosion rate was monitored using linear polarization resistance (LPR) measurements. Three additional sequential dilutions, each separated by varied time intervals, were performed. This was done to progressively decrease the bulk

inhibitor concentration to a negligible level, thereby enabling a more accurate examination of inhibitor desorption behavior during the persistency phase. The results indicate a slight increase in the corrosion rate after dilution, with a significant initial change observed immediately following each dilution. This is consistent with the expectation that desorption of the inhibitor is faster at 40°C compared to 30°C. Successive dilution steps resulted in a progressively more pronounced increase in the corrosion rate. This observation suggests that continuous decrease of the corrosion inhibitor (CI) concentration through multiple dilutions significantly affects inhibitor persistency, particularly as the bulk CI concentration approaches negligible levels. In other words, these results indicate that accurate assessment of inhibitor persistency requires minimizing residual CI in the bulk solution.

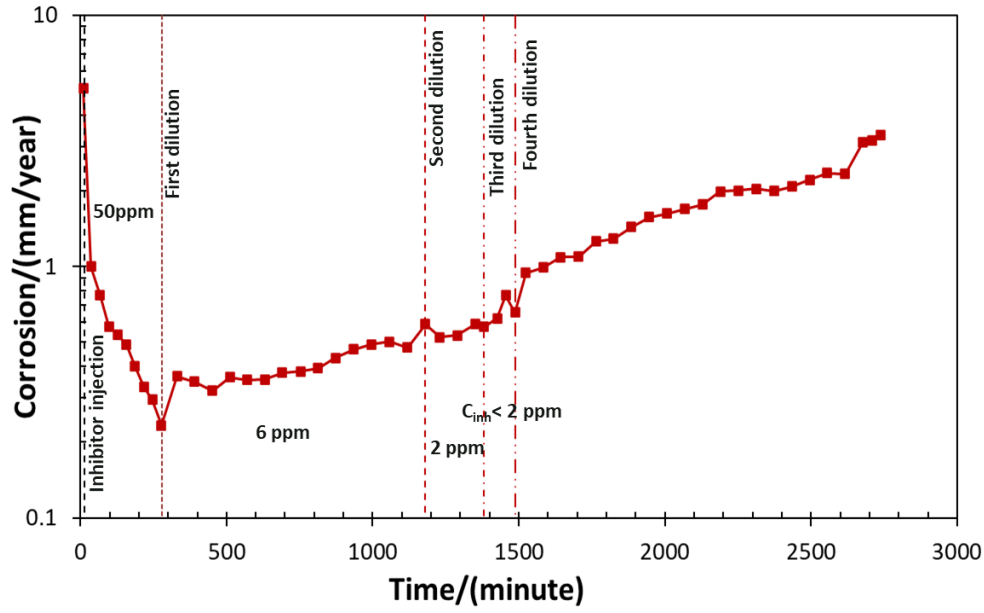

Figure 23. Corrosion rate versus time for first persistency experiment. (40°C, 0.97 bar pCO_2, X65 RCE, 1000 rpm, BDA-C14 inhibitor).

To further elucidate the underlying mechanisms of inhibitor persistency, a replicate experiment was performed, incorporating potentiodynamic sweeps at critical stages. Specifically, potentiodynamic sweeps were conducted at three distinct points: prior to the second dilution, prior to the third dilution, and at the end of the experiment. Notably, a rapid increase in corrosion rate was observed immediately following each sweep, suggesting accelerated inhibitor desorption in response to the abrupt reduction in CI concentration. The anodic and cathodic sweeps obtained during this experiment are presented in Figure 24. It is important to note that performing potentiodynamic sweeps can significantly alter the surface characteristics of the steel specimen. Therefore, it is generally recommended to terminate the experiment following the completion of the sweeps. However, in this particular case, the experiment was continued. Notably, there was no indication of inhibitor desorption during polarization, as the LPR measurements from two separate experiments—one including sweeps and the other without—were found to be very similar. Figure 25 presents the corrosion rate as a function of time for the experiment, which included two dilution events and potentiodynamic sweeps conducted during the testing period. The results show similar behavior to the experiment without polarization sweeps, as shown in Figure 24.

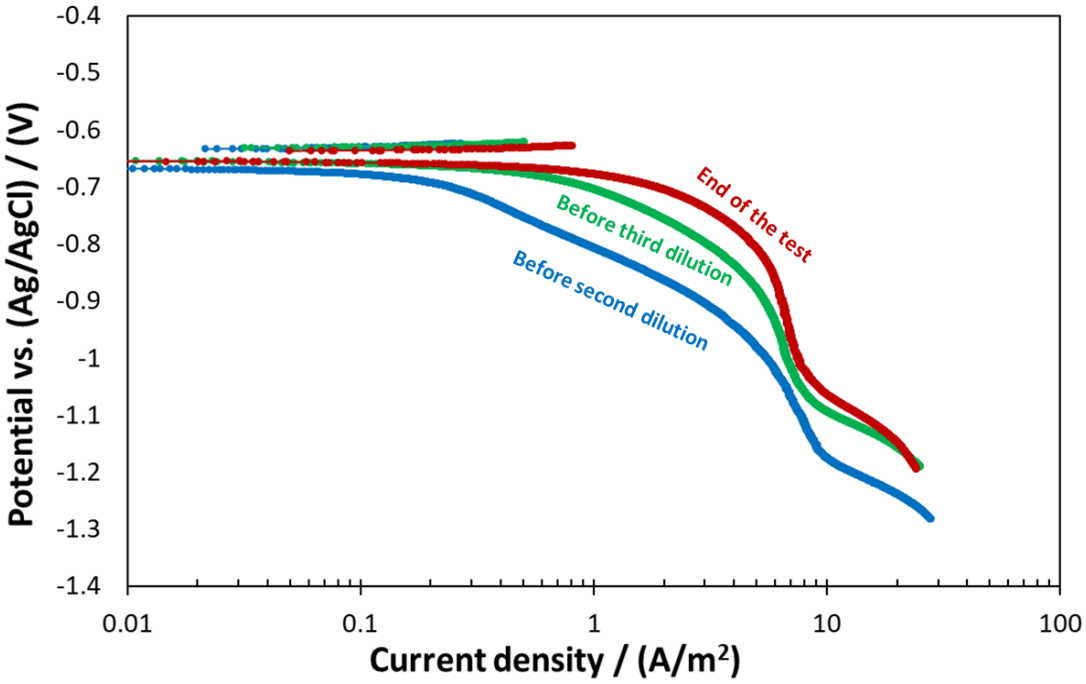

Figure 24. Potentiodynamic sweeps for persistency experiment. (40°C, 0.97 bar pCO_2, X65 RCE, 1000 rpm, BDA-C14 inhibitor).

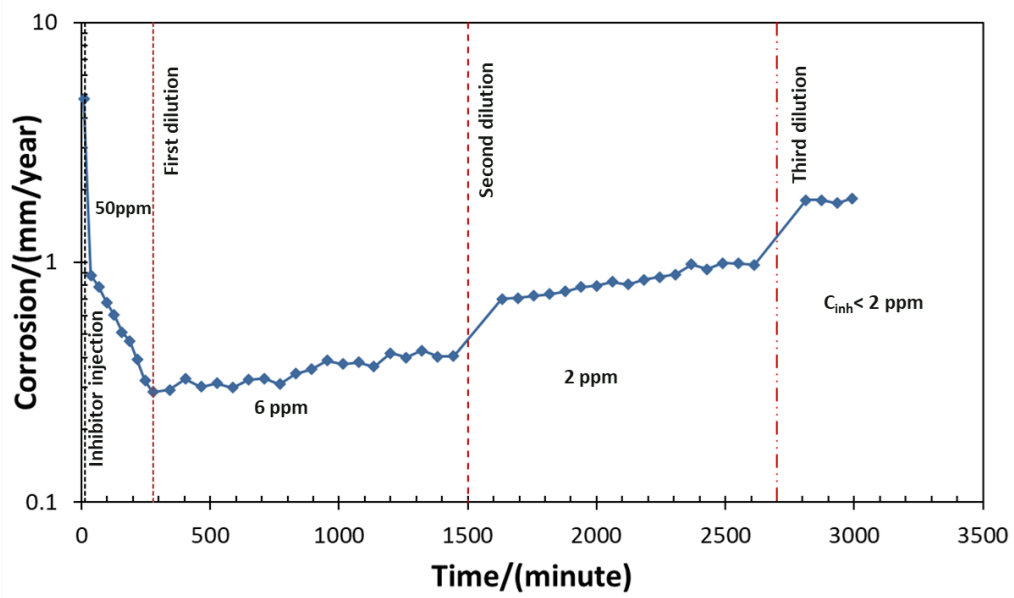

Figure 25. Corrosion rate versus time for the persistency experiment with two dilution events and potentiodynamic sweeps conducted during the test (40°C, 0.97 bar pCO_2, X65 RCE, 1000 rpm, BDA-C14 inhibitor).

Previous studies have demonstrated that polarization sweeps exhibit retardation in the presence of surface-adsorbed inhibitors, reflecting a decrease in corrosion reaction rates. Specifically, for model compound inhibitors, this retardation manifests as a reduction in the charge transfer rate without altering the limiting current observed in cathodic sweeps [43, 104-106]. Consequently, the polarization sweeps in this study displayed the anticipated mechanistic behavior: the charge transfer rate decreased with increasing inhibitor concentration.

4.3.3 Modeling BDA-C14 Inhibitor Adsorption/Desorption Behavior Using Langmuir Isotherm Model With Partial Dilution

As mentioned in section 2.3.3, the Langmuir isotherm model can be used to model inhibitor adsorption/desorption behavior, if the assumption behind this model can

be verified. This model expresses the change in surface coverage with regards to time, as shown in equation (6). This equation can be utilized to determine the adsorption and desorption kinetic constants of the inhibitor.

1- Adsorption behavior

By solving the equation (6) for surface coverage (θ), and considering $\theta = 0$ at $t = 0$ for the boundary conditions, an explicit function of θ with respect to time can be obtained:

$$\theta(t) = \left(\frac{K_{AD}C_{inh}}{1+K_{AD}C_{inh}}\right)\left(1 - e^{-(k_A C_{inh}+k_D)t}\right) \quad (16)$$

where θ is surface coverage factor, K_{AD} is equilibrium constant (M^{-1}), k_A is adsorption kinetic constant ($\mathrm{M}^{-1}.\mathrm{s}^{-1}$), k_D is desorption kinetic constant (s^{-1}), C_{inh} is inhibitor concentration (M), and *t* is time (s). This equation can be fitted to the experimental data to determine values of kinetic constants for BDA-C14 (by using least squares regression method). Figure 26 and Figure 27 show the results of equation (16) fitted to the experimental data at 30°C and 40°C. Using this equation fitted to experimental values, adsorption/desorption kinetic constants were calculated as shown in Table 3.

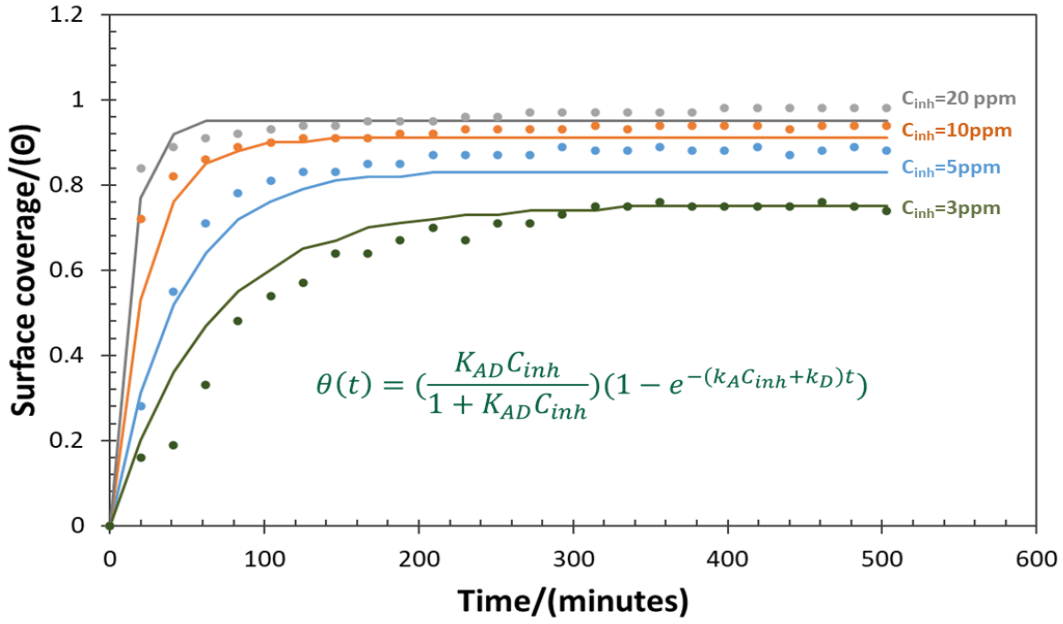

Figure 26. Langmuir adsorption model fitting with experimental data (30°C, 0.97 bar pCO_2, X65 RCE, 1000 rpm, BDA-C14 inhibitor).

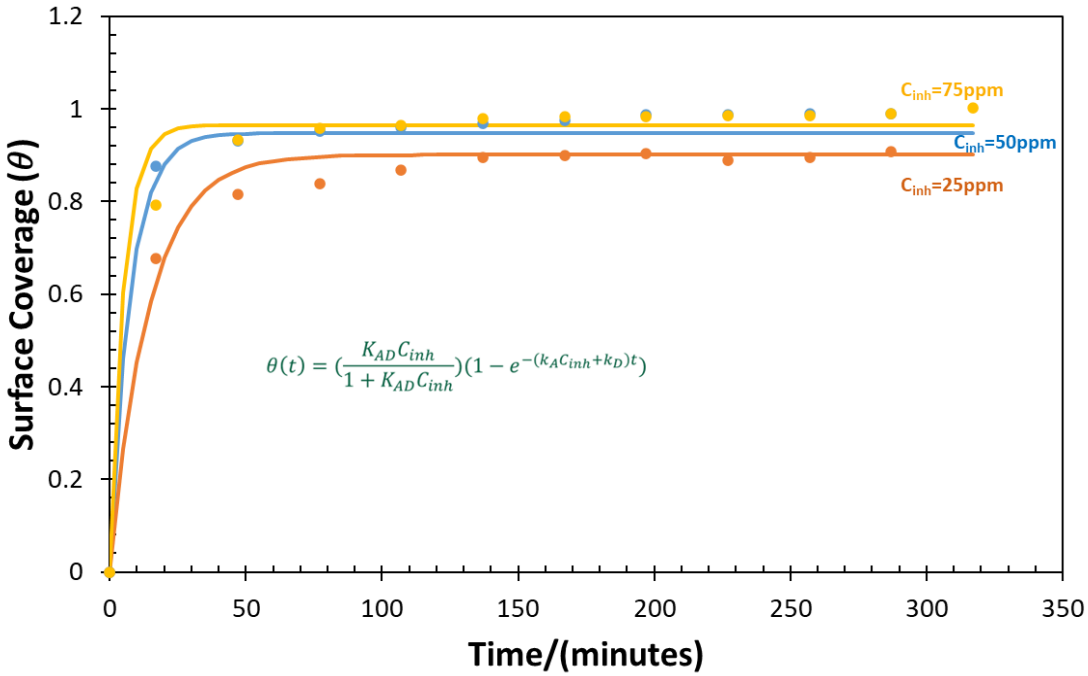

Figure 27. Langmuir adsorption model fitting with experimental data. (40°C, 0.97 bar pCO_2, X65 RCE, 1000 rpm, BDA-C14 inhibitor).

Table 3 Calculated values for adsorption/desorption kinetics at two different temperatures for BDA-C14.

Temperature	$k_A(mM^{-1}.s^{-1})$	$k_D(s^{-1})$	$K_{AD}(mM^{-1})$
30°C	2.4×10^{-2}	0.66×10^{-4}	371.42
40°C	1.6×10^{-2}	1.2×10^{-4}	135.8

2- Desorption behavior

By solving equation (6) for surface coverage (θ), and considering $\theta = 1$ at $t = 0$ for the boundary conditions and having constant C_{inh} after dilution, an explicit function of surface coverage factor (θ) with respect to time can be obtained for desorption step:

$$\theta(t) = \frac{k_D}{k_A C_{inh} + k_D} e^{-(k_A C_{inh} + k_D)t} + \frac{k_A C_{inh}}{k_A C_{inh} + k_D} \quad (17)$$

where k_A and k_D were calculated from adsorption part for BDA-C14 at 30°C and 40°C. Thus, the change in surface coverage with time can be modeled using equation (17) and, accordingly, change in corrosion rate with time can be calculated using the equation below:

$$CR_{\theta(t)} = CR_{\theta=0} - \theta(t) \times (CR_{\theta=0} - CR_{\theta=1}) \quad (18)$$

where $CR_{\theta=0}$ is the blank corrosion rate and $CR_{\theta=1}$ is the stable inhibited corrosion rate at maximum coverage. Figure 28 and Figure 29 compare the predicted and experimental corrosion rates at two different temperatures, considering the persistency step with a residual inhibitor concentration of 10.5 ppm_w (at 30°C) and 7 ppm_w (at 40°C).

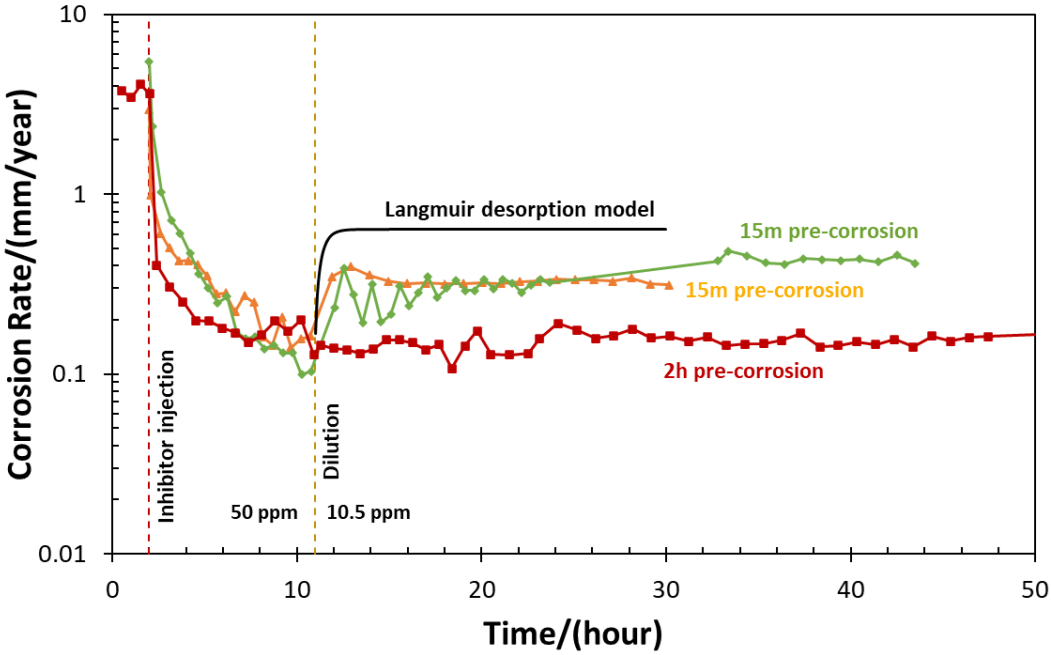

Figure 28. Langmuir desorption model data compared to experimental data with 2 hours or 20 minutes pre-corrosion. (30°C, 0.97 bar pCO_2, X65 RCE, 1000 rpm, BDA-C14 inhibitor).

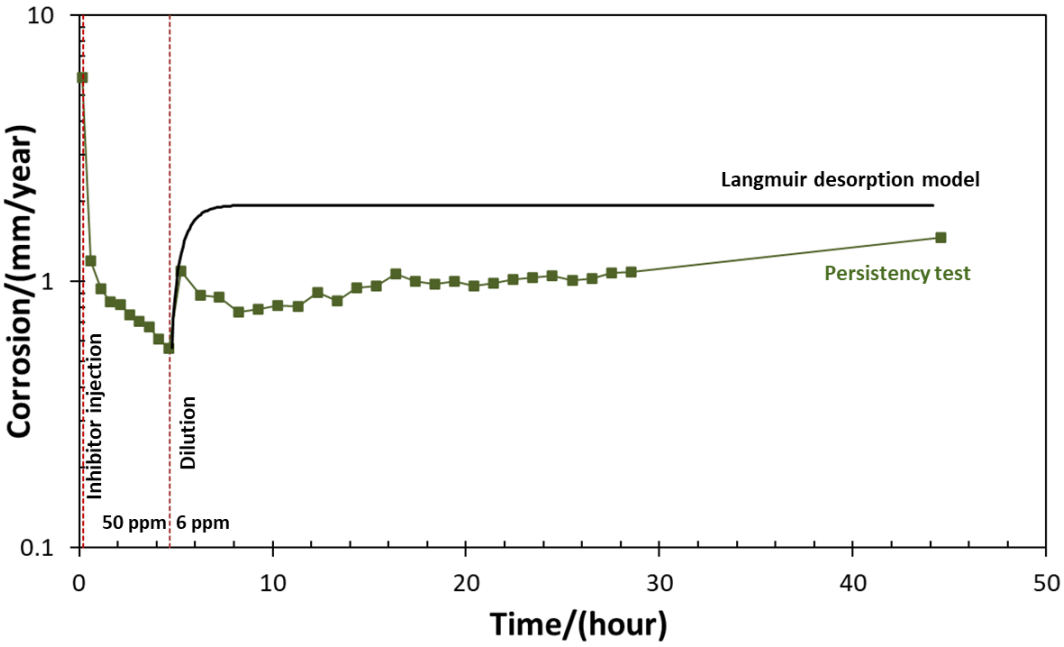

Figure 29. Langmuir desorption model data compared to experimental data. (40°C, 0.97 bar pCO_2, X65 RCE, 1000 rpm, BDA-C14 inhibitor).

Inhibitor desorption modeling at 30°C was performed by comparing the predicted corrosion rate to experimental data with different pre-corrosion times. The adsorption/desorption constants were calculated based on inhibition experiments with a 15-minute pre-corrosion period. As shown in Figure 28, the predicted corrosion rate using these kinetic constants exhibits a general trend similar to that of the experiment with 15 minutes of pre-corrosion. This suggests that pre-corrosion time affects adsorption and desorption kinetics by modifying the surface characteristics. Alternatively, a longer pre-corrosion period may lead to a decrease in surface saturation concentration, preventing inhibitor desorption after partial dilution, as observed in the experiment with 2-hour pre-corrosion.

While the desorption model demonstrates general agreement with the experimental corrosion rate trends observed at both temperatures, notably capturing the initial post-dilution increase and subsequent sustained inhibition, certain discrepancies are evident. Specifically, the model does not fully capture the stable corrosion rate observed experimentally after dilution. These discrepancies may arise from uncertainties in the equation fitting for kinetic constant calculations and inhibitor concentration measurements in the bulk phase post-dilution.

Overall, modeling inhibitor desorption using the Langmuir approach and comparing the predicted corrosion rate with experimental results provide valuable insights. The findings suggest that BDA-C14 follows adsorption/desorption kinetics,

consistent with its role as a water-soluble corrosion inhibitor used in continuous treatment.

4.4 Summary

The in-house synthesized quaternary ammonium inhibitor, BDA-C14, was utilized to evaluate inhibitor persistency under continuous treatment conditions. However, due to constraints regarding uninhibited brine availability, complete removal of inhibitor residuals from the bulk solution was not achieved. This resulted in partial inhibitor desorption from the surface, contributing to continued inhibition during the persistency phase. A summary of the results obtained with this partial dilution procedure at varying temperatures is provided below:

- Persistency at 30°C: Initial persistency tests of BDA-C14 at 30°C, conducted with two distinct pre-corrosion durations, revealed no significant change in corrosion rate following solution dilution. This lack of observable change may be attributed to the slow desorption kinetics at 30°C, potential uncertainties in inhibitor concentration measurements, and inadequate dilution, which sustained inhibition at the final concentration.
- Impact of Pre-Corrosion Time: Reducing the pre-corrosion time from 2 hours to 15 minutes resulted in a slight increase in the stable corrosion rate after dilution. However, the final corrosion rate remained significantly lower than the uninhibited rate, indicating persistent inhibitor activity even with shortened pre-corrosion.

- Effect of Initial Inhibitor Concentration: Experiments with varying initial inhibitor concentrations showed no significant impact on BDA-C14 persistency. Regardless of the starting concentration, the inhibitor maintained its effectiveness after dilution. This suggests that the surface saturation concentration, previously estimated between 20 to 50 ppm_w, is likely closer to 20 ppm_w. Additionally, as shown in Figure 14, even at lower initial concentrations, BDA-C14 provides a certain degree of inhibition.
- Temperature Dependence: Persistency experiments conducted at 40°C with BDA-C14 exhibited a higher final corrosion rate after dilution compared to those performed at 30°C. Furthermore, applying multiple stepwise dilutions, each using 5 L of uninhibited brine, resulted in a complete loss of inhibition and persistency at 40°C. This finding suggests that elevated temperatures enhance the desorption of inhibitor molecules, thereby reducing persistency.
- Modeling Desorption: The Langmuir isotherm model was applied to simulate BDA-C14 desorption at 30°C and 40°C under partial dilution conditions, where the CI concentration remained constant after dilution, with 15 minutes of pre-corrosion. A comparison between the modeled and experimental results at both temperatures indicated that although the predicted corrosion rate showed some deviations from the experimental data, these discrepancies were likely due to uncertainties in kinetic

constant calculations and CI concentration measurements. Nevertheless, the overall corrosion rate behavior was consistent with the experimental trends, showing an increase in corrosion rate after dilution while still maintaining partial inhibition. Furthermore, a comparison between the modeled results at 30°C and experimental data with 2-hour pre-corrosion revealed that pre-corrosion time influences inhibitor adsorption/desorption kinetics by altering the surface characteristics.

- Limitations: It is important to acknowledge that the partial dilution approach introduced limitations to the study. The presence of residual inhibitor molecules after dilution may have influenced the observed persistency behavior. It was postulated that future investigations should aim to employ a complete dilution process to ensure a more comprehensive evaluation of BDA-C14 persistency.

Chapter 5: Study of Continuous Treatment Persistency Using Continuous Dilution*

5.1 Introduction

Changes in the dilution methodology were implemented to address the limitations associated with partial dilution and achieve a more accurate evaluation of inhibitor persistency. This enhanced configuration facilitated continuous dilution of the solution following the inhibition step and could be maintained until the experiment conclusion. This methodology offered a more realistic representation of a potential interruption in continuous CI injection scenarios encountered in field applications. By enabling the removal of all residual inhibitor molecules from the glass cell, the revised setup provided a clearer picture of inhibitor persistency under such conditions. The chapter outlines the following key objectives:

- Evaluation of BDA-C14 Persistency at Elevated Temperatures: To assess the persistency behavior of BDA-C14 at elevated temperatures using the developed methodology (compared to previous experiments). This evaluation was conducted under conditions that eliminate residual

---

* A version of this chapter was published as:

#1: "Development of Methodologies for Continuous and Batch Inhibitor Film Persistency Investigation in the Laboratory," in AMPP Annual Conference+Expo 2022, paper no. 18056 (San Antonio, TX: AMPP 2022). (Reference number: [107])

#2: "Investigation of CO_2 Corrosion Inhibitor Adsorption and Desorption Behavior Using Langmuir Isotherm Model and Effects of Iron Carbide on CI Persistency," in AMPP Annual Conference+Expo 2023, paper no. 19451 (Denver, CO: AMPP 2023). (Reference number: [108])

inhibitor molecules from the system, thereby providing a more accurate representation of an interruption in continuous field treatment.

- Impact of Pre-Corrosion Time: To investigate the potential influence of iron carbide formation on inhibitor persistency. This investigation was focused on scenarios involving extended pre-corrosion or inhibition times, which could promote the formation of iron carbide on the metal surface.
- Modeling Inhibitor Behavior with Langmuir Isotherm: To develop a model of inhibitor adsorption/desorption behavior at varying temperatures using the Langmuir isotherm model. The resulting model was compared against the experimentally obtained results to assess its accuracy in predicting desorption behavior.

5.2 Experimental Procedure and Test Matrix

The general procedure of these experiments was similar to the previous chapter:

1- Pre-corrosion: Before each experiment, a meticulous preparation process was implemented. This involved rinsing the glass cell and associated equipment with isopropanol and DI water. A new solution was then prepared specifically for the upcoming experiment. Subsequently, the entire glass cell underwent CO_2 sparging for a duration of one hour. The pre-treated specimen was then mounted onto the rotating shaft and carefully positioned within the solution. The rotation process was initiated, and the sample underwent pre-corrosion for a period of 2 hours or 15 minutes. Throughout this pre-corrosion step, Open Circuit Potential (OCP), Electrochemical Impedance Spectroscopy

(EIS), and Linear Polarization Resistance (LPR) measurements were acquired at 30-minute intervals (one measurement for 15 minutes pre-corrosion experiments).

2- Inhibition: As described in detail within the common experimental methodology section, 2 mL of the prepared inhibitor solution was injected into the cell. Following the inhibitor injection, OCP, EIS, and LPR measurements were collected every 30 minutes until a stable, uninhibited corrosion rate was achieved.

3- Dilution: Following the establishment of a stable corrosion rate, a meticulous dilution procedure was initiated. This process involved the simultaneous removal of inhibited solution from the bottom of the glass cell and the introduction of fresh, uninhibited brine solution at the top. To maintain a consistent dilution rate, a constant flow rate of 40 mL/minute was employed, resulting in a complete solution exchange every 45 minutes. The integrated overflow mechanism (as depicted in Figure 30) ensured a constant liquid level throughout the dilution stage, guaranteeing that the specimen remained fully immersed. Given the large capacity of the reservoir (140 L), the solution could be diluted continuously until complete desorption of the inhibitor from the sample surface was achieved.

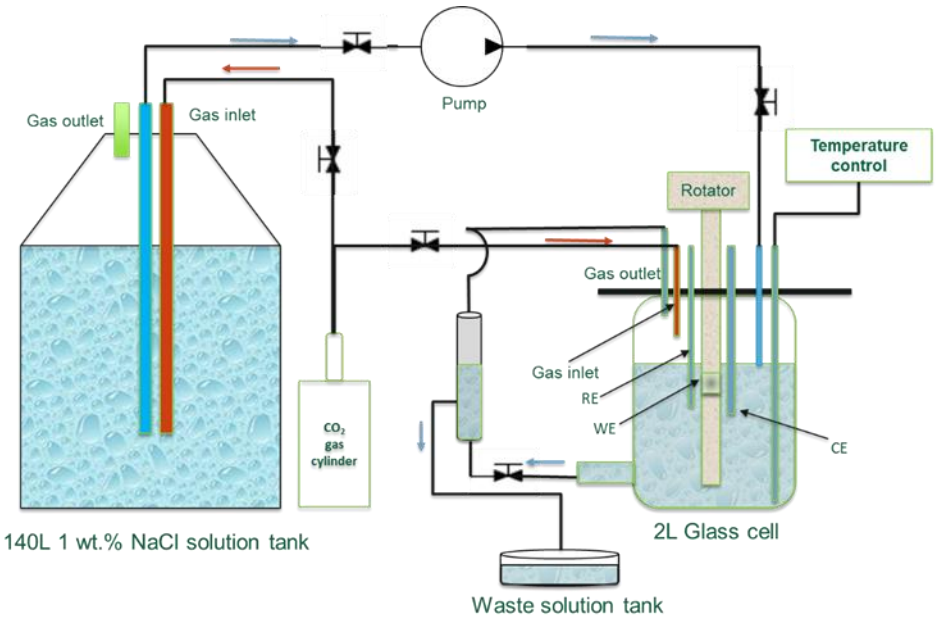

Figure 30. Schematic of the setup used in persistency experiments with continuous dilution.

Table 4. Experimental matrix for continuous treatment persistency experiments with continuous dilution.

Parameter	**Conditions**
Working electrode	API 5L X65 (0.035 wt.%C)
Solution	1 wt.% NaCl
Sparged gas	CO_2
Total pressure	1 bar
Rotational speed	1000 RPM
Temperature	(30 °C, 40°C) ± 1°C
pH	4.0 ± 0.1
Corrosion inhibitor (CI) model compound	Quaternary ammonium type (BDA-C14)
Measurement methods	OCP, LPR, EIS
Contact time (time before dilution)	9 hours, 29 hours
Initial inhibitor concentration	50 ppm (SSC)
Presence of hydrocarbon	No – brine only
Pre-corrosion before CI injection	15 minutes, 2 hours

5.3 Results and Discussion

5.3.1 Study of Persistency Using Continuous Dilution at 40℃

The persistency of BDA-C14 was evaluated at 40°C for the initial set of continuous treatment persistency experiments involving continuous dilution. In all experiments conducted at this temperature, the sample was pre-corroded for 15 minutes,

followed by the injection of 50 ppm_w BDA-C14. After approximately 5 hours the corrosion rate stabilized, and the solution was continuously flushed with uninhibited brine until the end of the experiment. Throughout the dilution process, samples were extracted from the solution for inhibitor concentration analysis. In the first two experiments, a needle valve was employed to regulate the dilution flow rate; however, this method proved to be inconsistent in maintaining a constant flow rate. Figure 31 and Figure 32 are for the experiments with fluctuating dilution flowrate. An additional modification, incorporating a flow meter, yielded more precise results. The subsequent experiment was conducted with a more stable dilution flow rate, as depicted in (Figure 33). The results are still very much valid and comparable, the use of a flowmeter making the conduction of the experiment much more practical. The experimental results obtained for BDA-C14 persistency under continuous dilution conditions revealed a consistent pattern. Immediately following the complete removal of inhibitor residuals from the glass cell, the corrosion rate rapidly increased to the uninhibited value, indicative of inhibitor desorption from the metal surface. This observation suggests that BDA-C14, when employed as a model compound continuous inhibitor, exhibits no persistency in the absence of residual inhibitor molecules within the bulk solution. In contrast, under identical experimental conditions but with a partial dilution approach, the inhibitor demonstrated a degree of persistency. This comparative analysis highlights the critical role of continuous dilution in influencing the performance and persistency of corrosion inhibitors.

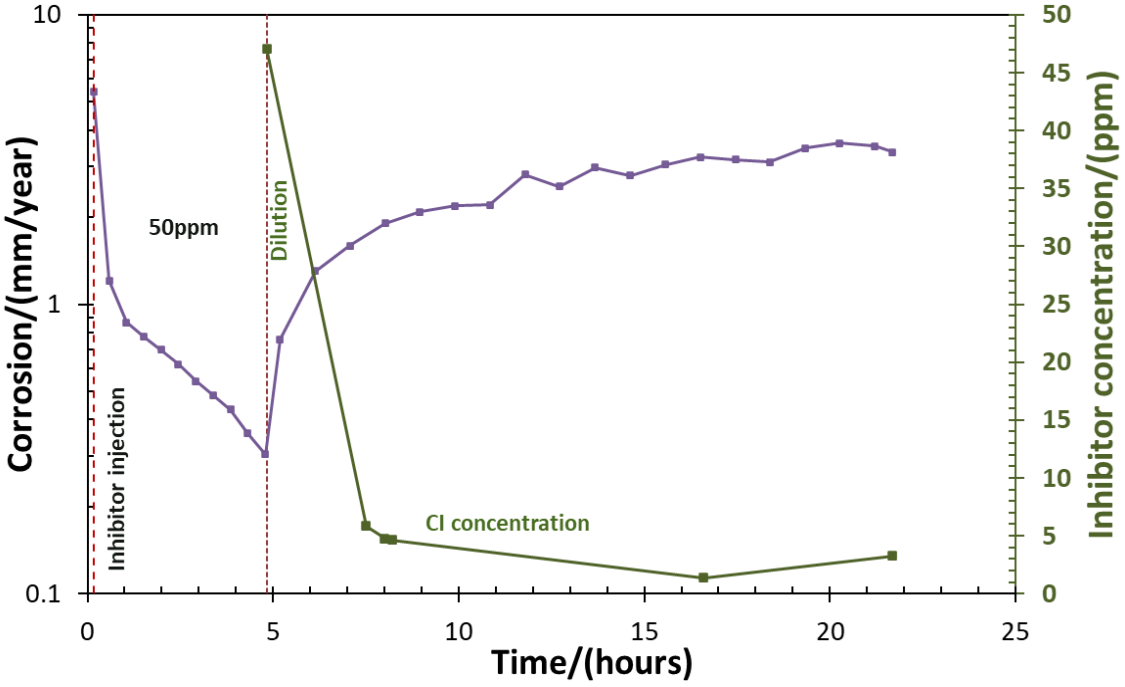

Figure 31. Corrosion rate versus time for 15 minutes pre-corrosion with continuous dilution with non-constant flow rate (40°C, 0.97 bar pCO_2, X65 RCE, 1000 rpm, BDA-C14 inhibitor).

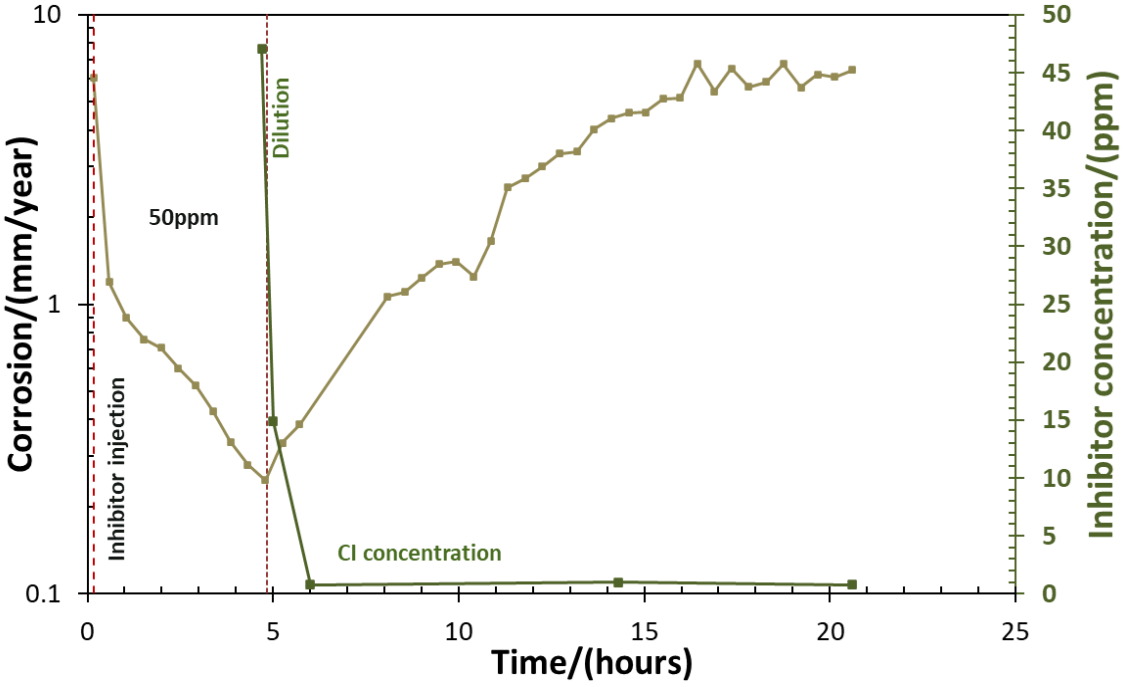

Figure 32. Corrosion rate versus time for 15 minutes pre-corrosion with continuous dilution with non-constant flow rate - repeat (40ºC, 0.97 bar pCO_2, X65 RCE, 1000 rpm, BDA-C14 inhibitor).

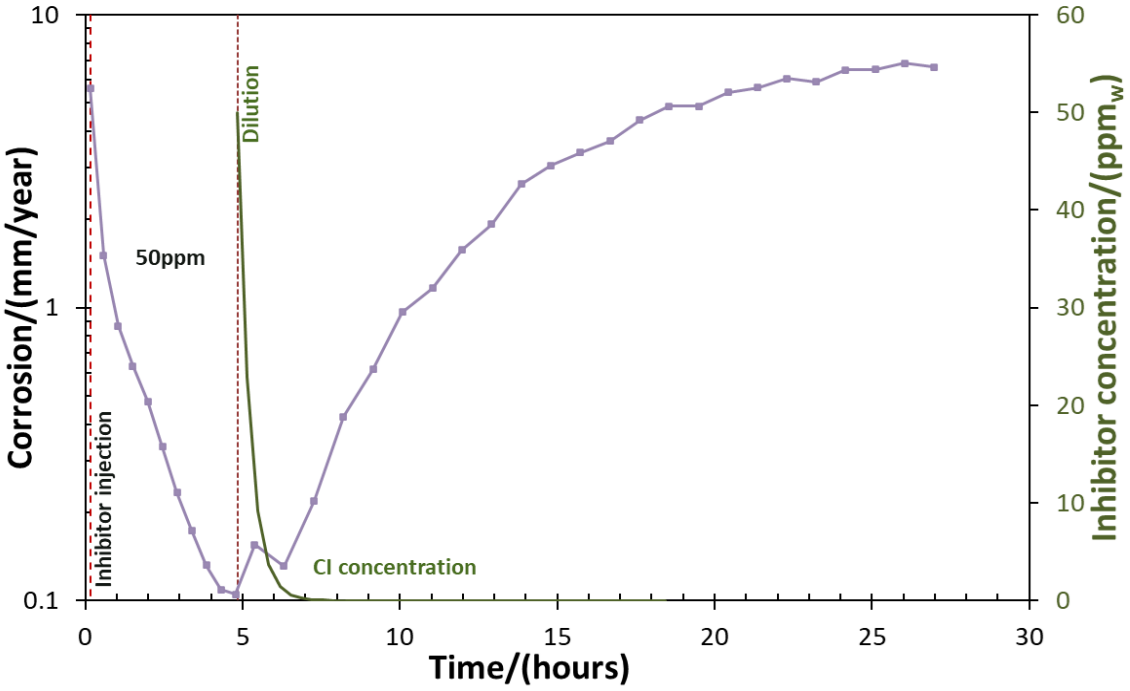

Figure 33. Corrosion rate versus time for 15 minutes pre-corrosion with continuous dilution with constant flow rate (40°C, 0.97 bar pCO_2, X65 RCE, 1000 rpm, BDA-C14 inhibitor).

Inhibitor concentration profile in Figure 33 was calculated using a mass balance with constant flow rate which gives an expression for the change in concentration as follows:

$$C_{Inh}(t) = C_{inh_0} e^{-\frac{Q}{V}t} \tag{19}$$

where $C_{Inh}(t)$ and C_{inh_0} are the inhibitor concentration at time t (minutes) and initial concentration in ppm_w respectively. Q is the dilution flow rate (L/minute), and V is solution volume (L).

5.3.2 Study of Persistency Using Continuous Dilution at 30℃

5.3.2.1 Persistency Experiments at Baseline Conditions. Three replicate experiments were conducted at 30°C to investigate inhibitor adsorption and desorption behavior under continuous dilution. These experiments were performed under baseline conditions, as described in the previous chapter, with 15 minutes of pre-corrosion and a 9-hour contact time. Figure 34 shows the results for three attempts which show a good reproducibility of the experiments. The average corrosion rate before addition of the inhibitor was 3.7 mm/year which reduced to 0.15 mm/year after 9 hours of the inhibitor injection. However, the corrosion rate remained stable for 1.5 hours after the dilution. Results suggest that the reason for this behavior was due to the complete removal of inhibitor from the main glass cell. In other words, corrosion rate did not increase until all the inhibitor residuals were removed from the glass cell by the continuous dilution. This could also be due to the surface saturation concentration, initially estimated to be between 50 and 20 ppm_w, actually being closer to 20 ppm_w. The period during which no change in corrosion rate is observed may correspond to the time required for the inhibitor concentration to decrease from 50 to 20 ppm_w

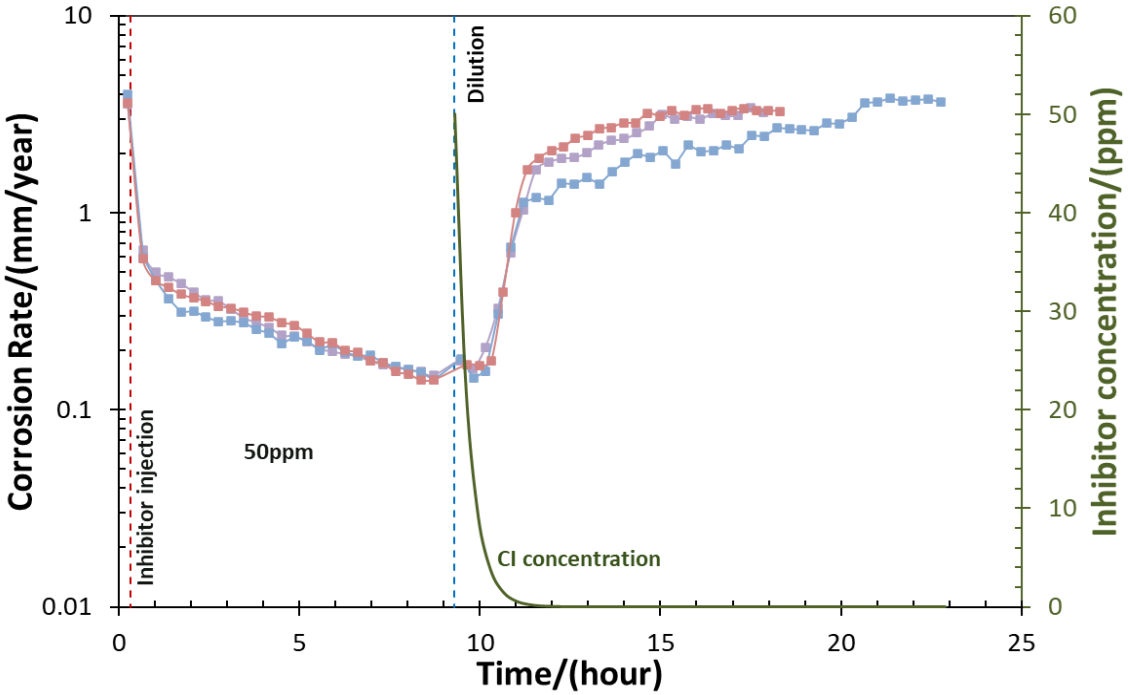

Figure 34. Corrosion rate and CI concentration versus time for 15 minutes pre-corrosion and three different repeats (30°C, 0.97 bar pCO_2, X65 RCE, 1000 rpm, BDA-C14 inhibitor).

Results in Figure 34 clearly show that constant dilution, in which the corrosion inhibitor concentration reaches zero concentration, results in full desorption of the inhibitor and no persistency of BDA-C14.

5.3.2.2 Persistency Experiment With Longer Contact Time. Two repeat experiments were conducted to investigate the effects of longer contact time between the RCE and the inhibitor in solution over a period of 29 hours. The inhibited corrosion rates at approximately 9 hours were comparable to those observed in Figure 34, reaching approximately 0.15 mm/yr. However, these rates continued to decrease, stabilizing at 0.085 and 0.04 mm/yr, respectively, in Figure 35, corresponding to an efficiency of approximately 98.4%. In both cases, an immediate increase in corrosion rate was

observed upon initiation of the dilution process. Nevertheless, neither test reverted to the initial corrosion rate, even after 30 to 65 hours of dilution. Following the first hour of dilution, a significant reduction in the slope of the corrosion rate versus time curve was observed, leading to a gradual and nearly continuous loss of mitigation over time until the conclusion of each test. Although the corrosion rate exhibited an increasing trend with a very small slope, the final corrosion rate (~1.2 mm/year) achieved after 65 hours of exposure during the dilution phase remained significantly lower than the uninhibited value of 3.7 mm/year. While extending the experiment for a longer duration could potentially allow the corrosion rate to reach that of the uninhibited brine, it was not practical to continue for such a long period.

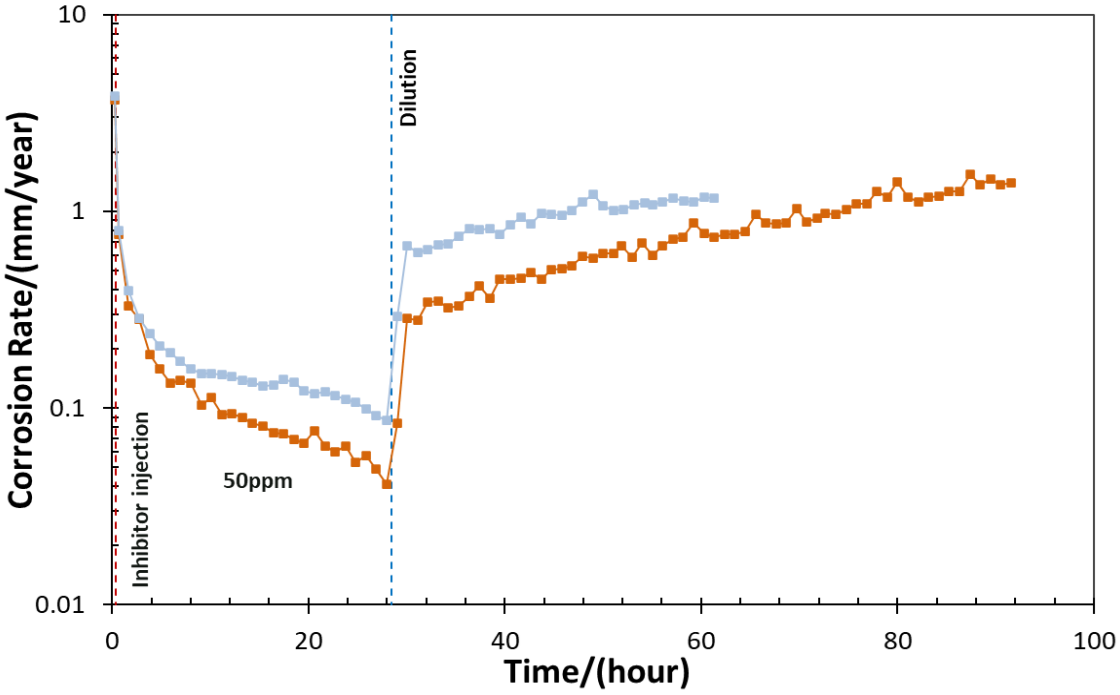

Figure 35. Corrosion rate and versus time for longer contact time of 29 hours with two different repeats (30°C, 0.97 bar pCO_2, X65 RCE, 1000 rpm, BDA-C14 inhibitor).

In each of the aforementioned tests, the working electrode was removed, polished, and reintroduced into the same solution to assess residual inhibitor levels and the overall corrosivity of the aqueous solution. For each test, the resulting corrosion rate was comparable to the initial corrosion rate (3.7 mm/year) observed in the uninhibited solution, confirming the effective removal of all inhibitor molecules from the glass cell. This finding suggests that extending the contact time from 9 to 28 hours resulted in slightly slower inhibitor desorption kinetics. Although the inhibition efficiency was not acceptable after the dilution, it is hypothesized that subtle changes in surface roughness and the formation of a thin iron carbide layer on the metal surface may have influenced surface characteristics and, consequently, inhibitor desorption kinetics. Further experiments were conducted to better investigate this hypothesis by extending the pre-corrosion time, ensuring sufficient formation of the iron carbide layer on the surface.

5.3.2.3 Persistency Experiment With Longer Pre-Corrosion Time. Another set of experiments was done to clarify the effects of initial pre-corrosion, or iron carbide layer development, on inhibitor desorption behavior and its persistency. Figure 36 shows two different experiments with 2 hours pre-corrosion and 9 hours of contact time. The initial corrosion rates before inhibitor injection were 3.7 ± 0.0.5 mm/yr with inhibited rates of 0.05 ± 0.01 mm/yr after 9 hours (98.6% efficiency). As compared to Figure 34, the results clearly show that the desorption kinetics of the BDA-C14 were influenced by the increasing pre-corrosion time, which is thought to be related to having more iron carbide formed on the metal surface. A slight increase in corrosion rate was observed

when dilution started, and about 1 hour of inhibitor persistency was seen before the corrosion rate began to increase. Compared to Figure 34 (with 15 minutes pre-corrosion), 2-hour pre-corrosion led to a slower and incomplete inhibitor desorption.

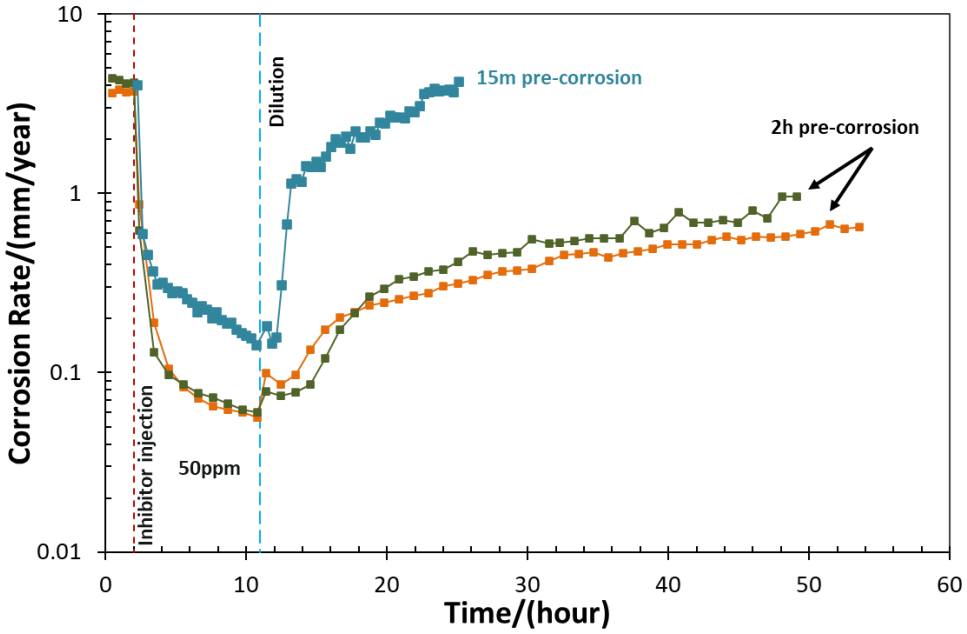

Figure 36. Corrosion rate versus time for 2 hours pre-corrosion and two different repeats comparing to 15 minutes pre-corrosion results (30°C, 0.97 bar pCO_2, X65 RCE, 1000 rpm, BDA-C14 inhibitor).

These results indicate that an increase in the iron carbide layer formed on the metal surface can alter surface characteristics and influence desorption kinetics. The formation of the iron carbide layer appears to decrease the rate of inhibitor desorption, potentially enhancing inhibitor persistency.

5.3.3 Modeling BDA-C14 Inhibitor Adsorption/Desorption Behavior Using Langmuir Isotherm Model With Continuous Dilution

As shown in the previous chapter, the adsorption/desorption constants of BDA-C14 at baseline conditions were calculated using the Langmuir isotherm model. However, the desorption model was based on constant inhibitor concentration after the partial dilution. However, in this case, the inhibitor concentration changes over time as a result of the continuous dilution of the solution.

Desorption behavior in continuous dilution conditions could also be analyzed using equation (6). However, this equation requires a numerical method due to the non-constant CI concentration after dilution with the time. Thus, at the time of the dilution, by considering $\theta = 1$ at $t = 0$ and $C_{inh}(t) = C_{inh_0} e^{(-\frac{Q}{v}t)}$, the surface coverage can be calculated over time. Detailed calculations are provided in Appendix B: Desorption Equation Solution in Continuous Dilution. Consequently, the corrosion rate as a function of time following the initiation of continuous dilution, for both temperatures, along with corresponding calculated kinetic values, can be determined and plotted using equation (18). Figure 37 and Figure 38 show the predicted corrosion rate and experimental data for the dilution step with 15 minutes pre-corrosion and 9 hours contact time at 40°C and 30°C, respectively.

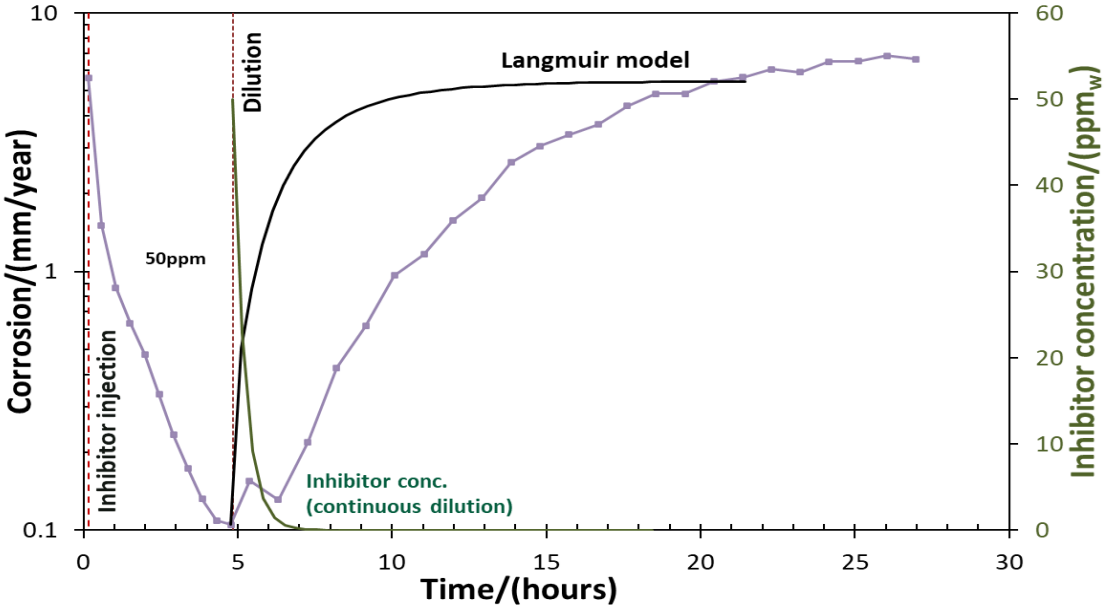

Figure 37. Modeled corrosion rate for the desorption part using Langmuir isotherm model versus experimental data (40°C, 0.97 bar pCO_2, X65 RCE, 1000 rpm, BDA-C14 inhibitor).

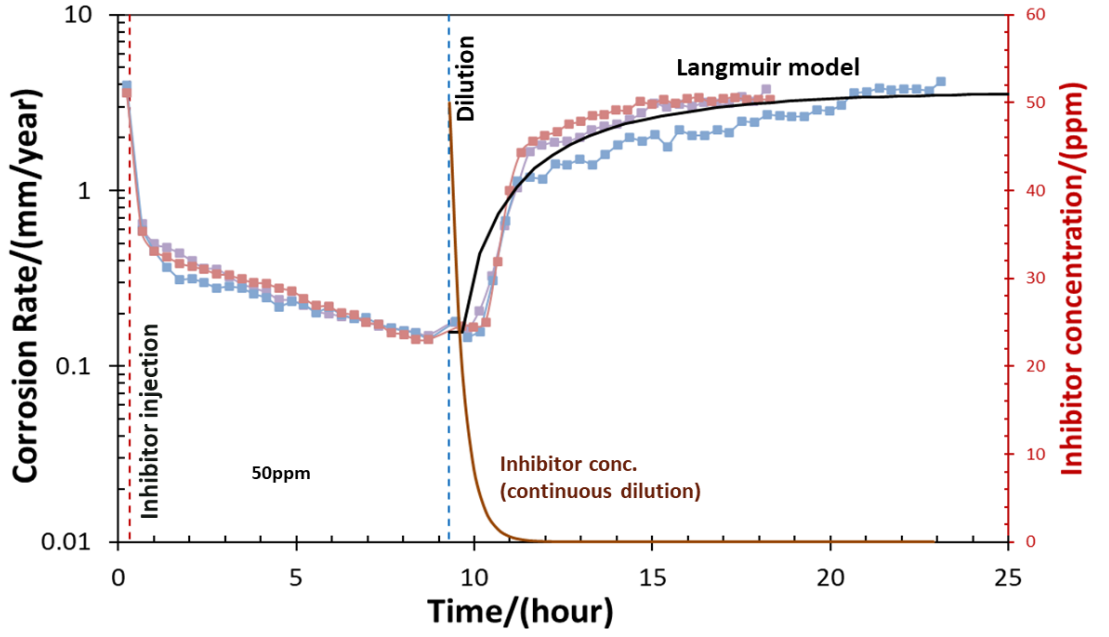

Figure 38. Modeled corrosion rate for the desorption part using Langmuir isotherm model versus experimental data (30°C, 0.97 bar pCO_2, X65 RCE, 1000 rpm, BDA-C14 inhibitor).

As can be observed from Figure 37, the calculated corrosion rates are different in the transient region from the experimental data at 40°C. Nevertheless, the general trend of change of the corrosion rate after dilution was successfully simulated using the Langmuir isotherm model. The observed deviations from the model in the transient region may be attributed to the limitations of the Langmuir model in capturing the behavior of the inhibitor at 40°C. Additionally, experimental uncertainties in determining the surface saturation concentration and the kinetic constants k_A and k_D could also influence the corrosion rate results during the transient phase. Results for the modeling at 30°C (Figure 38) show that the Langmuir isotherm model successfully modeled the desorption behavior of the BDA-C14 on a freshly polished surface at this temperature. The modeling results pertaining to the desorption behavior of the BDA-C14 inhibitor at both temperatures suggest that this model compound primarily adheres to an adsorption/desorption mechanism, exhibiting limited persistency upon complete removal of inhibitor residues from the bulk solution.

Predicted corrosion rates using Langmuir isotherm model at 30°C were compared with the results of experiments involving longer contact time and longer pre-corrosion. Figure 39 presents a comparison between the predicted corrosion rate model and experimental data for the experiment with a longer contact time but the same 15-minute pre-corrosion period. Figure 40 provides a similar comparison for the experiment with a longer pre-corrosion duration of 2 hours. It should be noted that this desorption prediction

model is based on adsorption/desorption constants derived from experimental data obtained with a 15-minute pre-corrosion period and a 9-hour contact time.

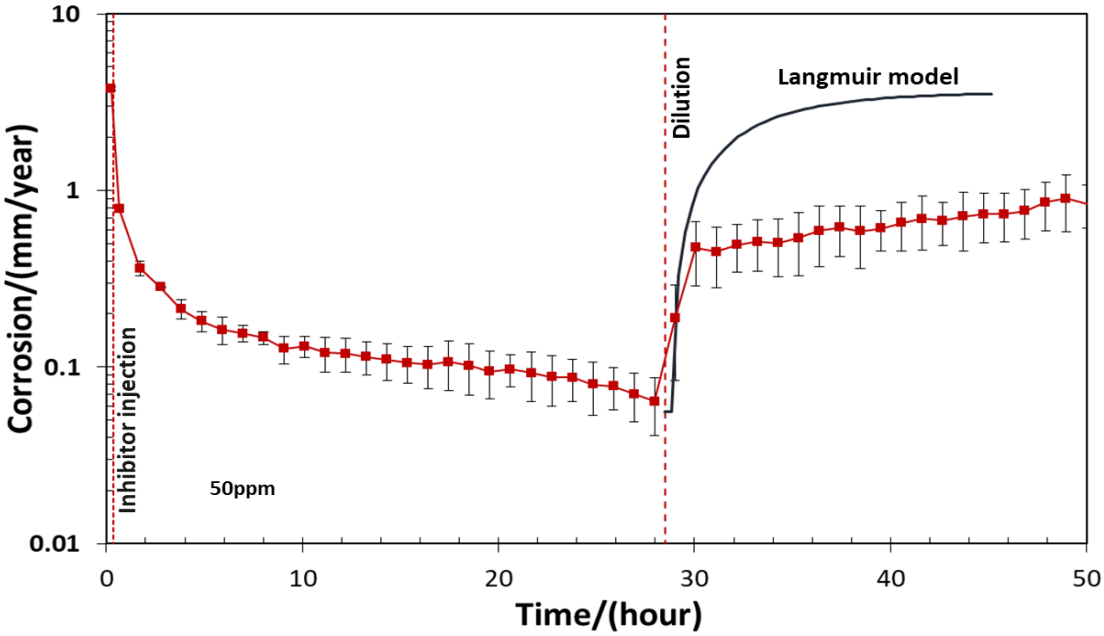

Figure 39. Modeled corrosion rate versus time compared to experimental data for longer contact time of 29 hours (30°C, 0.97 bar pCO_2, X65 RCE, 1000 rpm, BDA-C14 inhibitor).

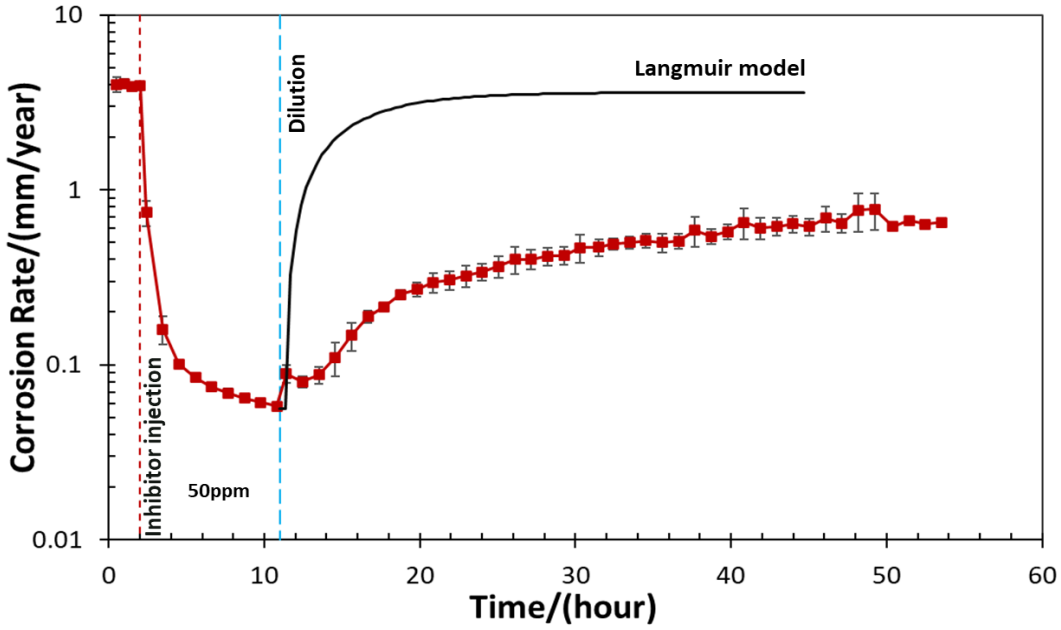

Figure 40. Modeled corrosion rate versus time compared to experimental data for longer pre-corrosion of 2 hours (40°C, 0.97 bar pCO_2, X65 RCE, 1000 rpm, BDA-C14 inhibitor).

Modeling results for experiments with longer contact time or longer pre-corrosion time show that the presence of iron carbide residues, associated with longer contact time or pre-corrosion, affected the desorption kinetics as hypothesized in the previous chapter. Thus, modeling was not able to predict the desorption behavior of the BDA-C14 when the surface characteristic and corresponding desorption kinetics changed. In addition, the slight delay often observed between the moment the inhibitor dilution starts and the moment the corrosion rate starts to increase may be associated to the time needed for the inhibitor concentration to decrease from 50 ppm_w to its surface saturation concentration (known to be 20 ppm_w from other studies [101]). Thus, inhibitor molecule coverage of

the metal surface remained maximum until the CI concentration in the bulk solution decreased below surface saturation concentration (20 ppm_w).

5.4 Summary

A new experimental setup was used for mimicking the effect of a sudden loss of continuous inhibition treatment on the corrosion of steel. Continuous dilution was successfully implemented and demonstrated its effectiveness in minimizing residual corrosion inhibitor content in solution over time. This approach addressed a key limitation of partial dilution in corrosion inhibitor persistency studies for continuous treatment. This method for dilution was employed in the corrosion inhibitor persistency study due to its ease of control and reliability in assessing the impact of various parameters, such as inhibitor contact time and controlled flow rate/fluid exchange rate, in long-term studies. A summary of the results with this continuous dilution procedure at different temperatures is presented as follows:

- BDA-C14, a model compound inhibitor, exhibited no persistency when all inhibitor residues were removed from the bulk solution at both temperatures. This indicates that the model compound inhibitor adheres to the adsorption/desorption mechanism, resulting in a lack of persistency after dilution, similar to other water-soluble inhibitors.
- Persistency experiments at higher temperature (40°C) showed that BDA-C14 has higher desorption kinetics and lower persistency as expected.
- The formation of an iron carbide layer on the surface, resulting from extended contact time or pre-corrosion duration, influenced desorption

kinetics. This suggests that the iron carbide layer enhances inhibitor persistency by reducing inhibitor desorption rates.

- The Langmuir isotherm model proved to be a valuable tool for modeling the adsorption and desorption of the inhibitor in continuous inhibition treatment. Modeling results suggest that continuous treatment inhibition operates in accordance with an adsorption/desorption mechanism, which is strongly influenced by the bulk inhibitor concentration but can also be affected by changes in surface characteristics, such as iron carbide formation).

Chapter 6: Study of Batch Inhibition Treatment Persistency With Commercial Inhibitor Package[†]

6.1 Introduction

As stated in the first chapter, of the two main methods (batch and continuous injection) for applying corrosion inhibitors in the oil and gas industry, continuous injection is by far the more practical and cost effective [21, 49]. However, when continuous inhibitor injection fails to provide adequate protection, batch inhibition is implemented as an alternative approach. Several methods exist for administering inhibitors within a batch inhibition regime. In transportation pipelines, an inhibitor slug is introduced between two moving displacement devices (pigs). The subsequent movement of these pigs results in the formation of a thick inhibitor film on the pipe internal surface. Conversely, in downhole tubular systems, a highly concentrated inhibitor slug is injected from the wellhead to the bottom hole (typically via the annulus between the production tubing and the casing), from where it flows back up through the tubing, allowing sufficient residence time to establish a uniform protective film on the steel wall. One of the most challenging steps in batch inhibition studies is the methodology that is employed in the laboratory to simulate the field application. There are two main methods that have been used for batch inhibition study in terms of inhibitor film formation in the literature. In the first methodology, the specimen is first dipped into the neat or diluted inhibitor solution for a defined time that aims to represent the contact time. Then, the specimen is

---

[† †] A version of this chapter was published as: "Effects of Temperature and Presence of Hydrocarbon on Commercial Batch Inhibitor Persistency using a Developed Methodology," in AMPP Annual Conference+Expo 2025, paper no. 00335 (Nashville, TN: AMPP 2025). (Reference number: [109])

dripped dry and transferred to the uninhibited brine and electrochemical measurements are conducted on the specimen with or without limited brine renewal [66, 70, 73, 75, 76, 110]. This method is called "*ex situ* dip and drip" method. In the second methodology, the inhibitor is applied to the specimen in a deoxygenated glass cell using either the dip and drip method or a spray nozzle to provide a controlled coverage of the specimen. Then, uninhibited brine is introduced to the glass cell without transferring the specimen [68, 69]. This method is called "*in situ* modified dip and drip" method. The first method is susceptible to oxygen contamination during the inhibitor application step and both methods exhibit limitations in brine renewal.

Thus, with the aim of developing a new methodology to surpass these limitations, this chapter outlines the following key objectives:

- Develop an apparatus and methodology that better simulates the batch inhibition treatment in the field, avoiding oxygen contamination and enabling the removal of all the inhibitor residuals after inhibitor application.
- Perform parametric studies by investigating the effects of CI contact time, temperature, and presence of hydrocarbon phase on commercial CI persistency. The use of a commercial corrosion inhibitor was intended to ensure that the developed methodology could be applied to an inhibitor commonly used for batch inhibition in the field, thereby validating the methodology.

6.2 Experimental Procedures and Test Matrix

As discussed in section 2.5.2, the current literature reflects diverse methodologies employed for studying inhibitor persistency. However, these approaches often face two main challenges: (1) oxygen contamination during the inhibitor film formation step, and (2) the inability to completely remove residual inhibitor from the solution. A modified methodology with a dedicated experimental setup was developed to address these limitations and enhance the simulation of real-world batch inhibition persistency. Figure 41 shows the schematic of the experimental setup used in batch inhibition persistency in this study.

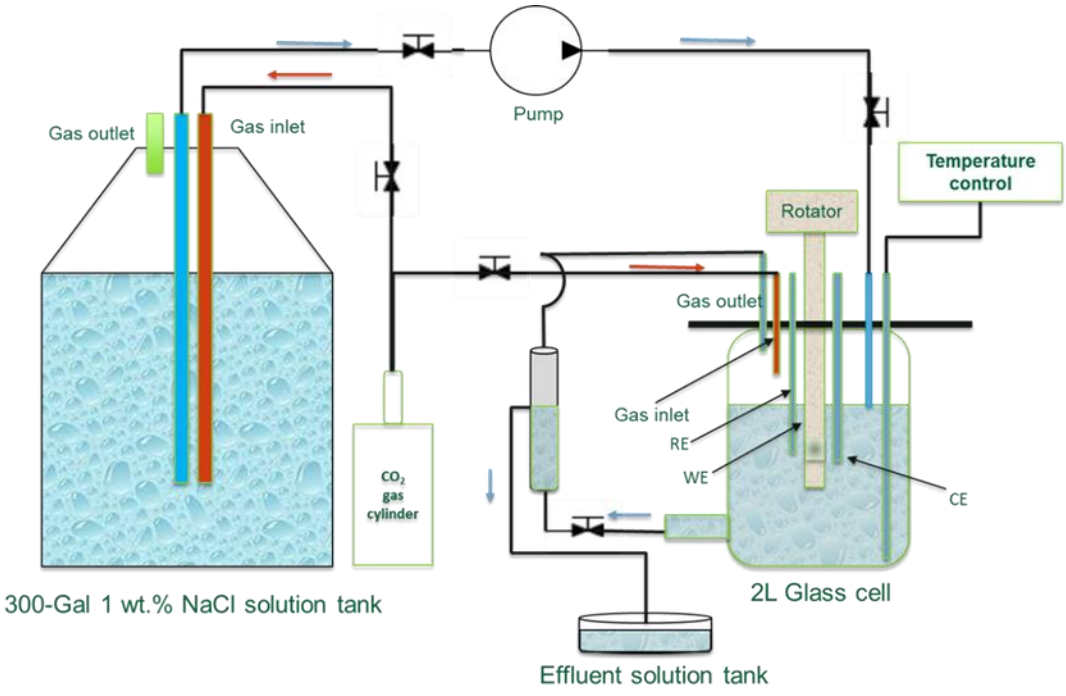

Figure 41. Schematic of the system setup used in batch inhibition study.

General procedural steps that were used in batch inhibition experiments are as follows:

1. Sparge prepared uninhibited brine overnight with CO_2.
2. Empty, dry, and sparge glass cell for 30 min.
3. Install RCE specimen into the glass cell and sparge for another 10 min.
4. Prepare inhibitor solution in a separate vial attached to a specialized holder (Figure 42).
5. Remove the stopper from glass cell lid & lower the vial into the glass cell to position it around the specimen without touching it.
6. Set RCE rotation (300 rpm) for a specific contact time (flow with inhibitor contact).
7. Stop RCE rotation and remove vial from around specimen without touching.
8. Take the vial out of the glass cell, put stopper back, and sparge for another 5 min.
9. Introduce pre-sparged uninhibited brine continuously at a constant flow rate.
10. After specimen is in full contact with the brine, conduct electrochemical measurements (OCP, EIS, and LPR) at constant time intervals for duration of test.

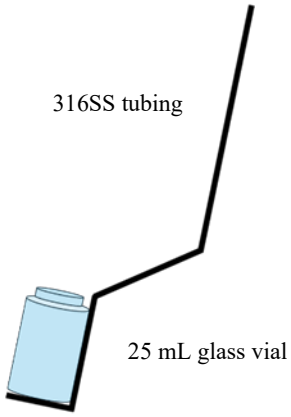

Figure 42. Schematic of the specialized holder for inhibitor film formation procedure.

Table 5 shows the test matrix for batch inhibition persistency studies using commercial inhibitor.

Table 5. Experimental matrix for batch inhibition treatment persistency experiments with commercial CI.

Parameter	**Conditions**
Working electrode	API 5L X65 (0.035 wt.% C)
Solution	1 wt.% NaCl
Sparged gas	CO_2
Total pressure	1 bar
Rotational speed	1000 RPM
Temperature	(30 °C, 45°C, 60°C) ± 1°C
pH	4.00-4.45± 0.1
Corrosion inhibitor type	Commercial inhibitor
Measurement methods	OCP, LPR, EIS
Contact time	5 minutes or 10 seconds
Initial inhibitor concentration	Neat inhibitor package (as received)
Presence of hydrocarbon	0 – 1% (v/v) LVT-200‡
Pre-corrosion before CI application	No pre-corrosion

‡ A generic hydrotreated light petroleum distillate containing carbon numbers predominantly in the range of C9 through C16 used as a model oil.

6.3 Results and Discussion

6.3.1 Effect of Temperature on Commercial CI Persistency

The efficacy of the proposed methodology as a representative tool for field batch inhibition was evaluated using a commercial batch corrosion inhibitor. As previously mentioned, a commercial batch corrosion inhibitor was used due to its observed persistency in field applications, making it a suitable choice for validating the developed methodology. Figure 43 presents the results of two replicate experiments in which the neat inhibitor was applied to the specimen for a 5-minute contact time under the specified conditions. This commercial inhibitor demonstrated excellent inhibition efficiency (approaching 100%) and persistency. Corrosion rate measurements were further corroborated by mass loss measurements, as the specimen exhibited negligible mass loss after the experiment. Additionally, potentiodynamic sweeps (Figure 44) conducted at the end of the second replicate experiment revealed that, compared to uninhibited conditions, the charge transfer rates for all reactions and the limiting current decreased by several orders of magnitude in the batch inhibition experiment with the commercial inhibitor, which was not observed with continuous type CI, further confirming the inhibitor exceptional efficiency.

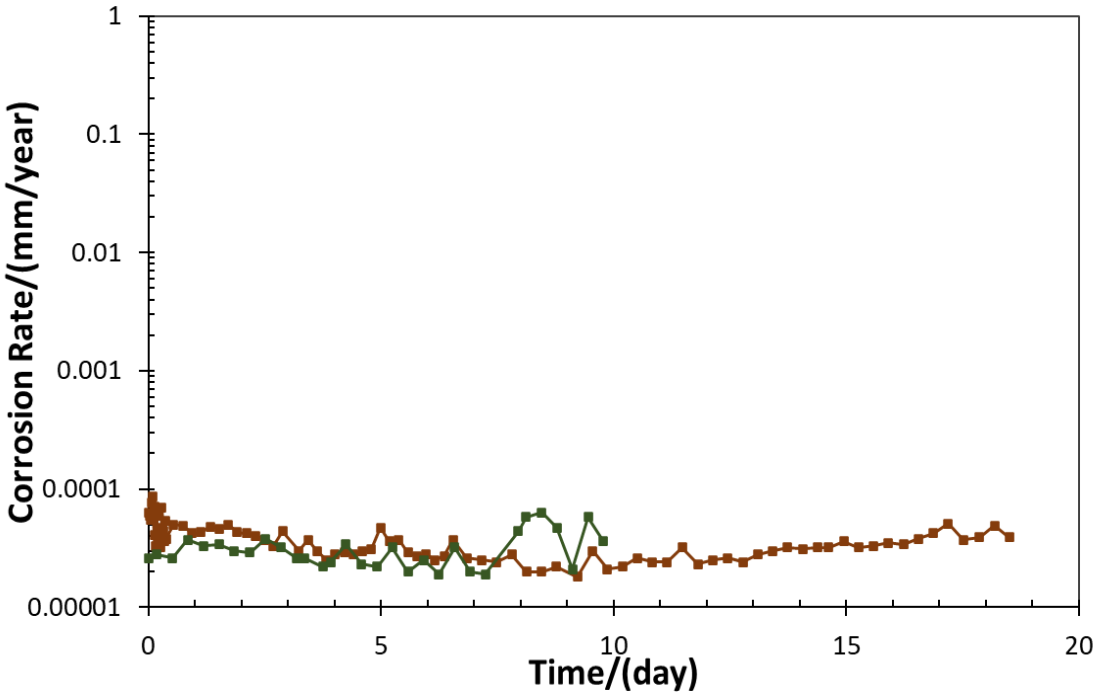

Figure 43. Batch inhibition persistency experiment with commercial inhibitor (30°C, 0.97 bar pCO_2, 1000 rpm, pH 4.0, 1 wt.% NaCl).

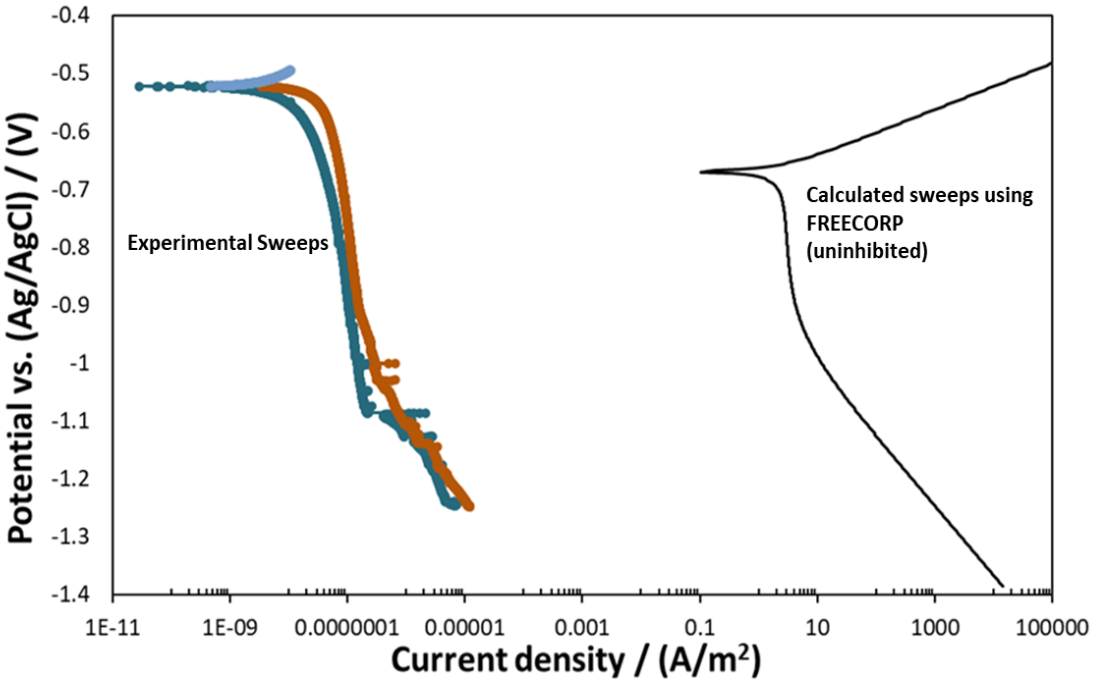

Figure 44. Potentiodynamic sweeps of the specimen with commercial CI vs. uninhibited conditions (30°C, 0.97 bar pCO_2, 1000 rpm, pH 4.0, 1 wt.% NaCl).

It is reported that in batch application, the contact time is in a range of 10 to 15 seconds depending on the CI slug volume and the velocity [73]. The extended contact time of 5 minutes in the previous experiment was selected to ensure proper inhibitor film formation, which was later adjusted in subsequent experiments. For the next step, the effects of shorter contact time and higher temperature were studied. Figure 45 shows three different repeats of an experiment in which the contact time was 10 seconds, and the temperature was initially 30°C for 1.5 days. Since no change in corrosion efficiency was observed and waiting for a few more days, as in the previous experiment, was impractical, the temperature was increased to 45°C to examine the effects of elevated temperature. Results showed that the contact time has little effect on inhibitor efficiency.

The increase in temperature caused an increase in the corrosion rate, however, the inhibitor remained persistent and showed similar inhibitor efficiency based on a higher baseline corrosion rate at the higher temperature.

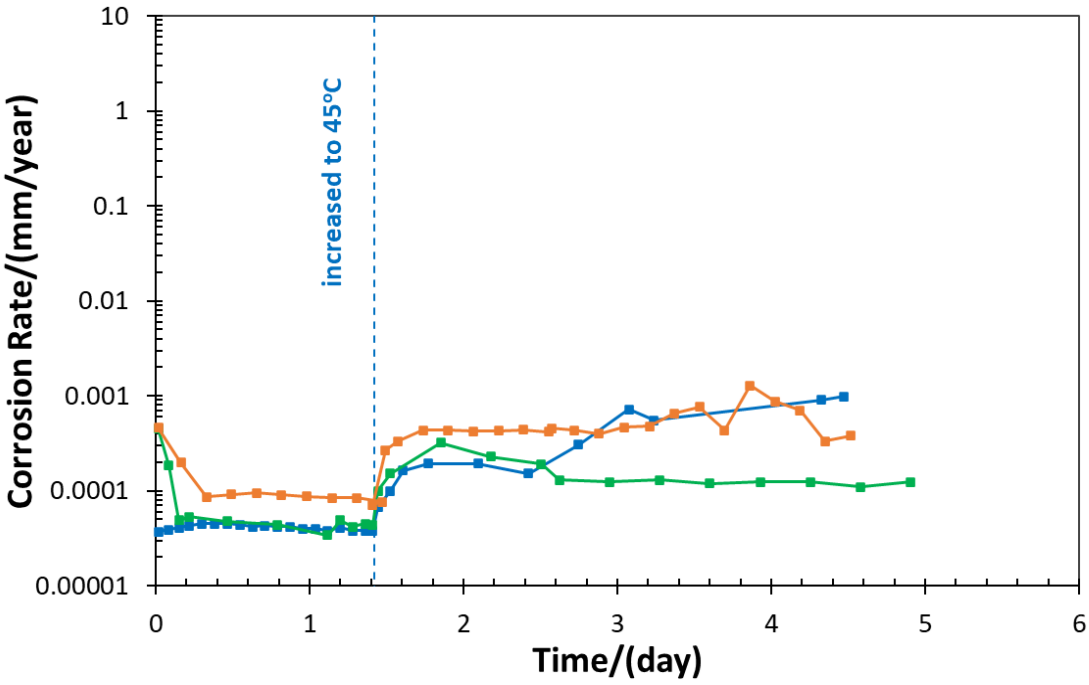

Figure 45. Effect of shorter contact time and elevated temperature on commercial batch CI persistency (30°C to 45°C, 0.97 bar pCO_2, 1000 rpm, pH 4.0, 1 wt.% NaCl).

Since this commercial batch CI showed excellent persistency throughout the laboratory testing period, further investigations were warranted, particularly at elevated temperatures. The underlying hypothesis suggests a decline in persistency at higher temperatures, allowing for the observation of persistency degradation over the course of the experiment. Two different sets of experiments were done for the next steps. In the first set, an experiment started at an initial temperature of 30°C, which was increased to

60°C after 1.5 days. The results of this experiment, depicted in Figure 46 and compared to previous findings, indicated an apparent increase in corrosion rate following the temperature elevation. Despite this increase, the inhibitor maintained excellent persistency within the experimental timeframe. To further evaluate inhibitor performance at 60°C, additional experiments were conducted, maintaining a constant temperature throughout the entire experimental duration. Figure 47 presents a comparative analysis between an experiment initiated at 30°C with a subsequent temperature increase to 60°C and an experiment conducted consistently at 60°C. In the experiment with a constant temperature of 60°C, an increase in corrosion rate occurred after 3.5 days, indicating a partial loss of inhibition that was not observed in previous electrochemical measurements. The specimen exhibited signs of localized corrosion at the end of the experiment, which is believed to have originated from the partial loss of inhibition. Figure 48 illustrates multiple repetitions of the batch inhibition experiment conducted at 60°C. Across all iterations, there was a consistent observation of partial loss in inhibition and persistency after 3 to 3.5 days into the experiment. This implies that this commercial batch CI, when employed for protection at 60°C, exhibits a persistency window of approximately 3 days.

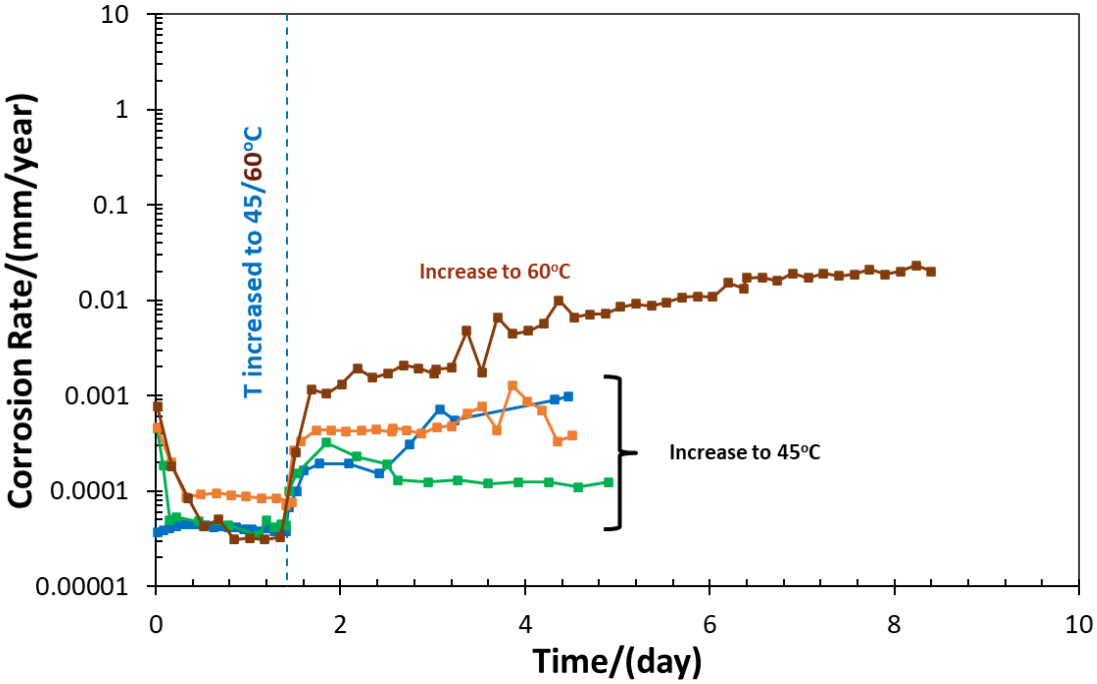

Figure 46. Effect of elevated temperature on commercial batch CI persistency (30°C to 45/60°C, 0.97 bar pCO_2, 10s contact time, 1000 rpm, pH 4.0, 1 wt.% NaCl).

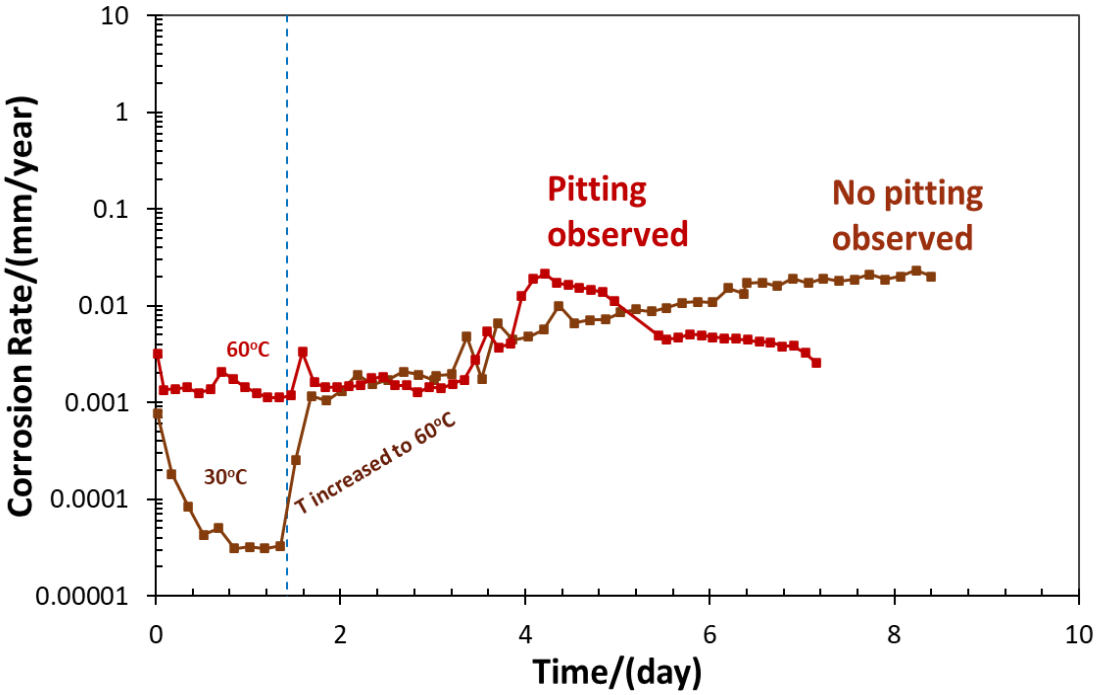

Figure 47. Effect of elevated temperature on commercial batch CI persistency (0.97 bar pCO_2, 10s contact time, 1000 rpm, pH 4.45, 1 wt.% NaCl).

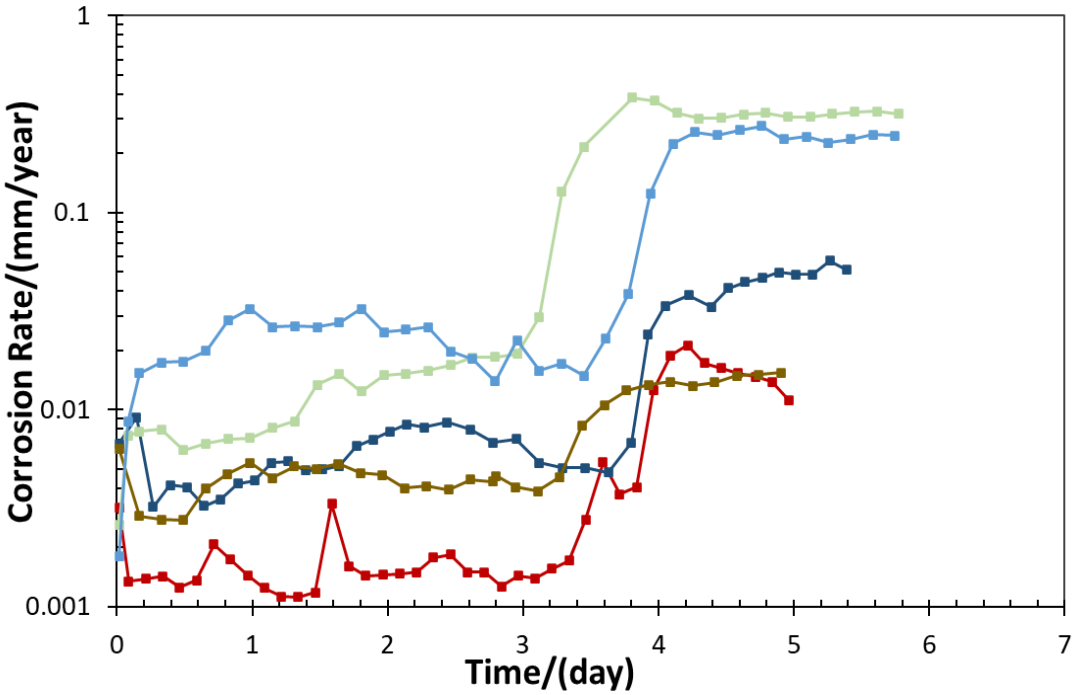

Figure 48. Different repeats for batch inhibition persistency experiment with commercial inhibitor at 60°C (0.97 bar pCO_2, 10s contact time, 1000 rpm, pH 4.45, 1 wt.% NaCl).

Figure 49 presents an image of the specimen at the end of one of the repeated experiments (corresponding to the green line in Figure 48), as retrieved, along with the profilometric surface analysis. The deepest pit depth was measured at 273 μm (the experiment represented in green line was run for 9 days and pitting corrosion calculation was done for 6 days after inhibition loss) which corresponds to a pitting rate of 16.6 mm/year. This means that the localized corrosion rate to inhibited corrosion rate ratio was $\frac{16.6}{0.3} = 55.3$, which is considered to indicate a very high probability for localized corrosion [111]. Even when compared to the uninhibited general corrosion rate under the same environmental conditions, which was measured between 11-13 mm/year, it seems to show that a slight galvanic effect may be occurring which increased the pitting rate. It

is obvious that the specimen had undergone harsh localized corrosion after loss of persistency.

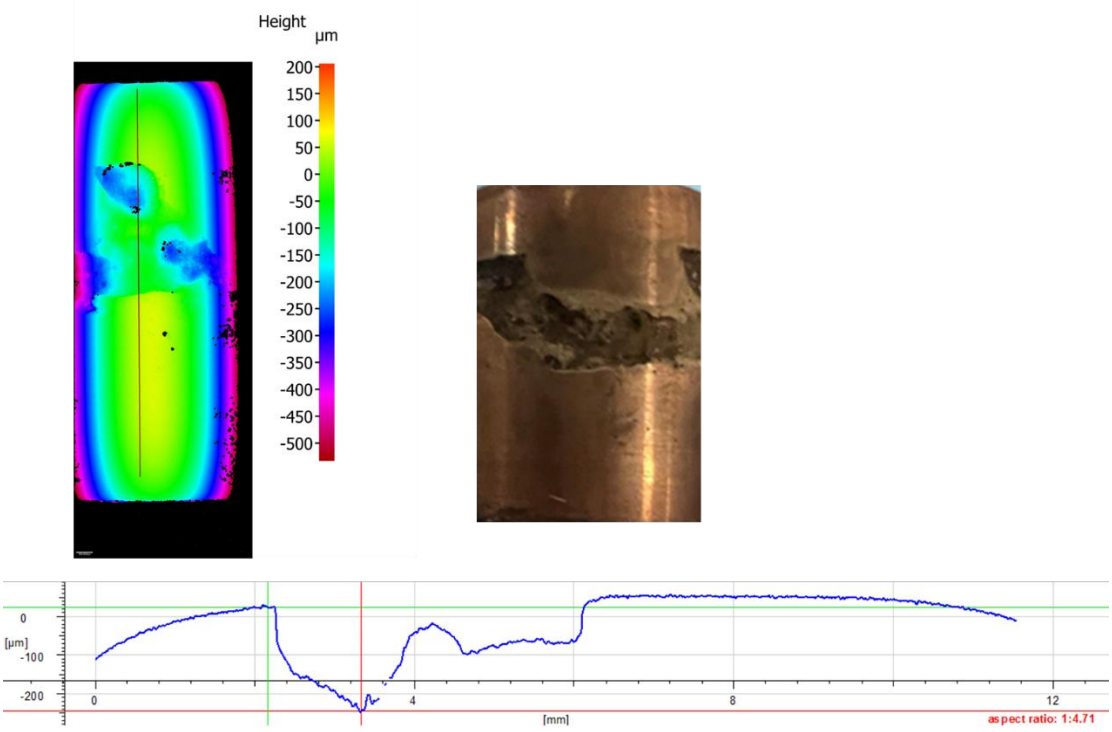

Figure 49. Profilometer analysis (left and bottom) with associated picture of the sample with severe localized corrosion after loss of inhibition at 60°C.

Additional experiments at 60°C were repeated without any solution dilution. This was done to verify that the inhibitor's failure was exacerbated by the continuous flow-through methodology of the experimental procedure and not solely attributed to the higher temperature. Figure 50 presents a comparison between the results of this undiluted experiment and the average results of the experiments with continuous dilution. This comparison verified that the loss of inhibition was highly dependent on the dilution method, which more closely mimics field conditions. In other words, the continuous

dilution methodology employed in these experiments is a crucial parameter for correlating laboratory batch inhibition studies with operational field conditions.

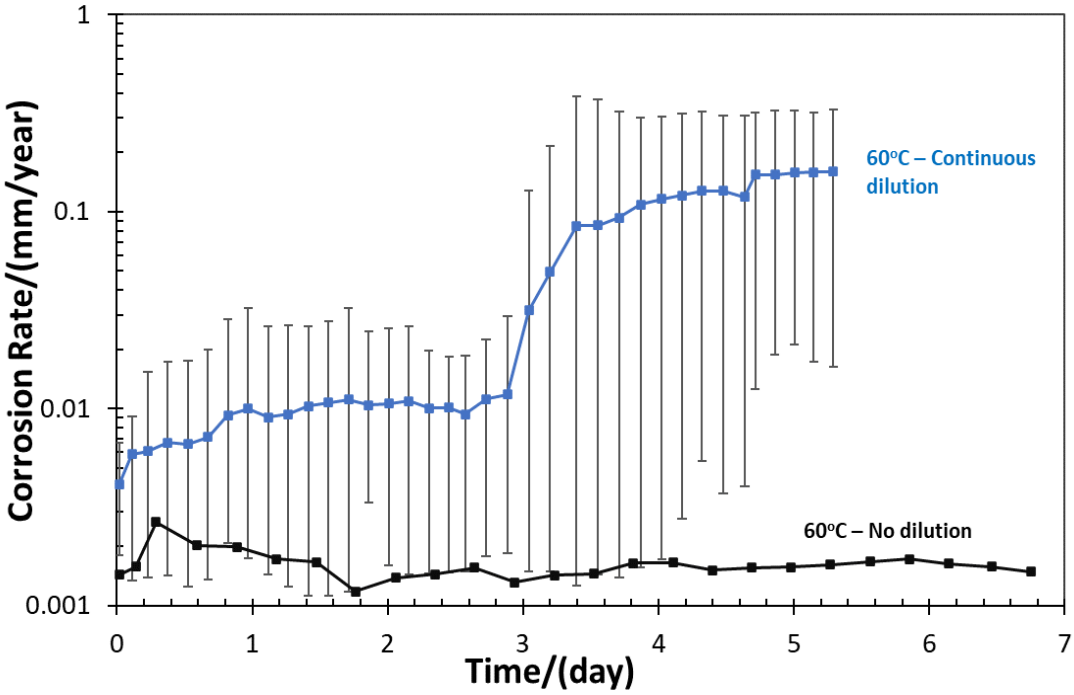

Figure 50. Comparison of batch inhibition experiment with and without continuous dilution (60°C, 0.97 bar pCO_2, 10s contact time, 1000 rpm, pH 4.45, 1 wt.% NaCl).

Another set of experiments were conducted at 80°C to investigate the effects of even higher temperature on this commercial batch CI. Figure 51 shows the results of two different repeats at this temperature. Results show that although the inhibition efficiency is high (~99%), the inhibited corrosion rate was close to the unacceptable corrosion rate threshold for field application (set at 4 mil/year or 0.1 mm/year [112]). Consequently, no further experimental work was conducted at this temperature.

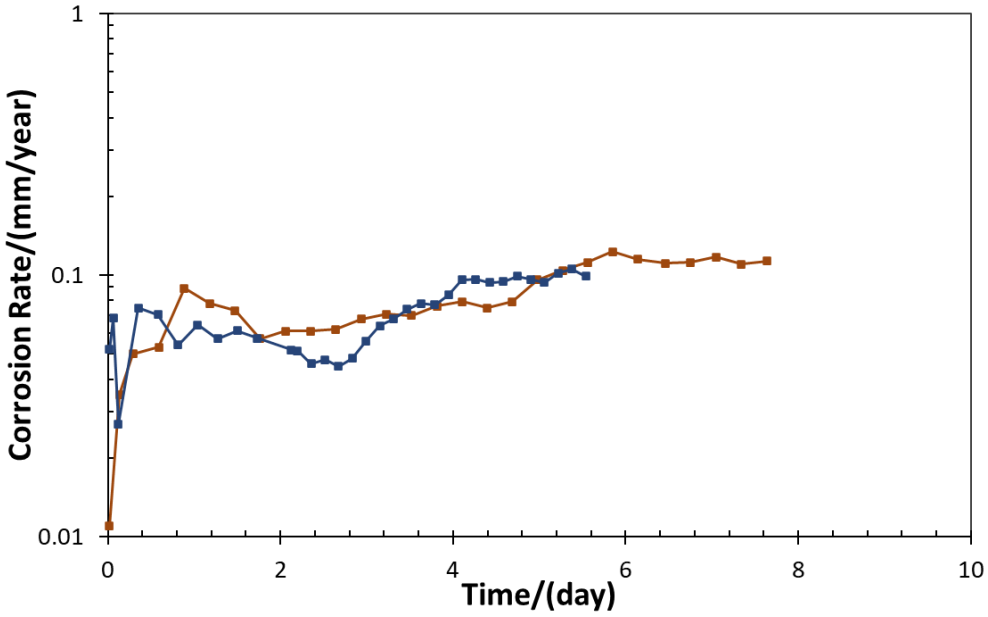

Figure 51. Batch inhibition persistency experiment with commercial inhibitor at 80°C (10s contact time, 0.97 bar pCO_2, 1000 rpm, pH 4.65, 1 wt.% NaCl).

6.3.2 Effect of Presence of Hydrocarbon on Commercial CI Persistency

One of the parameters that can affect inhibitor behavior and persistency is the presence of a hydrocarbon phase. This is particularly relevant since all pipelines carrying oil and gas fluids operate in two-phase oil/water flow or three-phase gas/oil/water flow. Previous studies showed that oil wetting of the specimen can affect the corrosion rate and surface characteristics [80, 81]. As is shown in Figure 52, the hypothesis here is that hydrocarbon molecules that are dispersed in water phase, can interact with the inhibitor hydrocarbon tail which can enhance the inhibitor performance and persistency time.

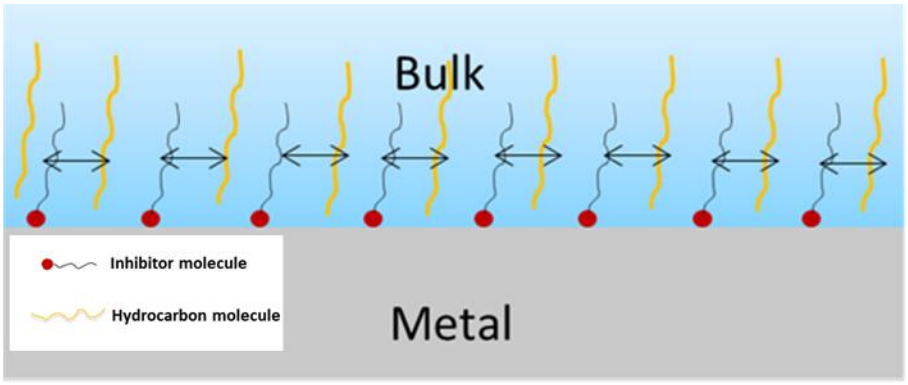

Figure 52. Interaction between inhibitor and oil molecules near the metal surface.

Experiments were conducted involving the introduction of 20 mL of LVT-200 on top of 1780 mL of brine (1 wt.% NaCl), equivalent to 1.1% (v/v) to investigate the impact of hydrocarbon presence on commercial batch corrosion inhibitor (CI). The experimental procedure entailed the initial addition of 1780 mL of brine into the glass cell, followed by the subsequent introduction of 20 mL of pre-sparged LVT-200 into the system. The entire solution was continuously diluted at a rate of 40 mL/minute. The continuous addition of fresh solution through the oil layer into the glass cell was observed to entrain and disperse oil droplets into the bulk solution. This observation aligns with the fact that LVT-200 exhibits extremely low solubility in water (~1.5 g/L)[§]. To counteract the dispersion of hydrocarbon molecules and the gradual loss of oil due to continuous dilution, LVT-200 was replenished every 24 hours, ensuring the sustained presence of the oil phase until the conclusion of the test. Figure 53 shows different repeats of the batch inhibition experiments in the presence of hydrocarbon molecules compared to the

[§] chrome-extension://efaidnbmnnnibpcajpcglclefindmkaj/https://deep-south-chemical.com/PDF%27s/SDS/LVT_200_PEN1090-00-C_US_GHS_English-Copy.pdf.

average results obtained in the absence of LVT-200. Results show that the presence of hydrocarbon and its subsequent dispersion into the brine phase enhanced the CI efficiency, increasing it from 99.94% to 99.99%, while also prolonging its persistency for a minimum of six days. These findings support the initial hypothesis by demonstrating the positive impact of hydrocarbon molecules compared to the experiments conducted without their presence. This raises two possible hypotheses. One scenario is that the hydrocarbon components in the commercial CI package play a critical role in inhibitor persistency. These components render the inhibitor package non-water-soluble, preventing it from dissolving into the bulk phase and thereby enhancing its persistency. However, when the inhibitor loses its persistency, it suggests that the inhibitor package on the surface has dissolved into the bulk phase. In this case, the presence of hydrocarbons in the system may counteract this dissolution by replenishing the dissolved components of the inhibitor package. An alternative scenario is that hydrocarbon molecules in the system reach the metal surface, interact with the inhibitor molecules, and slow down their desorption, thereby enhancing inhibitor persistency. These hypotheses are further examined in the next chapter.

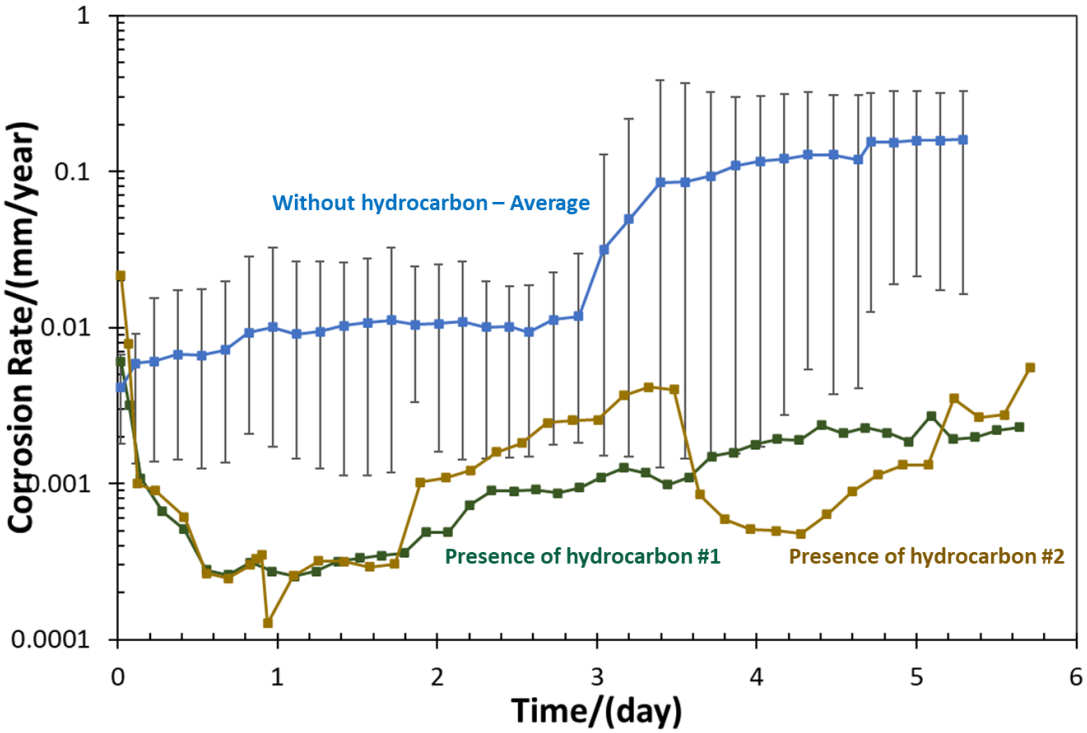

Figure 53. Comparison of batch inhibition experiment with and without presence of hydrocarbon (60°C, 0.97 bar pCO_2, 10s contact time, 1000 rpm, pH 4.45, 1 wt.% NaCl).

6.4 Summary

A commercial batch CI was used to validate the experimental procedure developed for batch inhibition persistency experiment. Although the inhibitor had excellent efficiency and persistency at lower temperatures, it showed only 3 days persistency at 60°C. The following conclusions can be taken from these experiments:

- Continuous dilution of the solution is a critical parameter in laboratory batch inhibition experiments as it ensures minimal residual inhibitor in the bulk solution, thereby closely mimicking field conditions.
- All instances of observed inhibition failure and loss of persistency resulted in pitting corrosion of the metal surface.

- Presence of LVT-200 dispersed in the water phase enhanced the persistency of the inhibitor, which suggests that the incorporation of hydrocarbon molecules (either as LVT-200 or as a solvent in the CI package) with the CI film plays a key role in batch CI persistency.

Chapter 7: Parametric Study of Batch Inhibition Persistency With Model Compound Inhibitor Package[**]

7.1 Introduction

As discussed in the preceding chapter, a novel methodology was developed to enhance the simulation of inhibitor persistency in batch inhibition treatments. However, the commercial inhibitor utilized in the previous chapter, owing to its proprietary formulation, did not permit a comprehensive understanding of the underlying mechanisms governing inhibitor persistency and the impact of inhibitor molecular structure on CI persistency. Consequently, the primary objective of this chapter is to address this shortcoming. This is achieved by developing and utilizing an inhibitor package with known formulation comprising a synthesized model compound and well-defined solvents and carriers. The performance of this model inhibitor package is anticipated to be lower than that of the commercial product. However, the objective of this section is not to develop a superior inhibitor chemistry but rather to gain insight into the operational parameters that influence persistency. The specific goals of this chapter are as follows:

- Identify a suitable model compound inhibitor that exhibits a measurable level of corrosion inhibitor (CI) persistency in batch treatment following the removal of

---

[**] A version of this chapter was published as:

#2: "Effects of Temperature and Presence of Hydrocarbon on Commercial Batch Inhibitor Persistency using a Developed Methodology," in AMPP Annual Conference+Expo 2025, paper no. 00335 (Nashville, TN: AMPP 2025). (Reference number: [109])

#1: "Methodology for Corrosion Inhibitor Persistency Studies in Batch Inhibition," *CORROSION* (2024), 80 (10). (Reference number: [113])

residual inhibitor from the glass cell. A longer alkyl tail in the inhibitor structure reduces water solubility; thus, it is hypothesized that an inhibitor with a longer alkyl tail will demonstrate improved persistency for the same inhibitor type.

- Identify the key parameters influencing inhibitor persistency:
  - Solvent type: The choice of inhibitor solvent in the batch CI package is critical in determining its physical properties, such as viscosity and solubility in water. Therefore, it is hypothesized that a solvent with lower water solubility and a high affinity to solubilize the inhibitor molecule will enhance the persistency of the inhibitor package.
  - Flow velocity: Increased flow velocity leads to higher mass transfer/shear stress and a faster dissolution rate, which can influence inhibitor persistency. This effect can be examined by increasing the rotational speed of the rotating cylinder electrode (RCE), as the higher rotational speed would enhance fluid movement, thereby improving mass transfer and potentially accelerating the dissolution of the inhibitor package from the surface.
  - Presence of hydrocarbon: Previous studies have demonstrated that the presence of oil can affect inhibitor behavior [77-81]. As shown in the previous chapter, hydrocarbon molecules can incorporate into the corrosion inhibitor (CI) film formed on the surface, thereby enhancing persistency. Consequently, the presence of hydrocarbon can increase the model compound batch CI persistency significantly.

- Develop a modeling approach for predicting corrosion inhibitor persistency in batch inhibition, considering various parameters.

7.2 Experimental Procedures and Test Matrix

The experimental setup and methodology employed in this chapter closely resemble those described in the preceding chapter. The experimental parameters that were selected to test the hypothesis and research questions explained above are discussed here:

Inhibitor type: Firstly, the same quaternary ammonium-type inhibitor used in the continuous treatment, but with a longer alkyl tail (BDA-C16), was selected to facilitate a better comparison between batch and continuous treatment; the longer alkyl tail was chosen to reduce water solubility while maintaining the same head group. Finally, the inhibitor type was modified to a phosphate ester, as this class of inhibitors exhibits higher inhibition efficiency at lower concentrations. A detailed explanation of the theoretical rationale for selecting each inhibitor is provided in the respective sections.

Solvent: Two types of solvent were selected for this part: one that could be used to solubilize the inhibitor and another one that acted as a "carrier" for the inhibitor package. Isopropanol and butoxyethanol were selected as they are known to dissolve the solid inhibitor. Oil-soluble solvents and a viscous solvent were utilized to investigate the effects of "carrier" solvent type on inhibitor persistency.

Presence of hydrocarbon: LVT-200 model oil was used in one set of experiments, as in the previous chapter, to examine the effects of straight chain hydrocarbon molecules and their potential incorporation into the CI film formed on the surface.

RCE rotational speed: In all experiments, except those investigating the effects of shear stress, the rotational speed was maintained at 1000 rpm. However, rotational speeds of 0 and 2000 rpm were selected to examine the effects of decreased and increased shear stress on batch CI persistency.

Table 6 presents the experimental matrix for the experiments conducted in this chapter.

Table 6. Experimental matrix for batch inhibition treatment persistency experiments with model compound CI.

Parameter	**Conditions**
Working electrode	API 5L X65 (0.035 wt.%C)
Solution	1 wt.% NaCl
Sparged gas	CO_2
Total pressure	1 bar
RCE rotational speed	0, 1000 and 2000 rpm
Temperature	30 $^{\circ}$C ± 1°C
pH	4.00 ± 0.1
Corrosion inhibitor type	Benzyldimethylammonium (BDA)-C16, BDA-C22, Phosphate ester (PE-C14)
Measurement methods	OCP, LPR, EIS
Contact time	5 minutes or 10 seconds
Initial inhibitor concentration	1.5, 7.5 and 15 wt.%
Inhibitor solvent	Isopropanol, butoxyethanol, LVT-200, alkylphenolethoxylate, diesel
Presence of hydrocarbon	0 – 1% (v/v) LVT-200
Pre-corrosion before CI application	No pre-corrosion

7.3 Results and Discussion

7.3.1 Study of Batch Inhibition With BDA-C16 and BDA-C22 Using Different Solvents

The first step in conducting batch persistency experiments with a known model compound inhibitor was to select the appropriate inhibitor type. BDA-C14 was utilized in the continuous treatment CI persistency phase of this study. Therefore, to ensure a better comparison with the experiments in continuous treatment, the same inhibitor type (quaternary ammonium) was chosen for the initial batch CI persistency experiments. However, since the alkyl tail with 14 carbons exhibited adsorption/desorption behavior without persistency, a longer alkyl tail (hexadecyl, 16 carbons) was selected to reduce water solubility and potentially enhance persistency. However, BDA-C16 needed to be tested in terms of inhibition efficiency in a continuous treatment experiment before conducting any batch inhibition experiments. Thus, 136 mg solid BDA-C16 was dissolved in 3 ml isopropanol (5.8 wt.%) and 2 ml of that solution was added to 1.8 L NaCl 1wt.% to make CI concentration of 50 ppm_w in the solution. Figure 54 shows the results for this experiment in which BDA-C16 was added to the glass cell after 15 minutes pre-corrosion. These three repeats show that BDA-C16 baseline inhibition decreased the corrosion rate from 4.00 mm/year to 0.02 mm/year with a good repeatability.

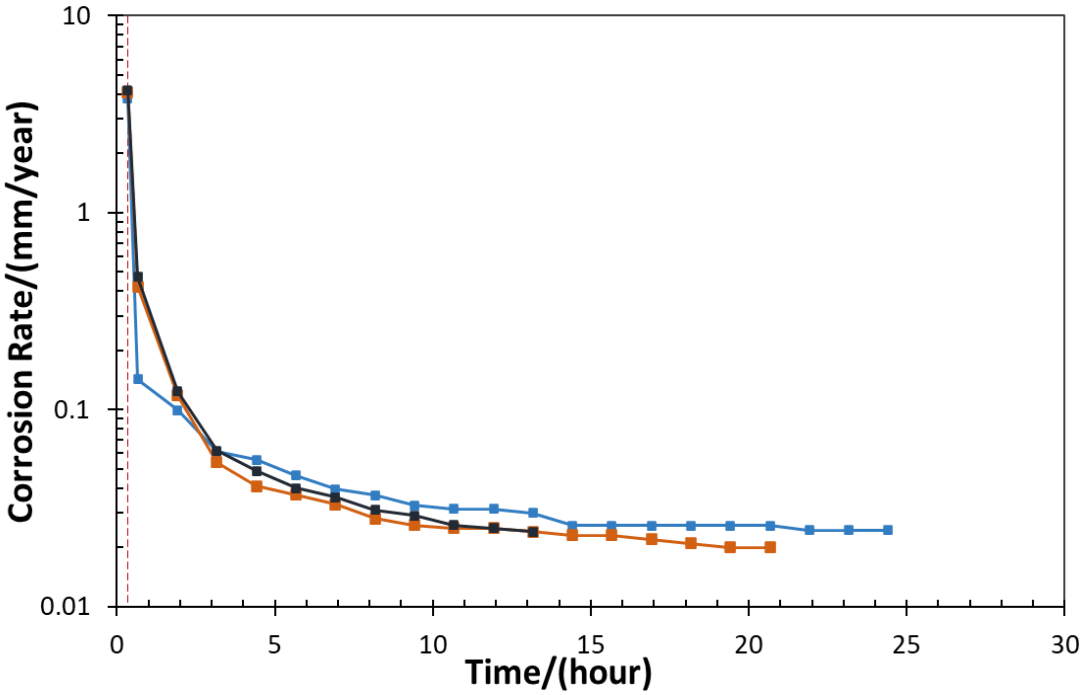

Figure 54. Baseline inhibition results for BDA-C16 (30°C, 0.97 bar pCO_2, 1000 rpm, pH 4.0, 1 wt.% NaCl).

The next step was to test BDA-C16 in batch inhibition to confirm that the proposed methodology is effective in ascertaining the persistency of this model compound inhibitor. The first experiment was conducted with BDA-C16 and isopropanol as solvent, because of the high solubility of BDA-16 at 15 wt%. As mentioned earlier, BDA-C16 had also been previously tested as a continuous type CI and was shown to mitigate corrosion to 0.1 mm/yr at a concentration as low as 50 ppm_w [100]. This inhibitor is, however, not expected to be very persistent on its own. Using the same experimental procedure as proposed in section 6.2, the steel specimen was dipped into the 15 wt.% BDA-C16 in isopropanol for 5 minutes contact time to provide the "excessive amount of time" for the batch treatment methodology. After conducting the inhibitor film

formation procedure as defined in this research, the uninhibited brine was introduced to the glass cell and the electrochemical measurements were conducted. Figure 55 shows two repeats of this experiment with 15 wt.% BDA-C16 dissolved in isopropanol and their associated change in corrosion rate/inhibitor concentration with time. It is noteworthy that the absorbance of different samples taken from the solution after dilution was measured using UV-Vis spectroscopy. The corrosion inhibitor (CI) concentration was then calculated based on the procedure explained in section 3.4.3 and the calibration curve developed for BDA-C16 by Pan, *et al*. [114]. The results show that after introducing the brine to the glass cell, the inhibitor concentration dropped significantly showing the ability of inhibitor removal in this methodology. In addition, the corrosion rate started at higher value than the baseline inhibited corrosion rate (measured at 0.1 mm/y [100]) and increased to uninhibited value (~4 mm/year) after 50 hours, showing no inhibitor persistency.

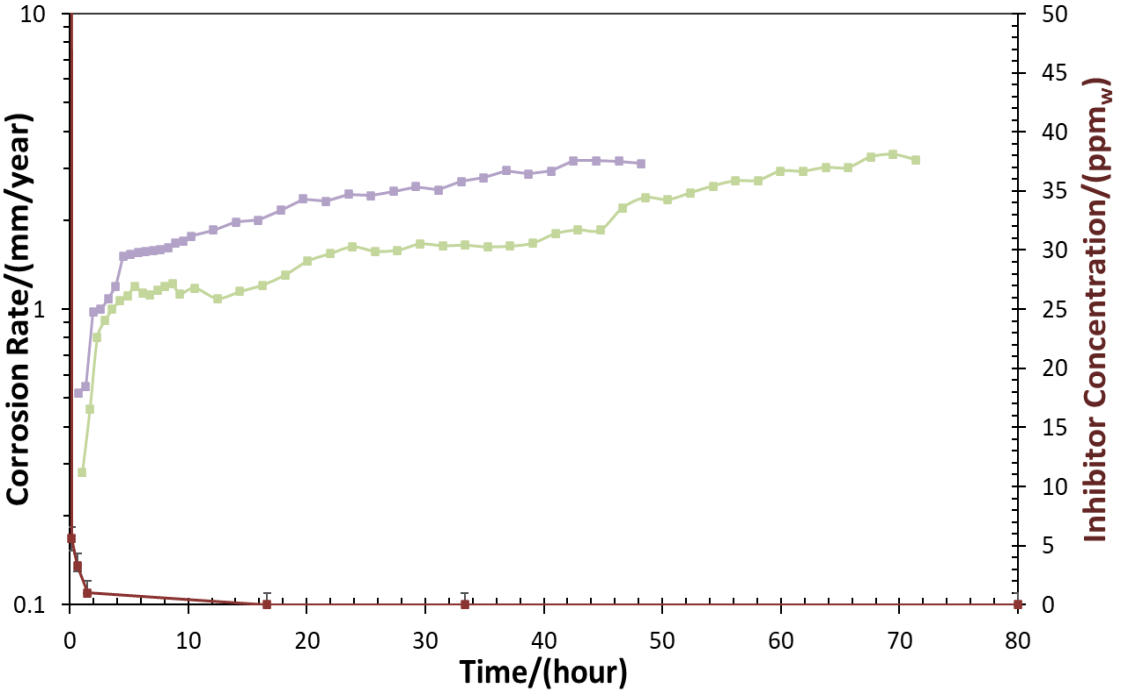

Figure 55. Batch inhibition persistency experiment with 15 wt.% BDA-C16 in isopropanol (30°C, 0.97 bar pCO_2, 1000 rpm, pH 4.0, 1 wt.% NaCl).

The next research question addressed the effects of solvent on inhibitor persistency. The hypothesis behind the next set of experiment was that linear aliphatic hydrocarbon molecules could incorporate with the inhibitor adsorbed layer and enhance the persistency of the inhibitor. Thus, for the next step, LVT-200 was used as the solvent for BDA-C16. The specimen was dipped into an inhibitor solution with 7.5 wt.% BDA-C16 in LVT-200 (instead of isopropanol). The highest solubility of BDA-C16 in LVT-200 was used in this experiment. Figure 56 shows the results for corrosion rate/inhibitor concentration versus time. Results show that although the initial corrosion rate was again higher than the baseline inhibited corrosion rate for BDA-C16, but remained low for 2 hours and gradually increased over time to reach the uninhibited value after 15 hours of

exposure. This suggests that the presence of alkanes in the system seems to lead to a short period of persistency (which was not seen with using isopropanol only). Therefore, the incorporation of hydrocarbon into the CI adsorbed layer was confirmed.

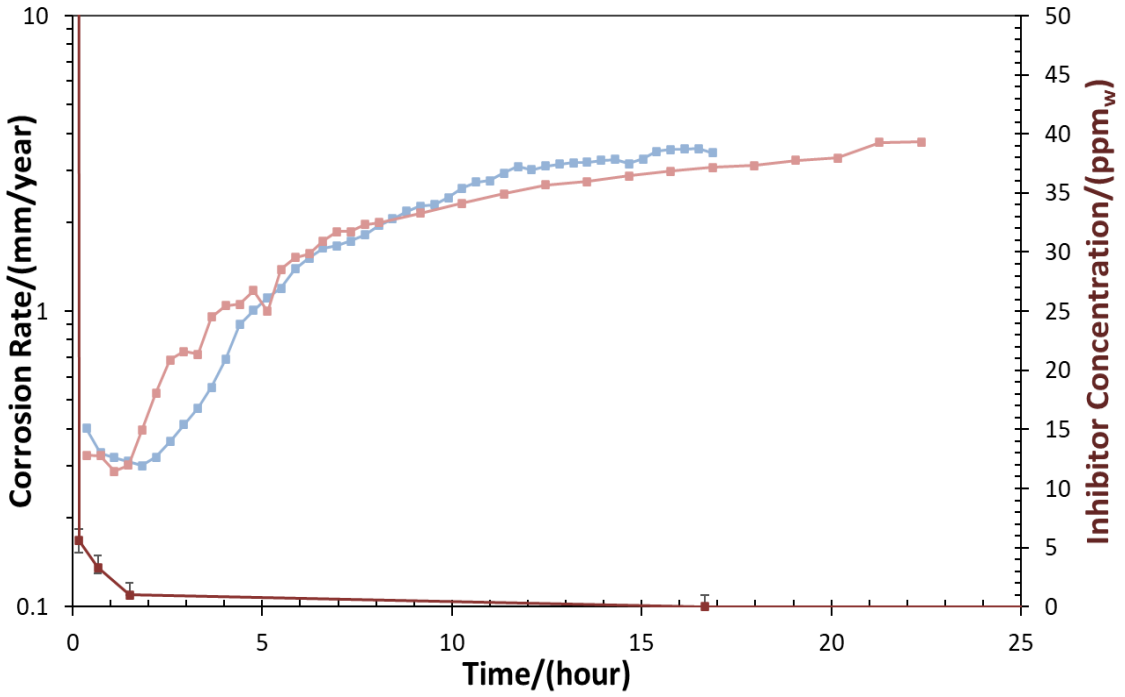

Figure 56. Batch inhibition persistency experiment with 7.5 wt.% BDA-C16 in LVT-200 (30°C, 0.97 bar pCO_2, 1000 rpm, pH 4.0, 1 wt.% NaCl).

Other experiments were conducted with BDA-C22 in order to investigate the effect of a longer alkyl tail, -$C_{22}H_{45}$, on batch inhibition persistency. As noted in the introduction, increasing the alkyl tail length of quaternary ammonium inhibitors enhances their hydrophobicity. This property, characteristic of amphiphilic molecules, is expected to improve their persistence. BDA-C22 is not soluble in isopropanol or LVT-200. Thus, butoxyethanol was used to make 7.5 wt.% BDA-C22 inhibitor solution. Figure 57 shows

the results for BDA-C22 batch inhibition persistency. Since BDA-C22 exhibited limited solubility in water, developing a UV-vis calibration curve for its concentration was not feasible. However, due to the similarity in dilution flow rate and initial inhibitor concentration, the concentration profile of BDA-C22 was assumed to be similar to that of BDA-C16 in the previous experiment, and this is presented in Figure 57. In both repeat experiments, the corrosion rate initially showed poor inhibition and rapidly increased to values approaching those observed in the absence of inhibitor. Results suggest that there was no discernible effect of a longer alkyl tail on the CI persistency of BDA-22 compared to BDA-C16. This may be related to the relatively small increase in alkyl tail length between BDA-C16 and BDA-C22.

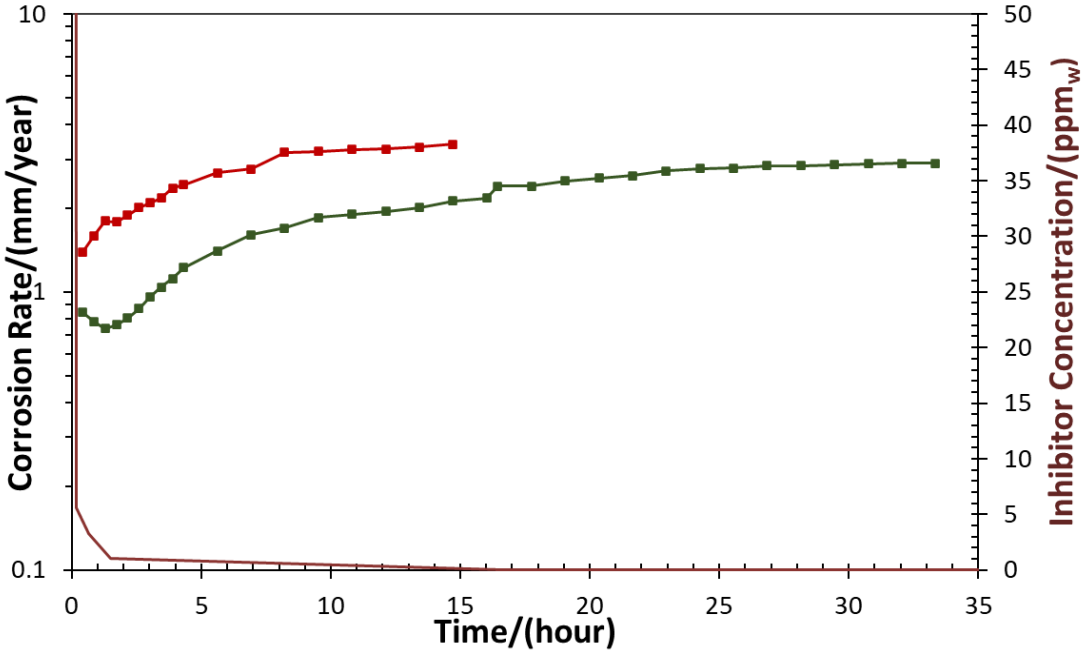

Figure 57. Batch inhibition persistency experiment with 7.5 wt.% BDA-C22 in butoxyethanol (30°C, 0.97 bar pCO_2, 1000 rpm, pH 4.0, 1 wt.% NaCl).

7.3.2 Study of Batch Inhibition With PE-C14 Using Different Solvents

BDA-C16 and BDA-C22 alone did not demonstrate acceptable persistency in batch treatment, whereas the commercial inhibitor package exhibited high effectiveness and persistency. While the properties of the corrosion inhibitor play a crucial role in its performance, the persistency of commercial CI formulations is hypothesized to be influenced by additional factors. Specifically, it is proposed that the observed persistency is not solely a function of the active CI component desorption rate. Rather, solvents and carriers within the formulation are posited to create an initial protective barrier, thereby delaying CI desorption. This mechanism suggests that inhibition persistency is determined by the time required for complete dissolution of these solvents and carriers, followed by the subsequent desorption of the active inhibitor layer. Therefore, "known" inhibitor packages, composed of a model compound inhibitor and well-defined solvents or carriers, are considered for further investigation of this hypothesis. Herein, it was proposed that phosphate ester model compound inhibitor (PE-C14) that previously showed high efficiency in continuous treatment and lower water solubility [48] (compared to BDA-C16 and BDA-C22) could be used with a viscous solvent such as alkylphenolethoxylate (AE) to provide both an excellent initial inhibition and measurable persistency. The use of a viscous solvent could decrease the dissolution rate of the CI package, as outlined in the proposed mechanism. However, PE-C14 has very low solubility in AE. Therefore, another solvent that has high solubility for PE-C14 was needed in this “known” inhibitor package. Given the relatively high solubility of PE-C14 in butoxyethanol (BE), it was postulated that an inhibitor package composed of PE-C14,

AE, and BE would be more suitable for investigating the underlying mechanisms governing CI persistency during batch treatment. It is noteworthy that LVT-200 showed limited ability to solubilize PE-C14 and that is why it was not used here. Figure 58 and Figure 59 show the structure for this model compound inhibitor and these two carriers, respectively. In addition, Table 7 shows the viscosity and PE-C14 relative solubility in these two solvents.

Figure 58. Molecular structures of in-house synthesized tetradecyl phosphate ester (PE-C14) (73.5% monoester & 25.5% diester) (reprinted with permission from [48]).

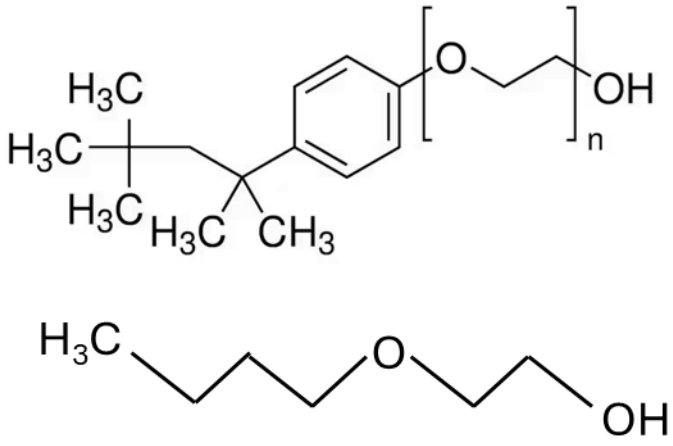

Figure 59. Molecular structure of the viscous alkylphenolethoxylate type solvent (top; n = 9–10 ethylene oxide units) and 2-butoxyethanol (bottom).

Table 7. Viscosity and solubility for PE-C14 for two solvents.

Solvent	Viscosity (cP)	PE-C14 relative solubility
Butoxyethanol (BE)	2.9	High
Alkylphenolethoxylate (AE)	300	Low

The first step was to test the PE-C14 in a continuous treatment experiment to ensure good efficiency of this model inhibitor in a CO_2 corrosion environment. Therefore, 68 mg PE-C14 was added to 3 mL isopropanol and then 2 mL of the solution was added to 1.8 L working solution after 15 minutes of pre-corrosion at 30°C to achieve 25 ppm_w PE-C14 in the brine. Figure 60 shows the corrosion rate results versus time for two different repeats.

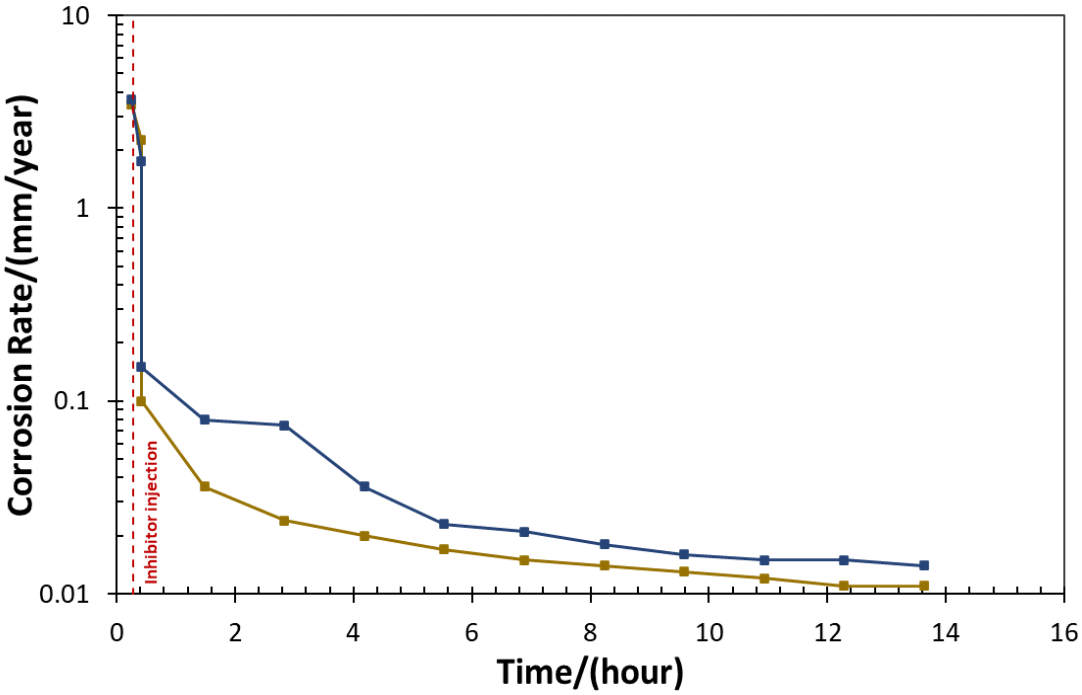

Figure 60. Corrosion rate versus time with PE-C14 injected after 15 minutes pre-corrosion in continuous treatment (30°C, 0.97 bar pCO_2, 25 ppm_w PE-C14, 1000 rpm, pH 4.00, 1 wt.% NaCl).

Results for PE-C14 in continuous treatment confirmed the high efficiency of this model compound inhibitor. Subsequently, batch inhibition persistency experiments were conducted with different solutions. Initially, PE-C14 was dissolved in BE (1.5 wt.%) to investigate the persistency of PE-C14 in a solvent with low viscosity but high solubility for PE-C14. Figure 61 shows the results of two repeats with this inhibitor package, represented by the green line. These results show that although PE-C14 is highly soluble in BE, the inhibitor molecules desorbed from the surface as soon as the fresh uninhibited brine was introduced into the glass cell. This was expected since BE is highly soluble in water. Before using AE with PE-C14 and BE, experiments were necessary to examine the effects of AE only on CO_2 corrosion. Figure 61 shows the repeats for corrosion rate

versus time with pure AE without inhibitor, represented by the red line. These results show that AE had some inhibition effect on corrosion rate, however, the inhibition efficiency and persistency was very low. For the next step, 1.5 wt.% PE-C14 was made with 18 mL AE and 3 mL BE. Figure 61 shows the results for two repeats of experiment with this "known" inhibitor package, represented by the blue line. The 90% efficiency threshold, represented by the dotted line in Figure 61, was used to define the persistency time (as the duration during which the inhibition efficiency remains above 90%). Based on this definition, this inhibitor package exhibited a persistency time of 4 hours. The corrosion rate results for this CI package revealed a distinct inhibition and desorption behavior of PE-C14. Previously, PE-C14 exhibited immediate desorption upon dilution; however, in this study, a delay followed by gradual desorption was observed. This suggests that the use of a viscous solvent temporarily acted as a barrier to inhibitor desorption. A plausible explanation is that the viscous solvent gradually dissolved into the bulk solution, with the duration of this process corresponding to the observed delay in inhibitor desorption representing the CI persistency. Once the viscous solvent was fully removed from the surface, the inhibitor began to desorb, leading to an increase in the corrosion rate until it reached the uninhibited level. Thus, it could be postulated that this behavior consists of two general steps: first, the dissolution of the CI package solvent into the bulk, and second, the desorption of the monolayer inhibitor molecules from the metal surface. These findings, based on an inhibitor package composed of two solvents (AE and BE) and the model compound inhibitor (PE-C14), indicate that PE-C14 could be further explored in batch inhibition persistency studies when dissolved in a viscous

solvent that enhances persistency. As a final step, the combined effect of both solvents, without the inhibitor, was tested and the results are presented in Figure 61 represented by the orange line. Although the mixture of viscous AE and BE without inhibitor showed some level of inhibition, inhibition efficiency and persistency were still much lower than in the presence of PE-C14.

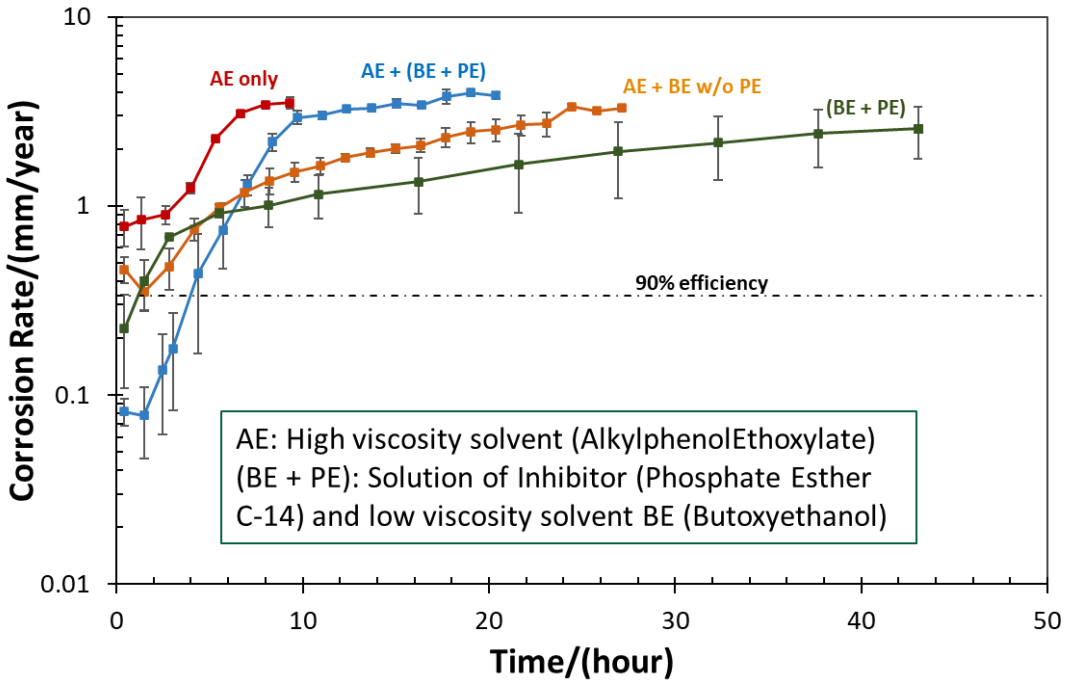

Figure 61. Batch inhibition persistency experiment of different packages with or without PE-C14 (30°C, 0.97 bar pCO_2, 1000 rpm, pH 4.00, 1 wt.% NaCl).

As a summary of these sets of experiments with model compound inhibitor and two known solvents/carriers, Table 8 shows the inhibition efficiency and persistency of different packages that were tested.

Table 8. Summary of inhibition efficiency and persistency for 4 different solvents.

Inhibitor package	**Initial inhibition efficiency**	**Persistency**
BE + PE	93.8 %	< 1 hour
AE (without PE)	87.5 %	N/A
AE + BE (without PE)	55.8 %	N/A
AE + PE + BE	97.6 %	4 hours

Batch inhibition persistency using PE-C14 and a viscous solvent demonstrated that the addition of a viscous solvent to the CI package enhances inhibitor persistency, as hypothesized. This suggests that upon dilution, the viscous solvent, which acts as a barrier to inhibitor desorption, first gradually dissolves into the bulk solution. Once the viscous solvent has completely left the surface, the inhibitor begins to desorb, following desorption kinetics.

7.3.3 Effects of Flow and Presence of Hydrocarbon on Batch CI Persistency With PE-C14 Package

The previous section enabled the identification of a model inhibitor in a known package (CI + solvent) with limited, but defined, persistency. The next phase of the study was focused on investigating the general mechanism behind persistency behavior. To gain insights into the underlying process and examine the proposed mechanism, parametric studies were conducted to investigate the influence of two key factors: flow velocity, which affects mass transfer and dissolution rate, and the presence of hydrocarbons. Both factors play a crucial role in the persistency mechanism and were

analyzed to better understand their impact on inhibitor behavior. The primary hypothesis was that reducing rotational speed, analogous to decreased flow velocity in a pipeline, decrease the mass transfer resulting in slower dissolution rate of the CI package and higher persistency. Conversely, increasing flow velocity could potentially accelerate the CI package dissolution rate and shorter persistency. Additionally, previous chapters highlighted the significant impact of hydrocarbon presence on inhibitor persistency. Thus, the presence of hydrocarbon was also investigated on this known package CI persistency. Figure 62 and Figure 63 present the results of experiments investigating the influence of flow velocity and presence of hydrocarbon on the persistency of this known inhibitor package consists of PE-C14, BE, and AE.

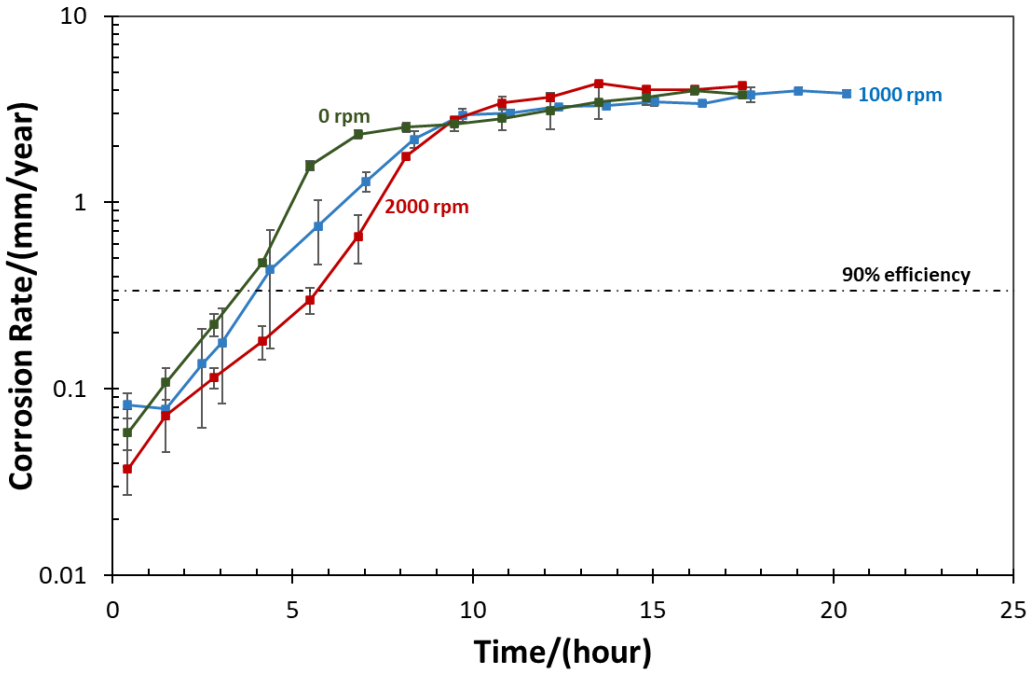

Figure 62. Batch inhibition with 1.5 wt.% PE-C14 in BE, with AE at different rotational speeds (30°C, 0.97 bar pCO_2, pH 4.00, 1 wt.% NaCl).

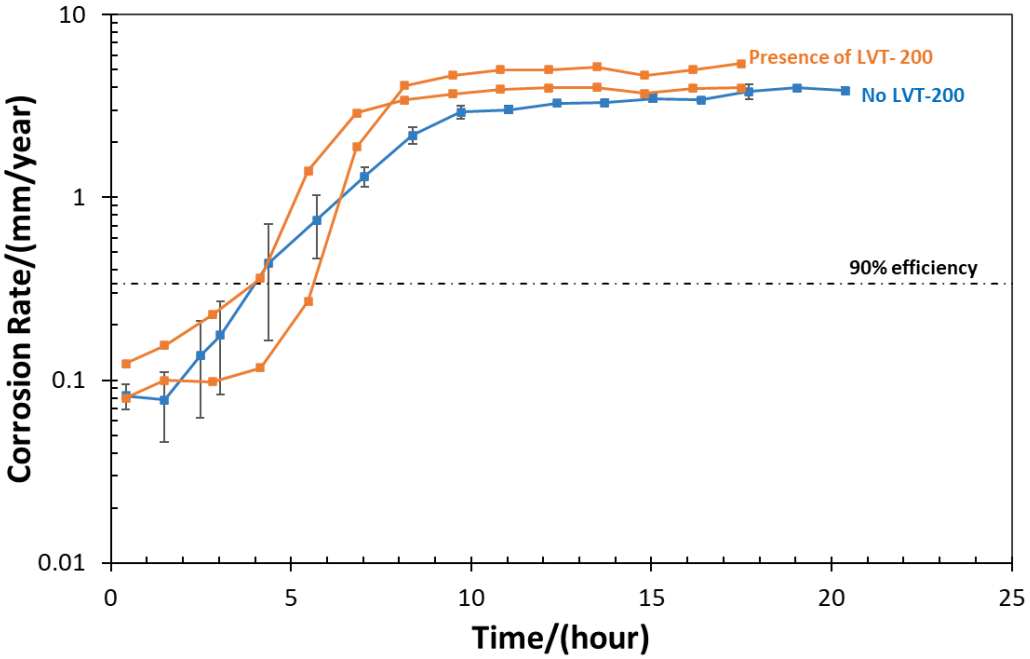

Figure 63. Batch inhibition with 1.5 wt.% PE-C14 in BE, with AE with and without presence of hydrocarbon (30°C, 0.97 bar pCO_2, pH 4.00, 1 wt.% NaCl).

In terms of changes in rotational speed, it was hypothesized that an increase in rotational speed would enhance mass transfer, potentially increasing the dissolution rate. However, the results did not align with this hypothesis, suggesting that either the rate of package solvent dissolution was not dependent on mass transfer or that the range of speed changes was not significant enough to have an impact. Additionally, in the previous chapter, the presence of hydrocarbons was shown to increase the persistency of the commercial inhibitor. However, the presence of hydrocarbons did not significantly affect the persistency of the "known" inhibitor package in this study. This observation is somehow surprising as incorporation of the aliphatic LVT (with carbon chain length C14 being the most common) was expected considering the similar tail length of PE-C14 [115]. However, other factors, such as the adsorbed inhibitor molecule orientation could

also play a role. Since the results of the parametric studies in this section were insufficient to verify the proposed mechanism for CI persistency outlined in section 7.3.2, the next phase of the study involved formulating a modified PE-C14 package using a less water-soluble solvent. The persistency of this modified package was then evaluated to further investigate the mechanism behind batch CI persistency.

7.3.4 PE-C14 Inhibitor Package Persistency With Diesel

The literature review indicates that batch inhibitor packages typically contain oil-soluble components, such as diesel or other aromatic solvents. Additionally, diluents such as crude oil, condensates, and diesel are commonly used as carrier fluid with the aim of improving contact time and enhancing inhibitor film thickness [73, 75, 76, 110]. Based on these findings, a commercially available diesel fuel, classified as ultra-low sulfur diesel (ULSD), with a maximum sulfur content of 10 ppm, was selected as the primary solvent for PE-C14. Diesel contains a mixture of aromatics and saturated hydrocarbons which has a much lower solubility in water than LVT-200 (0.005 g/L for diesel[††] and 1.5 g/L for LVT-200[‡‡]), potentially improving the persistency of the corrosion inhibitor. However, due to the partial solubility of PE-C14 in diesel, 3 mL of BE was still added to 18 mL of diesel with 1.5 wt.% PE-C14. The persistency of this modified inhibitor package was evaluated under the same experimental conditions as previous PE-C14 experiments. Figure 64 presents the results of two replicate experiments on the persistency of this oil soluble package (diesel, BE, and PE-C14) in comparison to the

---

[††] https://inchem.org/documents/icsc/icsc/eics1561.htm
[‡‡] chrome-extension://efaidnbmnnnibpcajpcglclefindmkaj/https://deep-south-chemical.com/PDF%27s/SDS/LVT_200_PEN1090-00-C_US_GHS_English-Copy.pdf

previous PE-C14 package, which contained BE and AE at the same CI concentration. Additionally, another experiment was conducted using same volume of diesel and BE without PE-C14 to isolate and assess its effects on CO_2 corrosion under the given conditions.

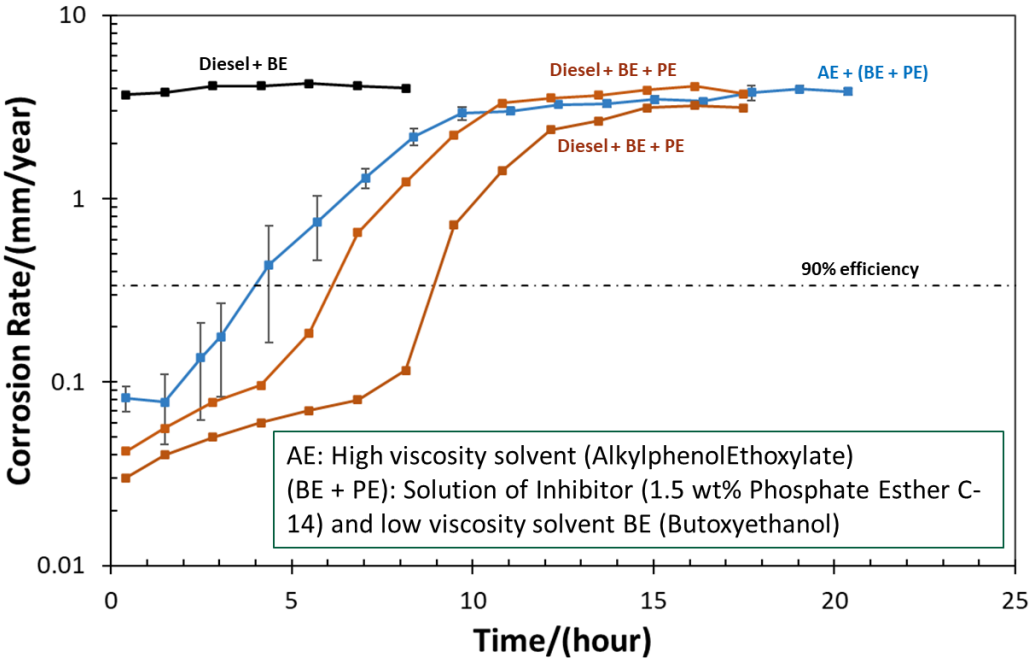

Figure 64. Batch inhibition with 1.5 wt.% PE-C14 in diesel and BE, compared to the previous package with AE (30°C, 0.97 bar pCO_2, pH 4.00, 1 wt.% NaCl).

The results presented in Figure 64 indicate that the experiments conducted with diesel, BE, and PE-C14 displayed a marked increase in persistency. The initial corrosion rate was relatively lower, and the increase in corrosion rate during the persistency stage remained gradual for approximately five hours. This was followed by a much steeper increase in corrosion rate, surpassing the 90% efficiency threshold after six to nine hours. These observations align with the hypothesis proposed earlier involving two primary

mechanisms governing inhibitor film degradation. Initially, the inhibitor film, which incorporates diesel, gradually dissolves into the aqueous phase and is carried out of the glass cell with the outlet flow. Diesel interacts with the adsorbed inhibitor molecules on the surface, forming a protective film that acts as a barrier to inhibitor desorption into the aqueous phase. As long as diesel remains on the surface, the inhibitor layer remains intact, preventing its desorption into the bulk solution. This mechanism explains the initially low slope observed in the corrosion rate, as the inhibitor persists on the surface for an extended period before gradual desorption occurs. Subsequently, the final layer of inhibitor molecules adsorbed onto the metal surface begins to desorb, resulting in a more pronounced increase in corrosion rate, as observed in the second high-slope phase of the results. A model based on diesel dissolution and PE-C14 desorption is presented in the following section to better examine this hypothesis and compare it with experimental data.

7.3.5 Batch Inhibition Persistency Model Based on Dissolution and Desorption

Pan, *et* al. [114], previously developed a model for inhibitor persistency in top-of-the-line corrosion (TLC) applications, based on the water solubility of the inhibitor. The model is founded on the principle that, immediately after inhibitor application, the surface concentration of the inhibitor is higher than its SSC. Over time, this concentration decreases as condensate droplets remove inhibitor molecules from the surface. Inhibitor persistency is therefore defined as the duration during which the CI surface concentration remains above the SSC. Once the concentration drops to the SSC, desorption begins, and the inhibitor loses its persistency. Although this model was developed for TLC

conditions, a similar approach was used in this work to model the persistency of batch corrosion inhibitors. The hypothesis underlying batch CI persistency modeling is based on a two-step mechanism: (1) dissolution of the inhibitor/solvent layer formed on the metal surface, primarily involving the solvent component of the package, and (2) desorption of the inhibitor from the metal surface. For the package containing 18 mL of diesel, 3 mL of butoxyethanol, and 1.5 wt.% PE-C14, it is assumed that the first step is a rate-determining process governed by the diesel dissolution rate. Once all the diesel in the glass cell dissolves into the aqueous phase and is removed with the outlet flow, the process transitions to the second step, which is controlled by the desorption kinetics of PE-C14.

7.3.5.1 Solvent (Diesel) Dissolution Rate Calculation. Equation (20) represents the mass balance equation used to determine the dissolution rate of diesel into the aqueous phase:

$$\frac{dm}{dt} = \dot{m}_{in} - \dot{m}_{out} \tag{20}$$

where m, $\dot{m}_{in}$, and $\dot{m}_{out}$ represent the mass of diesel in the glass cell, the inlet and outlet mass flow rate of diesel respectively. Since there is no diesel presents in the inlet flow and no diesel generation, the change in diesel mass over time can be simplified. It is noteworthy that here it is assumed that there is no mechanical transport of the diesel as a separate phase. In other words, it is assumed that diesel loss is only due to the dissolution to the aqueous phase without having any mechanically dispersed diesel molecules leaving the surface. This relationship is then integrated over the total duration required for complete diesel removal from the glass cell, as expressed in equations (21) to (23):

$$\frac{dm}{dt} = -\dot{m}_{out} = -Q \times S \tag{21}$$

$$\int_0^T dt = \int_M^0 \left(-\frac{dm}{Q \times S}\right) \tag{22}$$

$$T = \frac{M}{Q \times S} \tag{23}$$

where M, T, Q, and S represent the diesel initial mass (g), dissolution time (min), dilution flowrate ($\frac{L}{\text{min}}$), and diesel solubility in water ($\frac{g}{L}$)[§§].

The total mass of diesel deposited on the steel surface following the inhibitor application step can be estimated by considering the corrosion inhibitor (CI) package thickness reported in the literature (0.025 to 0.076 mm [76]) and the surface area covered by the inhibitor package, as shown in Figure 65.

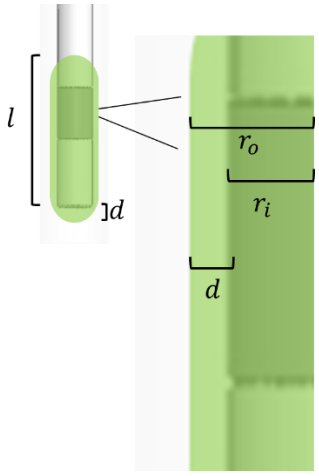

Figure 65. Schematic of the area covered by the inhibitor package after inhibitor application step in batch treatment experiment. (d, l, r_i, and r_o are the film thickness, length of the shaft covered by the film, shaft radios without and with CI respectively)

[§§] https://inchem.org/documents/icsc/icsc/eics1561.htm

Based on these assumptions, the total mass of diesel can be determined using equation (24):

$$M = \rho(l\pi(r_o^2 - r_i^2)) + d\pi r_o^2 \quad (24)$$

where ρ represents the diesel density in ($\frac{g}{mm^3}$), and all other parameters are expressed in millimeters (mm). The total time required for diesel dissolution in water can then be determined using equation (23).

7.3.5.2 PE-C14 Desorption Modeling. As previously discussed, the second step of the proposed model involves the desorption behavior of PE-C14, which is described using the Langmuir isotherm model. The adsorption and desorption kinetics have been investigated in our laboratory by Ren *et al*. [48]. By utilizing the adsorption (k_A) and desorption (k_D) rate constants along with equations (17) and (18), the predicted corrosion rate at the onset of PE-C14 desorption from the surface can be determined. Furthermore, the corrosion rate is assumed to remain approximately constant during the dissolution step, which has been calculated by equation (23) to last 7.3 hours. Based on these modeling results, the corrosion rate behavior can be simulated and compared with the experimental data presented in Figure 66.

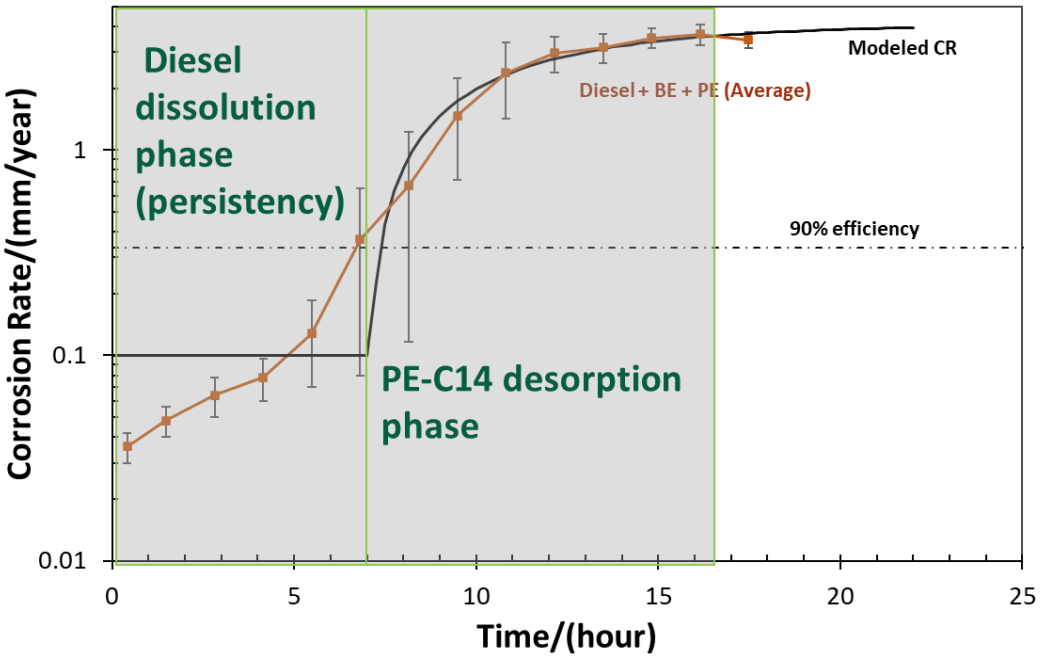

Figure 66. Modeled corrosion rate using dissolution step period (7.3 hours) and Langmuir isotherm model (30°C, pH 4.00, 1 wt.% NaCl).

The comparison between the modeling results and the experimental data for this inhibitor package validates the underlying hypothesis of the proposed model, which postulates that batch inhibition persistency occurs in two distinct steps, as previously discussed. The most critical step is the dissolution of the inhibitor package. During this phase, the inhibition efficiency remains its maximum efficiency; however, the inhibitor film thickness gradually decreases due to dissolution. This observation aligns with existing literature, which emphasizes that a key characteristic of batch inhibitors is their oil solubility and highlights the crucial role of inhibitor film thickness in their effectiveness [73, 75, 76, 110].

7.4 Summary

Building upon the methodology developed and the commercial inhibitor evaluated in the previous chapter, this chapter investigated the mechanisms governing batch CI persistency with known components. Experiments were conducted utilizing various model compound inhibitors and solvents. The central research question addressed herein concerned the mechanism of batch CI persistency, specifically why inhibitors in continuous treatment desorb upon removal from the bulk solution, while batch CIs exhibit a period of protection even when the bulk CI concentration is negligible. To address this, an inhibitor package with known components was required to facilitate analysis of batch CI behavior during the persistency phase. Following the evaluation of various corrosion inhibitor molecules and solvents, a package exhibiting limited persistency was identified. Subsequent parametric studies led to the development of a model explaining the general behavior of batch CIs and the rationale behind inhibitor persistency time. A summary of the key findings from this chapter is presented below:

- BDA-C16 and BDA-C22 exhibited insufficient persistency in batch treatment. However, the use of a hydrocarbon solvent (model oil) slightly improved CI persistency, suggesting that the incorporation of hydrocarbon molecules with CI molecules on the specimen enhances their retention.
- PE-C14, when tested for batch inhibition, exhibited little to no persistency when combined with butoxyethanol as a solubilizing agent.

- The use of the high-viscosity solvent alkylphenolethoxylate as a carrier for PE-C14, in combination with butoxyethanol, enhanced CI persistency by decreasing the dissolution rate of the CI package formed on the metal surface.
- Diesel was used as an oil-soluble component to reduce the water solubility of the inhibitor package and to investigate the dissolution mechanism. This package enhanced CI persistency, confirming the hypothesis that inhibitor package solubility is the main factor for determining CI persistency.
- The modeling was conducted based on the rate-determining dissolution of oil into water, followed by the desorption kinetics of the main inhibitor molecule from the surface. The modeling results supported the proposed mechanism of persistency behavior, confirming that it is governed by solubility. Although this model may serve as a preliminary framework for understanding batch inhibition persistency, it has several limitations:
    - The solubility of inhibitor packages depends on the collective properties of all their components. This poses a challenge, particularly for commercial inhibitors with proprietary or undisclosed formulations, where accurate solubility data are difficult to obtain.
    - The model is primarily based on the dissolution behavior of the inhibitor package. As such, it does not account for other influential factors, such as the incorporation of hydrocarbon molecules into the inhibitor film, which may significantly affect CI film persistency.

- The model also fails to capture scenarios involving partial loss of the inhibitor film, which can lead to severe localized corrosion. In such cases, although the film is still partially present on the surface, its protective function may be entirely compromised.

Chapter 8: Conclusions and Recommendations for Future Work

8.1 Conclusions

This study aimed to evaluate CO_2 corrosion inhibition persistency under two primary treatments: continuous CI injection and batch application. The overarching approach involved the development of an improved methodology for both treatment types, designed to more accurately reflect their practical application within the oil and gas industry. Subsequently, parametric studies were conducted to analyze and model inhibitor persistency behavior under each treatment scenario. Chapters 4 and 5 presented an investigation into continuous treatment protocols, specifically focusing on the impact of two distinct dilution methodologies. Conversely, Chapters 6 and 7 detailed experiments involving batch inhibition treatments, evaluating the persistency of both commercially available and model compound corrosion inhibitors. The main findings and conclusions derived from this study are summarized below:

Continuous treatment CI persistency:

- A quaternary ammonium model compound inhibitor (BDA-C14) was used in the persistency experiments as a continuous treatment corrosion inhibitor. Initial tests were performed using a previously developed setup capable of only partial dilution. At 30°C, with a 2-hour pre-corrosion period and subsequent dilution to 10 ppm_w, BDA-C14 demonstrated strong persistency. However, this behavior was likely influenced by the limited dilution capacity of the system and the extended pre-corrosion duration, both of which may have affected inhibitor desorption kinetics

and surface saturation concentration. To further investigate this effect, the pre-corrosion time was reduced from two hours to 15 minutes. Following dilution, a slight increase in the corrosion rate was observed, though the inhibitor continued to provide effective corrosion protection.

- Experiments conducted at 40°C using the preliminary setup revealed a higher corrosion rate following dilution, indicating an increased desorption rate of BDA-C14, as expected. However, some degree of inhibition remained, though it was entirely lost upon the application of additional dilution steps. These preliminary findings highlighted the necessity of an improved system setup to ensure the complete removal of residual inhibitor during the persistency phase of the continuous treatment experiments.
- After developing a system capable of flow-through dilution, inhibitor residuals were rapidly removed from the glass cell upon initiation of dilution. This continuous dilution was achieved using 140 L of uninhibited brine, which replenished the solution throughout the duration of the test. This methodology more accurately represents corrosion inhibitor (CI) persistency under continuous treatment conditions in the field, where the inhibitor concentration in the pipeline bulk gradually approaches zero as uninhibited flow replaces the treated fluid.
- BDA-C14 exhibited no persistency once all inhibitor residuals were completely removed from the glass cell at both temperatures. This finding

is crucial as it invalidates the partial dilution methodology still commonly used throughout the industry. It also confirms that BDA-C14, as a representative water-soluble inhibitor used in continuous treatment, follows adsorption-desorption kinetics without demonstrating any inherent persistency. However, these kinetics can be influenced by changes in the metal surface characteristics. As presented in Chapter 5, results from experiments with extended pre-corrosion and prolonged contact time provide strong evidence of this effect. Specifically, the findings indicate that increased surface roughness slows down inhibitor desorption kinetics, thereby delaying the complete loss of inhibition

- Based on the assumption that the continuous treatment corrosion inhibitor (CI) primarily follows adsorption/desorption kinetics, the Langmuir isotherm model was employed to simulate the desorption behavior of BDA-C14. Kinetic constants were determined by fitting the experimental inhibition data to the Langmuir model at both temperatures. The model was then used to predict desorption behavior as a function of CI concentration following dilution. The modeling results successfully captured the overall inhibitor performance, particularly the time required for complete inhibition loss and the resulting final corrosion rate. Comparison between the modeled data using 15-minute pre-corrosion and the 2-hour pre-corrosion experiment clearly demonstrated that extended pre-corrosion time altered the desorption kinetics. Additionally, the

calculated kinetic constants were higher at elevated temperatures, as expected.

Batch treatment CI persistency:

- The first step in the persistency study for batch treatment involved developing an improved methodology to overcome the limitations of previous approaches described in the literature. Two key parameters were considered in this methodology. First, the inhibitor was applied within the same cell where the experiment was conducted to prevent oxygen contamination, ensuring more reliable and controlled experimental conditions. Second, the uninhibited brine was continuously introduced into the glass cell throughout the test to guarantee the complete removal of the inhibitor, providing a more accurate representation of real-world batch treatment conditions.
- For the evaluation of the proposed methodology, a commercial batch CI was initially used in a batch treatment persistency experiment. The corrosion rate results demonstrated excellent inhibition efficiency and persistency, even with continuous solution replenishment throughout the test. However, the very long persistency of the inhibitor was not practical for this study. Therefore, higher temperatures were explored until the commercial inhibitor exhibited a loss of persistency after approximately three days at 60°C. Multiple experimental repetitions confirmed this trend, with localized corrosion observed after persistency loss. This condition

provided a suitable basis for parametric studies, as it allowed for the observation of both persistency and inhibition loss.

- The presence of hydrocarbons, a key parameter influencing inhibitor behavior, was investigated at 60°C using the commercial CI. The results indicated that dispersed hydrocarbon molecules in the aqueous phase interacted with the inhibitor film on the metal surface, enhancing its persistency by at least two additional days.
- Experiments with the commercial inhibitor limit a complete understanding of the mechanism behind batch persistency, as the exact composition of the commercial package is unknown. Therefore, synthesized model compound inhibitors were used in the next phase to gain deeper insight into the factors influencing batch treatment persistency.
- Two quaternary ammonium model compound inhibitors specifically BDA-C16 and BDA-C22, were evaluated for batch CI persistency experiments. Both exhibited insufficient persistency in batch treatment. However, the addition of a hydrocarbon solvent (LVT model oil) slightly improved CI persistency, suggesting that hydrocarbon molecules may incorporate into the inhibitor film, thereby enhancing its persistency.
- Another model compound inhibitor, PE-C14, which demonstrated higher efficiency at lower concentrations, was tested as a batch CI. When combined with butoxyethanol as a solubilizing agent, PE-C14 exhibited little to no persistency. However, using a high-viscosity solvent as a

carrier, along with butoxyethanol, enhanced CI persistency. This suggests that increasing the viscosity of the batch CI package could improve persistency by reducing the dissolution rate of the inhibitor film on the surface.

- Diesel was used as an oil-soluble component to reduce the water solubility of the inhibitor package and investigate the dissolution mechanism. This modification enhanced CI persistency, confirming the hypothesis that the solubility of the inhibitor package is a key factor in determining CI persistency.
- A model for batch inhibition persistency was developed, consisting of two distinct steps. The first step is the rate-determining dissolution of oil into water, which defines the inhibitor persistency time. Once the solution is fully removed from the surface, the second step begins, where adsorbed inhibitor molecules start to desorb. At this stage, the mechanism is governed by the desorption kinetics of the main inhibitor molecule. The modeling results supported this proposed mechanism of persistency behavior, confirming that solubility plays a key role in governing inhibitor persistency. Although this model provides insights into persistency behavior in batch treatment, the actual persistency behavior of commercial corrosion inhibitors in the field is assumed to be more complex. This model has limitations when applied to commercial CIs, as it does not account for the unique characteristics of such inhibitors. Additionally, it

overlooks the effects of hydrocarbon presence, which can influence inhibitor behavior. Moreover, the model is based solely on dissolution as the rate-determining step for persistency, potentially oversimplifying the complex dynamics of real-world systems.

8.2 Hypotheses Revisited

Based on the conclusions of this study, the initial hypotheses can now be revisited and evaluated with their corresponding judgments:

Hypothesis #1: In continuous treatment, the behavior of corrosion inhibitors (CIs) during the persistency phase is fundamentally governed by desorption kinetics. These kinetics, in turn, are modulated by CI characteristics, temperature, and surface properties. Consequently, the prediction of CI desorption/persistency behavior necessitates a comprehensive investigation of the parameters influencing the respective rate constant. It is hypothesized that lower temperatures and increased surface roughness, resulting from longer time pre-corrosion, retard the desorption of corrosion inhibitors (CIs), thereby enhancing their persistency.

Judgment: The results from the experiments in Chapters 4 and 5 demonstrated that inhibitor behavior under interruption conditions of continuous treatment is influenced by the inhibitor concentration in the bulk solution. Once the inhibitor concentration falls below the surface saturation concentration, desorption begins. However, the desorption kinetics of the inhibitor are highly dependent on the surface characteristics and temperature. The adsorption/desorption kinetic constants for each inhibitor can be determined under fixed conditions. Any change in surface characteristics or temperature

will affect these kinetics. Modeling results using the Langmuir isotherm model also confirmed that continuous CI follows the adsorption/desorption kinetics without exhibiting persistency behavior, thus supporting the first hypothesis.

Hypothesis #2: In contrast to continuous treatment, the persistency behavior of batch inhibition deviates from a strict adherence to adsorption/desorption mechanisms. In batch treatment, oil-soluble corrosion inhibitors (CIs) are applied, forming a substantially thicker film on the metal surface compared to continuous treatment. Consequently, the persistency of this inhibitor film is primarily governed by the dissolution rate of the film into the aqueous phase, followed by desorption kinetics. It is hypothesized that enhancing the oil solubility of the inhibitor package will extend the persistency duration of the batch corrosion inhibitor (CI). Furthermore, supplementary parameters influencing the inhibitor dissolution rate, including viscosity and the presence of hydrocarbons, are anticipated to modulate the observed persistency behavior

Judgment: A comparison of the results from commercial batch CI and model compound inhibitors revealed a significant difference in persistency behavior. The key parameter differentiating the commercial inhibitors from the model compound inhibitors in this study was assumed to be the oil solubility of the package. When the model compound inhibitor package became less water-soluble by using an oil-soluble solvent, inhibitor persistency increased. Additionally, modeling based on solubility demonstrated that batch inhibitor persistency is strongly dependent on the dissolution rate of the CI package. However, the presence of hydrocarbons can interact with the inhibitor package on the surface and influence this dissolution rate. Other phenomena, such as the strength

of the adsorption, could also affect commercial inhibitor packages persistency behavior. Therefore, while this hypothesis was confirmed for the model compound inhibitor package, it may not fully apply to commercial batch CIs.

8.3 Recommendations for Future Work

Although this study provided modeling for both continuous and batch treatment persistency, further development is needed, especially for establishing batch inhibition persistency, through more parametric studies. It is proposed that additional experiments for both continuous and batch inhibition be conducted as follows:

- Different model compound inhibitors beyond the quaternary ammonium type, such as CIs containing sulfur, should be tested using the methodology developed in this study [116, 117]. The adsorption/desorption kinetics of each inhibitor can be evaluated using the same approach or additional isotherm models. Subsequently, the desorption behavior can be modeled and compared to the corrosion rate after dilution. Furthermore, it is recommended that commercial continuous CIs be analyzed using this technique to enhance the evaluation of this approach.
- It is recommended that adsorption/desorption analysis for each known model compound inhibitor in continuous treatment be conducted under varying conditions, including different corrosion products on the surface, the presence of hydrocarbons, and intermittent oil wetting. These

parametric studies can further refine the modeling of continuous inhibition persistency.

- For batch inhibition persistency, it is recommended to develop improved inhibitor packages using oil-soluble inhibitor molecules and oil-soluble solvents. The dissolution rate of each formulated package can then be determined using the methodology employed in this study, allowing for a more comprehensive evaluation of the proposed model.
- It is also recommended to study the persistency of different commercial batch CI packages in batch treatment. By developing a method to calculate the dissolution rate constant for each inhibitor, the approach proposed in this study can be further evaluated to determine whether the dissolution of the inhibitor package is the sole mechanism behind long-term persistency or if other factors, such as chemisorption, should also be considered.

References

[1] E. McCafferty, “Societal aspects of corrosion,” in *Introduction to Corrosion Science*, 1st ed., New York: Springer, 2010, pp. 1–11.

[2] J. M. Malo, V. Salinas, J. Stray, “Current corrosion causes gasoline pipeline failure,” *Mater. Perform.*, vol. 33, no. 63, pp. 63–66, 1994.

[3] C. de Waard, D. E. Milliams, “Carbonic acid corrosion of steel,” *Corrosion*, vol. 31, no. 5, pp. 177–181, 1974.

[4] B. Ridd, T. J. Blakset, D. Queen, “Field trials for corrosion inhibitor selection and optimization using a new generation of electrical resistance probes,” in *CORROSION 1998*, paper no. 78 (San Diego, CA: NACE, 1998).

[5] P. Roberge, “Corrosion inhibitors,” in *Handbook of Corrosion Engineering*, 2nd ed., New York: McGraw-Hill Education, 2012.

[6] W. Li, J. Jing, J. Sun, F. Zhang, W. Huang, and Y. Guo, “Corrosion inhibitor distribution and injection cycle prediction in a high water-cut oil well: A numerical simulation study,” *Sustainability*, vol. 15, no. 7, p. 6289, 2023.

[7] J. Sonke, W. D. Grimes, “Guidelines for corrosion inhibitor selection for oil and gas production,” in *CORROSION 2017*, paper no. 8842 (New Orleans, LA: NACE, 2017).

[8] S. Webster, D. Harrop, A. J. McMahon, G. J. Partridge, “A new class of ‘green’ corrosion inhibitors: development and application,” in *CORROSION 1993*, paper no. 109 (Houston, TX: NACE, 1993).

[9] M. Lopez, J. Porcayo Calderon, M. Casales Diaz, “Internal corrosion solution for gathering production gas pipelines involving palm oil amide based corrosion inhibitors,” *Int. J. Electrochem. Sci.*, vol. 10, no. 9, pp. 7166–7179, 2015.

[10] D. A. Jones, “Corrosion inhibitors,” in *Principles and Prevention of Corrosion*, New York: MacMillan, 1996, pp. 503–512.

[11] A. Kahyarian, B. Brown, S. Nesic, “The unified mechanism of corrosion in aqueous weak acids solutions: A review of the recent developments in mechanistic understandings of mild steel corrosion in the presence of carboxylic acids, carbon dioxide, and hydrogen sulfide,” *Corrosion*, vol. 76, no. 3, pp. 268–278, 2020.

[12] L. G. S. Gray, B. G. Anderson, M. J. Danysh, and P. R. Tremaine, “Mechanism of carbon steel corrosion in brines containing dissolved carbon dioxide at pH 4,” in *CORROSION 1989*, paper no. 464 (Houston, TX: NACE, 1989).

[13] L. G. S. Gray, B. G. Anderson, M. J. Danysh, and P. R. Tremaine, “Effect of pH and temperature on the mechanism of carbon steel corrosion by aqueous carbon dioxide,” in *CORROSION 1990*, paper no. 40 (Houston, TX: NACE, 1990).

[14] S. Nesic, J. Postlethwaite, S. Olsen, “An electrochemical model for prediction of corrosion of mild steel in aqueous carbon dioxide solutions,” *Corrosion Sci*, vol. 52, no. 4, pp. 280–294, 2007.

[15] M. Nordsveen, S. Nesic, R. Nyborg, A. Stangeland, “A mechanistic model for carbon dioxide corrosion of mild steel in the presence of protective iron carbonate

films — part 1: theory and verification," *Corrosion Sci*, vol. 59, no. 5, pp. 443–456, 2003.

[16] S. Nesic, M. Nordsveen, R. Nyborg, A. Stangeland, "A mechanistic model for carbon dioxide corrosion of mild steel in the presence of protective iron carbonate films — part 2: a numerical experiment," *Corrosion Sci*, vol. 59, no. 5, pp. 489–497, 2003.

[17] H. Mansoori, "Influence of calcium and magnesium ions and their carbonate scales on CO_2 corrosion of mild steel," Ph.D. dissertation, Dept. Chem. Eng. Ohio Univ., Athens, OH, 2019.

[18] V. S. Saji and S. A. Umoren, *Corrosion inhibitors in the oil and gas industry*, Hoboken, NJ: Wiley, 2020.

[19] O. S. I. Fayomi, I. G. Akande, S. Odigie, "Economic impact of corrosion in oil sectors and prevention: an overview," in *Journal of Physics: Conference Series*, vol. 1378, no. 2, p. 022037, 2019.

[20] V. A. Solovyeva, K. H. Almuhammadi, W. O. Badeghaish, "Current downhole corrosion control solutions and trends in the oil and gas industry: A review," *Materials*, vol. 16, no. 5, p. 1795, 2023.

[21] S. Papavinasam, "Mitigation – internal corrosion," in *Corrosion Control in the Oil and Gas Industry*, 1st ed., San Diego: Gulf Professional Publishing, 2013, pp. 361–424.

[22] V. S. Sastri, *Corrosion Inhibitors: Principles and Application*, New York: John Wiley and Sons, 1998.

[23] V. S. Sastri, *Green Corrosion Inhibitors*, 2nd ed., New Jersey: John Wiley and Sons, 2011.

[24] B. D. B. Tiu, R. C. Advincula, "Polymeric corrosion inhibitors for the oil and gas industry: design principles and mechanism," *React. Funct. Polym.*, vol. 95, pp. 25–45, 2015.

[25] U.S. Public Health Service, "Toxicological profile for chromium," *Agency for Toxic Substances and Disease Registry*, Report no. ATSDR/TP-88/10, 1989.

[26] S. H. Yoo, Y. W. Kim, K. Chung, S. Y. Baik, J. S. Kim, "Synthesis and corrosion inhibition behavior of imidazoline derivatives based on vegetable oil," *Corrosion Sci*, vol. 59, pp. 49-54, 2012.

[27] C. Monticelli, "Corrosion inhibitors," in *Encyclopedia of Interfacial Chemistry*, Amsterdam: Elsevier, 2018, pp. 164–171.

[28] C. G. Dariva, A. F. Galio, "Corrosion inhibitors – principles, mechanisms and applications," in *Developments in Corrosion Protection*, M. Aliofkhazraei, Ed., Rijeka: IntechOpen, 2014.

[29] S. Papavinasam, "Evaluation and selection of corrosion inhibitors," in *Uhlig's Corrosion Handbook*, Ottawa: John Wiley and Sons, 1999, pp. 1121–1128.

[30] R. A. Sims, S. L. Harmer, J. S. Quinton, "The role of physisorption and chemisorption in the oscillatory adsorption of organosilanes on aluminium oxide," *Polymers*, vol. 11, no. 3, p. 410, 2019.

[31] L. Wang, H. Wang, A. Seyeux, S. Zanna, A. Pailleret, S. Nesic, P. Marcus, "Adsorption mechanism of quaternary ammonium corrosion inhibitor on carbon

steel surface using ToF-SIMS and XPS," *Corrosion Sci*, vol. 213, p. 110952, 2023.

[32] A. Kokalj, "Corrosion inhibitors: physisorbed or chemisorbed?," *Corrosion Sci*, vol. 196, p. 109939, 2022.

[33] N. Hackerman, A. Makrides, "Action of polar organic inhibitors in acid dissolution of metals," *Ind. Eng. Chem.*, vol. 46, no. 3, pp. 523–527, 1954.

[34] S. A. Umoren, M. M. Solomon, "Polymeric corrosion inhibitors for oil and gas industry," in *Corrosion Inhibitors in the Oil and Gas Industry*, 2020, pp. 303–320.

[35] S. A. Umoren, M. M. Solomon, "Protective polymeric films for industrial substrates: A critical review on past and recent applications with conducting polymers and polymer composites/nanocomposites," *Prog. Mater. Sci.*, vol. 104, pp. 380–450, 2019.

[36] A. Alareeqi, M. Hadizadeh, J. Duan, X. Ji, "Understanding the relationship between the structural properties of three corrosion inhibitors and their surface protectiveness ability in different environments," *Appl. Surf. Sci.*, vol. 542, p. 148600, 2021.

[37] E. Ituen, O. Akaranta, A. James, "Evaluation of performance of corrosion inhibitors using adsorption isotherm models: An overview," *Chem. Sci. Int. J.*, vol. 18, no. 1, pp. 1–34, 2017.

[38] W. J. Lorenz, F. Mansfeld, "Interface and interphase corrosion inhibition," *Electrochim. Acta*, vol. 31, no. 4, pp. 467–476, 1985.

[39] A. El-Awady, B. Abd-El-Nabey, S. Aziz, "Kinetic-thermodynamic and adsorption isotherms analyses for the inhibition of the acid corrosion of steel by cyclic and open-chain amines," *J. Electrochem. Soc.*, vol. 139, p. 2149, 1992.

[40] B. G. Ateya, B. E. El-Anadouli, F. M. El-Nizamy, "The adsorption of thiourea on mild steel," *Corrosion Sci*, vol. 24, no. 6, pp. 509–515, 1984.

[41] I. Langmuir, "The adsorption of gases on plane surfaces of glass, mica and platinum," *J. Am. Chem. Soc.*, vol. 40, no. 9, pp. 1361–1403, 1918.

[42] Y. Liu, L. Shen, "From Langmuir kinetics to first- and second-order rate equations for adsorption," *Langmuir*, vol. 24, no. 20, pp. 11625–11630, 2008.

[43] J. M. Dominguez Olivo, "Electrochemical model of carbon dioxide corrosion in the presence of organic," PhD Dissertation, Department of Chemical and Biomolecular Engineering, Ohio University, 2020.

[44] C. Cao, "On electrochemical techniques for interface inhibitor research," *Corrosion Sci*, vol. 38, no. 12, pp. 2073–2082, 1996.

[45] Lj. M. Vracar, D. Drazic, "Adsorption and corrosion inhibitive properties of some organic molecules on iron electrode in sulfuric acid," *Corrosion Sci*, vol. 44, pp. 1669–1680, 2002.

[46] S. Nesic, W. Wilhelmsen, S. Skjerve, and S. M. Hesjevik, "Testing of inhibitors for CO_2 corrosion using the electrochemical techniques," in *Proceedings of the 8th European Symposium on Corrosion Inhibitors (8 SEIC)*, paper no. 10 (Ferrara, Italy: University of Ferrara, 1995), pp. 1163–1192.

[47] T. Murakawa, S. Nagaura, N. Hackerman, “Coverage of iron surface by organic compounds and anions in acid solutions,” *Corrosion Sci*, vol. 7, no. 2, pp. 79–89, 1967.

[48] S. Ren, “Effect of corrosion residues and products of mild steel on corrosion inhibition mechanisms in CO_2 and H_2S environments,” PhD Dissertation, Department of Chemical and Biomolecular Engineering, Ohio University, 2023.

[49] J. A. Dougherty, “Effect of treatment method on corrosion inhibitor performance,” in *CORROSION 1997*, paper no. 97344 (Houston, TX: NACE, 1997).

[50] M. J. J. Simon-Thomas, “Corrosion inhibitor selection – feedback from the field,” in *CORROSION 2000*, paper no. 00056 (Orlando, FL: NACE, 2000).

[51] H. A. Craddock, *Oilfield chemistry and its environmental impact*, Hoboken, NJ: Wiley, 2017.

[52] M. Askari, M. Aliofkhazraei, R. Jafari, P. Hamghalam, A. Hajizadeh, “Downhole corrosion inhibitors for oil and gas production – a review,” *Appl. Surf. Sci. Adv.*, vol. 6, p. 100128, 2021.

[53] M. Achour, C. Johlman, D. Blumer, “Understanding the corrosion inhibitor partitioning in oil and gas pipelines,” in *Abu Dhabi International Petroleum Exhibition and Conference 2008*, paper no. 117942-MS (Abu Dhabi, UAE: SPE, 2008).

[54] Z. Kassenova, “Study of portioning of corrosion inhibitors between water and oil phases,” *Oil Gas Technol.*, vol. 132, pp. 15–18, 2021.

[55] M. M. Jordan, L. Sutherland, "Assessment of formation damage potential of corrosion inhibitor squeeze applications," in *CORROSION 2016*, paper no. 7290 (Vancouver, BC: NACE, 2016).

[56] R. L. Martin, G. F. Brock, J. B. Dobbs, "Corrosion inhibitor compositions and methods," U.S. Patent 6,866,797, Mar. 15, 2005.

[57] J. Yang, V. Jovancicevic, S. Mancuso, J. Mitchell, "High performance batch treating corrosion inhibitor," in *CORROSION 2007*, paper no. 7693 (Nashville, TN: NACE, 2007).

[58] E. Fischer, "Corrosion inhibitors for use in hydrocarbons," U.S. Patent 5,759,485, May 26, 1998.

[59] G. Lim, T. D. Williamson, T. D. Williamson Inc., "Advancements in spray pig applications," *PPSA seminar*, 2013.

[60] J. H. Meng, "Reliable corrosion inhibition in the oil and gas industry," *RR 1023 Research Report*, 2014.

[61] J. A. Dougherty, B. O. Alink, "Corrosion and inhibitor film life studies using a RCE flow-through test," in *CORROSION 2002*, paper no. 02195 (Denver, CO: NACE, 2002).

[62] S. Ramachandran, Z. Liu, C. Menendez, "Adsorption and desorption analysis of corrosion inhibition," in *CORROSION 2018*, paper no. 10805 (Phoenix, AZ: NACE, 2018).

[63] S. Ramachandran, Z. Liu, C. Menendez, J. Ott, L. Huang, "Adsorption desorption behavior of water soluble film persistent corrosion inhibitor," in *CORROSION 2019*, paper no. 12984 (Nashville, TN: NACE, 2019).

[64] Y. J. Tan, B. Kinsella, S. Bailey, "Monitoring batch treatment inhibitor performance continuously using electrochemical noise analysis," *Br. Corros. J.*, vol. 32, no. 3, pp. 212–216, 1997.

[65] Y. J. Tan, S. Bailey, B. Kinsella, "The monitoring of the formation and destruction of corrosion inhibitor films using electrochemical noise analysis (ENA)," *Corrosion Sci*, vol. 38, no. 10, pp. 1681–1695, 1996.

[66] R. De Marco, W. Durnie, A. Jefferson, B. Kinsella, A. Crawford, "Persistence of carbon dioxide corrosion inhibitors," *Corrosion*, vol. 58, no. 4, pp. 354–363, 2002.

[67] Y. Chen, G. R. Ruschau, J. A. Beavers, "Corrosion and inhibitor film persistency under flow conditions," in *CORROSION 2002*, paper no. 02237 (Denver, CO: NACE, 2002).

[68] M. Achour, J. Pierce, D. Daniels, H. Fang, "A novel laboratory test method to determine film persistency of batch inhibitors used to mitigate top of the line corrosion," in *CORROSION 2010*, paper no. 10101 (San Antonio, TX: NACE, 2010).

[69] M. Pan, M. Eslami, Y. Ding, Z. Belarbi, D. Young, M. Singer, "Methodology of batch inhibition applied for top and bottom of the line corrosion mitigation," in *CORROSION 2021*, paper no. 16751 (Houston, TX: NACE, 2021).

[70] Y. J. Tan, S. Bailey, B. Kinsella, "An investigation of the formation and destruction of corrosion inhibitor films using electrochemical impedance spectroscopy (EIS)," *Corrosion Sci*, vol. 38, no. 9, pp. 1545–1561, 1996.

[71] M. Achour, J. Pierce, and D. Daniels, "A novel laboratory test method to determine film persistency of batch inhibitors used to mitigate top of the line corrosion," in *CORROSION 2010*, paper no. 10101 (San Antonio, TX: NACE, 2010).

[72] S. Papavinasam, R. W. Revie, "Review of testing methods and standards for oilfield corrosion inhibitors," in *CORROSION 2004*, paper no. 04641 (New Orleans, LA: NACE, 2004).

[73] J. J. Wylde, M. Reid, A. Kirkpatrick, N. Obeyesekere, D. Glasgow, "When to batch and when not to batch: An overview of integrity management and batch corrosion inhibitor testing methods and application strategies," in *SPE International Symposium on Oilfield Chemistry*, paper no. 164080-MS (The Woodlands, TX: SPE, 2013).

[74] M. Finšgar, J. Jackson, "Application of corrosion inhibitors for steels in acidic media for the oil and gas industry: A review," *Corrosion Sci*, vol. 86, pp. 17–41, 2014.

[75] C. M. Menendez, J. M. Bojes, J. Lerbscher, "Obtaining batch corrosion inhibitor film thickness measurements using an optical profiler," *Corrosion*, vol. 67, no. 3, pp. 035003-1–035003-12, 2011.

[76] J. M. Bojes, M. Maddison, M. Girgis, H. Fear, “Batch inhibitor film distribution studies: Correlation of field data with laboratory results,” in *CORROSION 2001*, paper no. 01028 (Houston, TX: NACE, 2001).

[77] N. Norooziasl, A. F. Qadikolae, D. Young, B. Brown, S. Sharma, M. Singer, “Experiments and molecular simulations to study the effect of surface-active compounds in mixtures of model oils on CO_2 corrosion during intermittent oil–water wetting,” *Langmuir*, vol. 40, no. 19, pp. 9945–9956, 2024.

[78] C. Li, S. Richter, S. Nesic, “How do inhibitors mitigate corrosion in oil–water two-phase flow beyond lowering the corrosion rate?,” *Corrosion*, vol. 70, no. 9, pp. 958–966, 2014.

[79] Y. He, “Effect of intermittent wetting on corrosion inhibition in oil/water systems,” PhD Dissertation, Department of Chemical and Biomolecular Engineering, Ohio University, 2024.

[80] N. Norooziasl, D. Young, B. Brown, M. Singer, “Effect of oil/water intermittent wetting on CO_2 corrosion in the presence of acridine and myristic acid,” *Corrosion*, vol. 80, 2023.

[81] Z. M. Wang, J. Zhang, “Corrosion of multiphase flow pipelines: the impact of crude oil,” *Corros. Rev.*, vol. 34, no. 1–2, pp. 17–40, 2016.

[82] A. A. Al-Asadi, “Iron carbide development and its effect on inhibitor performance,” MS Thesis, Department of Chemical and Biomolecular Engineering, Ohio University, 2014.

[83] H. Fang, R. H. Huang, “Investigation of effects of iron sulfide on corrosion and inhibition of carbon steel in H_2S containing conditions,” in *CORROSION 2012*, paper no. 1651 (Salt Lake City, UT: NACE, 2012).

[84] E. Gulbrandsen, A. Stangeland, T. Burchardt, S. Nešić, S. M. Hesjevik, “Effect of precorrosion on the performance of inhibitors for CO_2 corrosion of carbon steel,” in *CORROSION 1998*, paper no. 98013 (San Diego, CA: NACE, 1998).

[85] E. Barmatov, T. L. Hughes, “Effect of corrosion products and turbulent flow on inhibition efficiency of propargyl alcohol on AISI 1018 mild carbon steel in 4 M hydrochloric acid,” *Corrosion Sci*, vol. 123, pp. 170–181, 2017.

[86] L. D. Paolinelli, T. Pérez, S. N. Simison, “The effect of pre-corrosion and steel microstructure on inhibitor performance in CO_2 corrosion,” *Corrosion Sci*, vol. 50, no. 9, pp. 2456–2464, 2008.

[87] A. Shamsa, R. Barker, Y. Hua, E. Barmatov, T. L. Hughes, A. Neville, “Impact of corrosion products on performance of imidazoline corrosion inhibitor on X65 carbon steel in CO_2 environments,” *Corrosion Sci*, vol. 185, p. 109423, 2021.

[88] H. Zhang, X. Pang, M. Zhou, C. Liu, L. Wei, K. Gao, “The behavior of pre-corrosion effect on the performance of imidazoline-based inhibitor in 3 wt.% NaCl solution saturated with CO_2,” *Appl. Surf. Sci.*, vol. 356, pp. 63–72, 2015.

[89] Y. Ding, B. Brown, D. Young, S. Nesic, M. Singer, “Effect of temperature on adsorption behavior and corrosion inhibition performance of imidazoline-type inhibitor,” in *CORROSION 2017*, paper no. 9350 (New Orleans, LA: NACE, 2017).

[90] M. P. Desimone, G. Gordillo, S. N. Simison, "The effect of temperature and concentration on the corrosion inhibition mechanism of an amphiphilic amido-amine in CO_2 saturated solution," *Corrosion Sci*, vol. 53, no. 12, pp. 4033–4043, 2011.

[91] M. A. Ameer, E. Khamis, G. Al-Senani, "Effect of temperature on stability of adsorbed inhibitors on steel in phosphoric acid solution," *J. Appl. Electrochem.*, vol. 32, no. 2, pp. 149–156, 2002.

[92] B. A. Abd El-Nabey, E. Khamis, G. E. Thompson, J. L. Dawson, "Effect of temperature on the inhibition of the acid corrosion of steel by benzaldehyde thiosemicarbazone: Impedance measurements," *Surf. Coat. Technol.*, vol. 28, no. 1, pp. 83–91, 1986.

[93] R. H. Hausler, G. Schmitt, C. Consulta, "Hydrodynamic and flow effects on corrosion inhibition," in *CORROSION 2004*, paper no. 04402 (New Orleans, LA: NACE, 2004).

[94] K. D. Efird, "Jet impingement testing for flow accelerated corrosion," in *CORROSION 2000*, paper no. 00052 (Orlando, FL: NACE, 2000).

[95] K. D. Efird, "Disturbed flow and flow-accelerated corrosion in oil and gas production," *J. Energy Resour. Technol.*, vol. 120, pp. 72–77, 1998.

[96] C. M. Canto Maya, "Effect of wall shear stress on corrosion inhibitor film performance," PhD Dissertation, Department of Chemical and Biomolecular Engineering, Ohio University, 2015.

[97] R. Woollam, “Is shear stress important in CI performance? Length scales important to understanding corrosion processes,” in *CORROSION 2007*, paper no. 07319 (NACE International, 2007).

[98] E. Ituen, O. Akaranta, A. James, “Evaluation of performance of corrosion inhibitors using adsorption isotherm models: An overview,” *Chem. Sci. Int. J.*, vol. 18, no. 1, pp. 1–34, 2017.

[99] W. J. Lorenz, F. Mansfeld, “Determination of corrosion rates by electrochemical DC and AC methods,” *Corrosion Sci*, vol. 21, no. 9, pp. 647–672, 1981

[100] N. Moradighadi, S. Lewis, J. D. Olivo, D. Young, B. Brown, S. Nesic, “Determining critical micelle concentration of organic corrosion inhibitors and its effectiveness in corrosion mitigation,” *Corrosion*, vol. 77, no. 3, pp. 266–275, 2021.

[101] K. Singla, B. Brown, and S. Nesic, “Importance of Location for Addition of Surfactant Inhibitors in Corrosion Experiments,” *Corrosion*, vol. 80, no. 6, pp. 603–607, Apr. 2024, doi: 10.5006/4514.

[102] R. C. Woollam, “Analysis of corrosion inhibitor performance curves using Langmuir adsorption kinetics,” in *CORROSION 2021*, paper no. 16859 (Houston, TX: NACE, 2021).

[103] N. Moradighadi, S. Lewis, J. M. Domínguez Olivo, D. Young, B. Brown, S. Nešić, “Effect of alkyl tail length on CMC and mitigation efficiency using model quaternary ammonium corrosion inhibitors,” in *CORROSION 2019*, paper no. 13004 (NACE International, 2019).

[104] R. Zvauya, J. L. Dawson, “Inhibition studies in sweet corrosion systems by a quaternary ammonium compound,” *J. Appl. Electrochem.*, vol. 24, no. 9, pp. 943–947, 1994.

[105] C. Cao, “On electrochemical techniques for interface inhibitor research,” *Corrosion Sci*, vol. 38, no. 12, pp. 2073–2082, 1996.

[106] W. J. Lorenz, F. Mansfeld, “Interface and interphase corrosion inhibition,” *Electrochim. Acta*, vol. 31, no. 4, pp. 467–476, 1986.

[107] M. H. Pan, K. S. Bahadori, M. Eslami, B. Brown, M. Singer, “Development of methodologies for continuous and batch inhibitor film persistency investigation in the laboratory,” in *AMPP 2022*, paper no. 18056 (San Antonio, TX: AMPP, 2022).

[108] K. S. Bahadori, B. Brown, and M. Singer, “Investigation of CO_2 corrosion inhibitor adsorption and desorption behavior using Langmuir isotherm model and effects of iron carbide on CI persistency,” in *AMPP 2023*, paper no. 19451 (Denver, CO: AMPP, 2023).

[109] K. S. Bahadori, B. Brown, M. Singer, “Effects of temperature and presence of hydrocarbon on commercial batch inhibitor persistency using a developed methodology,” in *AMPP 2025*, paper no. 00335 (Nashville, TN: AMPP, 2025).

[110] W. Mosher, T. Crosby, T. Lam, “Methodology for the evaluation of batch corrosion inhibitor films and their integrity,” in *AMPP 2021*, paper no. 16892 (Virtual Conference: AMPP, 2021)

[111] B. Brown, S. Nešić, "Aspects of localized corrosion in an H_2S/CO_2 environment," in *CORROSION 2012*, paper no. 1559 (Salt Lake City, UT: NACE, 2012).

[112] A. Crossland, R. Woollam, J. Vera, J. Palmer, G. John, S. Turgoose, "Corrosion inhibitor efficiency limits and key factors," in *CORROSION 2011*, paper no. 11062 (Houston, TX: NACE, 2011).

[113] K. Sh. Bahadori, M. Singer, B. Brown, D. Young, "Methodology for corrosion inhibitor persistency studies in batch inhibition," *Corrosion*, vol. 80, no. 10, pp. 964–966, 2024.

[114] M. Pan, "Simulation of batch inhibition applied to top-of-the-line corrosion mitigation," PhD Dissertation, Department of Chemical and Biomolecular Engineering, Ohio University, 2025.

[115] M. Eslami, S. Sharma, D. Young, and M. Singer, "Efficiency of volatile corrosion inhibitors in the presence of n-heptane: An experimental and molecular simulation study," *Corrosion*, vol. 80, no. 6, pp. 615–629, 2024.

[116] M. F. Mohamed, "Water chemistry and corrosion inhibition in high pressure CO_2 corrosion of mild steel," Master Thesis, Department of Chemical and Biomolecular Engineering, Ohio University, 2015.

[117] C. M. Canto Maya, "Effect of wall shear stress on corrosion inhibitor film performance," Master Thesis, Department of Chemical and Biomolecular Engineering, Ohio University, 2015.

Appendix A: Electrochemical and Transport Processes in CO_2 Environments

When CO_2 is in the aqueous phase, it can cause severe corrosion of mild steel as it generates an acidic environment, which is the main source of corrosion in oil and gas pipelines [43]. During the past 30 years, much more information has become available on CO_2 corrosion in aqueous systems. When CO_2 gas is in contact with water, it dissolves and increases the reduction current associated with mild steel corrosion [12-16]. When CO_2 gas dissolves in water, different chemical, electrochemical and transport processes sequentially occur in the solution [16]:

CO_2 gas dissolves into water:

$$CO_{2(g)} \rightleftharpoons CO_{2(aq)} \tag{25}$$

Aqueous CO_2 then hydrates and forms carbonic acid:

$$CO_{2_{(aq)}} + H_2O_{(l)} \rightleftharpoons H_2CO_{3_{(aq)}} \tag{26}$$

Carbonic acid forms bicarbonate and hydrogen ions:

$$H_2CO_{3_{(aq)}} \rightleftharpoons H^+_{(aq)} + HCO^-_{3\,(aq)} \tag{27}$$

Bicarbonate ions dissociate, form carbonate and additional hydrogen ions:

$$HCO^-_{3\,(aq)} \rightleftharpoons H^+_{(aq)} + CO^{2-}_{3\,(aq)} \tag{28}$$

In an aqueous system with CO_2 and mild steel, besides the main anodic reaction for iron that is mentioned in section 2.1, the main cathodic reactions are reported to be as follows:

$$2H^+_{(aq)} + 2e^- \rightarrow H_{2(g)} \tag{29}$$

$$2H_2CO_{3_{(aq)}} + 2e^- \rightarrow H_{2(g)} + 2HCO^-_{3\,(aq)} \tag{30}$$

$$2HCO_{3\,(aq)}^{-} + 2e^{-} \rightarrow H_{2(g)} + 2CO_{3\,(aq)}^{2-} \quad (31)$$

$$2H_2O_{(l)} + 2e^{-} \rightarrow H_{2(g)} + 2OH_{(aq)}^{-} \quad (32)$$

Different studies have shown that each of these cathodic reactions are dominant in different conditions [12-17]. However, in general, when the reactions are controlled by charge transfer, the dominant cathodic reaction is reduction of carbonic acid and if the reactions are controlled by the diffusion of the H^+, the dominant cathodic reaction is reduction of H^+ ions. More recent work has shown that, in the conditions selected for this study, the direct reduction of carbonic acid does not significantly occur, the main reaction being the reduction of H^+. However, the dissociation of carbonic acid remains a main contributor of acidity through a process called buffering effect.

Appendix B: Desorption Equation Solution in Continuous Dilution

This section discusses the calculations done for solving equation (6) in continuous dilution condition.

Inhibitor Concentration Equation

The only term in equation (6) that differs from partial dilution is $C_{inh}(t)$ which is not constant in continuous dilution period. Change in CI concentration with time can be calculated using a mass balance equation in the glass cell:

$$\frac{dN_{inh}}{dt} = \dot{N}_{inh_i} - \dot{N}_{inh_o} \tag{33}$$

where N_{inh}, $\dot{N}_{inh_i}$, and $\dot{N}_{inh_o}$ are moles of inhibitor in the bulk, and the inlet and outlet molar flowrate respectively. This equation can be simplified with the fact that there is no inhibitor entering the glass cell or consumed by any reaction:

$$\frac{dN_{inh}}{dt} = -\dot{N}_{inh_o} \tag{34}$$

Number of inhibitor moles in the bulk and the outlet molar flowrate can be also calculated using the equations below:

$$\dot{N}_{inh_o} = Q \times C_{inh} \tag{35}$$

$$N_{inh} = C_{inh} \times V \tag{36}$$

where Q, C_{inh}, and V are dilution flow rate ($\frac{L}{minute}$), inhibitor concentration in the bulk ($\frac{mol}{L}$), and solution volume (L). Thus, equation (34) can be simplified as follows:

$$\frac{dC_{inh}}{C_{inh}} = -\frac{Q}{V}dt \tag{37}$$

By integrating equation (37), the change in inhibitor concentration over time is given by the following equation:

$$C_{inh}(t) = C_{inh_0} e^{-\frac{Q}{V}t} \tag{38}$$

where C_{inh_0} is the initial CI concentration before dilution.

Now that the change in inhibitor concentration by the time is calculated, equation (6) can be rewritten as follows:

$$\frac{d\theta}{dt} = k_A C_{inh_0} e^{-\frac{Q}{V}t}(1-\theta) - k_D\theta \tag{39}$$

Equation (39) cannot be solved analytically; therefore, a numerical approach was employed in this research using Python™. Specifically, an ODE solver function in Python was utilized to approximate the solution by discretizing the problem into small time steps and iteratively computing function values through numerical methods. Then, the corresponding surface coverage for each time step was determined. Using these calculated surface coverage values, the corrosion rate at each time step was computed based on equation (18).

Thesis and Dissertation Services